NASA Reference Publication 1163

February 1986

NASA RP-1163

EL NINO AND OUTGOING LONGWAVE RADIATION:

AN ATLAS OF NIMBUS-7 EARTH RADIATION BUDGET OBSERVATIONS

NASA

NASA

NASA Reference Publication 1163

February 1986

NASA RP-1163

EL NINO AND OUTGOING LONGWAVE RADIATION:

AN ATLAS OF NIMBUS-7 EARTH RADIATION BUDGET OBSERVATIONS

H. Lee Kyle
Goddard Space Flight Center

Philip E. Ardanuy
Richard R. Hucek
Research and Data Systems Corporation

The Nimbus-7 ERB Experiment Team

NASA
National Aeronautics
and Space Administration

Scientific and Technical Information Branch

The Nimbus-7 ERB Experiment Team

Albert Arking, NASA Goddard Space Flight Center
Garrett Campbell, Department of Atmospheric Science, Colorado State University
John R. Hickey, The Eppley Laboratory, Inc.
Frederick House, Department of Physics and Atmospheric Science, Drexel University
Andrew Ingersoll, Division of Geological and Planetary Sciences, California Institute of Technology
Herbert Jacobowitz, National Oceanic and Atmospheric Administration, National Environmental Satellite, Data, and Information Service
H. Lee Kyle, NASA Goddard Space Flight Center
Robert Maschhoff, Gulton Data Systems Division
G. Louis Smith, NASA Langley Research Center
Larry L. Stowe, National Oceanic and Atmospheric Administration, National Environmental Satellite, Data, and Information Service
Thomas H. Vonder Haar, Department of Atmospheric Science, Colorado State University

Library of Congress Cataloging-in-Publication Data

Ardanuy, Philip E.
El Nino and outgoing longwave radiation.

(NASA RP ; 1163)
Bibliography: p.
1. Energy budget (Geophysics)--Atlases.
2. El Nino Current--Atlases. 3. Nimbus
(Meteorological satellite)--Atlases. I. Hucek,
Richard R. II. Kyle, H. Lee. III. Title. IV. Title:
El Nino and outgoing long wave radiation. V. Series.
QC809.E6A73 1986 551.5'272 85-31944

Table of Contents

INTRODUCTION

Five years of broad-band earth radiation budget (ERB) measurements taken by the Nimbus-7 ERB experiment have been archived. This period encompasses the 1982-1983 El Nino/Southern Oscillation event, which reached a peak near the beginning of the fifth data year (January 1983). A 41-month outgoing longwave radiation subset of this data set, extending from June 1980 through October 1983, has been further processed to enhance the spatial resolution. This atlas contains the analyses of the resultant fields and a set of anomaly maps based on a definition of pre-El Nino climatology. Together they provide the first broad-band glimpse of the terrestrial outgoing longwave radiative response to the El Nino event throughout its life cycle. Of particular interest are the quasi-stationary planetary-scale tropical and mid-latitude patterns which emerged as the El Nino reached its peak intensity.

BACKGROUND

Without question, the 1982-1983 El Nino event is associated with one of the largest-amplitude global climate perturbations in recent history. The meteorological ramifications of this event include: droughts in southern Africa, Indonesia, northern Brazil, and Australia; flooding in the central equatorial Pacific, Ecuador, southern Brazil, and Peru; intense tropical cyclones over French Polynesia and the Hawaiian Islands; and unusual storm activity across the southern United States from California to the Gulf of Mexico. These global phenomena are discussed in detail by Rasmusson et al. (1983a and 1983b), Rasmusson and Wallace (1983), and Rasmusson and Hall (1983). Arkin et al. (1983) produced a "quick-look" atlas of the event, including the sea-surface temperature, 850 mb and 200 mb wind, and the NOAA-7 Advanced Very High Resolution Radiometer (AVHRR) 11.5 μm-band outgoing longwave radiation fields. These illustrate the time evolution of the large-scale features preceding and during the event, from September 1982 through August 1983.

In order to be able to predict, on a year-to-year basis, fluctuations of our global climate system, and with it the periodic occurrences of the El Nino/Southern Oscillation (ENSO) events, it is important to develop a physical understanding of the ENSO phenomenon. The 1982-1983 ENSO occurrence was observed on many scales by many instruments. One of these was the set of broad-band ERB radiometers on board the Nimbus-7 polar orbiter. This spacecraft is sun synchronous, with local-noon and local-midnight equatorial crossing times. The experiment was operational and taking data prior to, during, and following the ENSO event.

OVERVIEW OF THE ERB EXPERIMENT

On October 22, 1978, the Nimbus-7 spacecraft was launched into a sun synchronous near-polar orbit, with local-noon ascending and local-midnight descending nodes, and a retrograde inclination to the equator of 99.3° (Jacobowitz et al., 1978). To minimize degradation in the optical trains of the various channels (caused by the interaction of deposited out-gassing contaminants and the solar UV), the experiment was not activated until November 16, 1978. At this time, full-time collection of ERB observations commenced, limited only by the constraint of available spacecraft power. The major imposition was that of a 3 day on/1 day off instrument duty cycle.

On board the Nimbus-7 observatory are a wide variety of remote sensing experiments, including the ERB experiment. The ERB instrument package consists of three sections: a ten-channel solar telescope, four wide-field-of-view (WFOV) fixed Earth-flux channels, and eight narrow-field-of-view (NFOV) scanning Earth-radiance channels. The experiment is described in detail by Jacobowitz et al. (1984). The solar and the WFOV Earth-flux channels are in their seventh year of operation, and both are still recording high-quality data. The scanner, on the other hand, failed in June 1980 after 20 months of data gathering. The NFOV scanner data for this early period have been analyzed by Jacobowitz and Tighe (1984). Solar data have been discussed in numerous places [see, for instance, Hickey and Alton] and continue to be collected, processed, and analyzed. Relevant to this atlas is the WFOV ERB data set as archived on the ERB MATRIX tapes and described by Jacobowitz et al. (1984). The WFOV radiometers are capable of measuring the shortwave and total outgoing components of the Earth's radiation budget at satellite altitude. From these spacecraft measurements "top of the atmosphere" (TOA) fluxes may be inferred.

In the Nimbus ERB instruments, a total channel is used to measure both reflected-solar and emitted-terrestrial radiation in a spectral band of .2 to 50 μm. At the same time, shortwave channels monitor reflected solar radiation in the spectral bands of .2 to 3.8 μm and .7 to 2.8 μm. The calibrated output of the channels and their differences then yields total reflected shortwave, emitted longwave, near-infrared reflected, ultraviolet and visible reflected, and total exitant irradiances.

Channels 12, 13, and 14 view the entire visible Earth disk at all times. Satellite-altitude (955 km) irradiance observations are taken at 4-second intervals throughout the 104-minute orbits. It should be emphasized at this time that this satellite-altitude data set may not be simply reduced to the TOA due to the non-uniform weighting of radiances incident within the fields-of-view (FOV's), as noted in King and Curran (1980). Thus, the WFOV observations are actually integrals across the radius of the 29.3° Earth central angle (ECA) visible Earth disk; the half-power point radius is approximately 10° ECA.

Although calibrated to high precision in the laboratory at three times prior to launch, with no evidence of any calibration drift (Hickey and Karoli, 1974), exposure to the in-flight orbital environment produced both trends and periodicities in the filtered channels (13 and 14) data set. This requires the application of a set of calibration adjustments (Kyle et al., 1984; Ardanuy and Rea, 1984; Maschhoff et al., 1984) to account for the implied calibration changes.

TECHNICAL APPROACH

The roots of the data set illustrated here lie in the data record taken by the ERB experiment on board the Nimbus-7 spacecraft. At present, 5 years of these observations have been archived. Because of a calibration change, only the latter 4 years (extending from June 1980 through October 1983) represent an internally consistent sequence of the Earth's radiation budget. The field most amenable to higher-level analyses at this time is that of the broad-band longwave flux at the so-called "top of the atmosphere." This parameter, during production, is binned into 2070 target areas, each approximately 500 km by 500 km. Time averages in a daily and in a monthly sense are subsequently generated and placed on the ERB MATRIX tape. The strengths of this data set are that: (1) these are broad-band (4 – 50 μm) measurements, making the resultant fields an energy parameter rather than simply an index; (2) they are global in extent; (3) the calibration is well known; (4) there are no discontinuities in the time coverage; and (5) due to the excellent "health" of the instrument and the spacecraft and due to reprocessing plans, a consistently calibrated extension of this data set spanning a decade may become available in the future.

What distinguishes the present data set from the archived Nimbus-7 data set is the extensive post-processing which it has received. Through the use of additional information, already present but "hidden" in the data, it is possible to improve substantially both the time and space sampling of the data set. The technique has already been developed (Smith and Green, 1981) and applied (Bess et al., 1981) to Nimbus-6 ERB data. It is accomplished here for the Nimbus-7 ERB data set by fitting a spectrally truncated 12th-degree spherical harmonic field to the binned observations. By incorporating the known angular instrument response, the effective spatial resolution is doubled along the track, and observations are effectively obtained at each target area for each day. This process has been applied to the 41-month data set.

The maps shown in this atlas were made from the ascending node (local noon Equator crossing time) outgoing longwave radiation fields on the ERB MATRIX tape. On the descending node (night) side of the orbit, direct sunlight contaminates the WFOV data over some 20° of latitude at both satellite sunrise and sunset. These contaminated data were not used, but the resultant gaps make both the descending node data and the day-night averages less susceptible to resolution enhancement. Recent studies (Kyle et al., 1985) indicate that there is a calibration bias in the archived WFOV longwave data. According to this study, the actual ascending node outgoing longwave should be some 11 W/m^2 larger than indicated on the maps. The average day-night means should be some 8 W/m^2 larger than the map values. However, care should be exercised in transforming map readings to day-night means, as there are large regional variations in the diurnal cycle in the outgoing longwave radiation — see, for example, Minnis and Harrison (1984). This bias problem will have little affect on the anomaly maps. Corrected MATRIX tapes will not be available for approximately 2 years.

SIMULATION

Although a complete treatment of the development process that resulted in the deconvolution algorithm used here is outside the scope of this atlas, some review is pertinent. As discussed in the previous section, a resampling of the WFOV data set is desirable in terms of both instrument coverage and spatial resolution. Two questions may be asked: what is the optimal spectral resolution, and what is the accuracy of the results? To answer these questions, a set of "truth" fields is required. For these, the set of 23 daily target-area NFOV ascending-node longwave fields for June 1979 was used. For simulation purposes, the NFOV-derived "truth" fields are assumed perfect: the goal, therefore, is to replicate as closely as possible the "perfect" solution. Knowing the orbit parameters for the Nimbus-7 spacecraft, it is possible to simulate, on an observation-by-observation, day-by-day basis, a set of synthetic WFOV longwave measurements. After deconvolution, the resultant spectral amplitudes can then be evaluated at each target area, and a global root-mean-square (RMS) comparison can be made with the truth field. The global minimum in the surface formed by a contour map of RMS deviation between the two fields as a function of spectral resolution (number of waves versus number of nodes) then yields the desired spectral truncation. This simulation yielded, for a rhomboidal truncation, the combination of 7 waves and 12 nodes, or 195 amplitudes. When the complete month is considered, a global RMS error of 8 W/m^2 is obtained. Although solutions to a higher wavenumber are possible, no global gain in accuracy is obtained. The improvement in accuracy appears to be greatest in the tropical half of the Earth between 30 °N and 30 °S latitude. As a consequence, tropical features such as the Intertropical Convergence Zone (ITCZ), the subtropical belts, and other non-zonally-symmetric features as well are more sharply defined in the deconvolved fields. Ardanuy and Kyle (1985) describe the development of the data set in more detail.

ANOMALIES DURING EL NINO

During the 1982-1983 El Nino event, significant perturbations in a diverse set of geophysical fields occurred. Of special interest to this study are those planetary-scale fields that act to modify the outgoing longwave radiation (OLR) field at the top of the atmosphere. The most important is the effective "cloudiness": specifically, perturbations from the climatological mean of cloud cover, height, thickness, water content, drop/crystal size distribution, and emissivity. Also important are changes in surface temperature and atmospheric water vapor content and, to a lesser extent, atmospheric temperature. Changes in one or more of these parameters, regionally or globally, will cause corresponding anomalies in the broad-band OLR at the top of the atmosphere.

To facilitate the examination of the time evolution of the El Nino event from the perspective of the set of top of the atmosphere OLR fluxes, monthly averaged time-anomaly fields have been generated. These are defined in terms of departures (W/m^2) from the climatology for that month. The term "climatology" is used loosely here to indicate the 2 years between June 1980 and May 1982. Thus, a 2-year mean pre-El Nino seasonal cycle is removed in the creation of the anomaly maps. Analysis of these fields indicates that the OLR anomaly response to the El Nino event of 1982-1983 can be characterized as having four modes of behavior: onset, intensification, expansion, and decay.

Onset of El Nino

The onset phase of the OLR response existed between July and September 1982. The phenomenological characteristics for the months were weak anomalies with little spatial extent. Indeed, were it not for the ensuing intensification of these anomalies into major perturbations, one would equate them with those other anomalies "typically" noted in non-El Nino years. They were, however, stationary and did intensify.

In July, the incipient El Nino was only apparent as a weak negative (-21 W/m^2) OLR anomaly at 175 °W on the equator and a corresponding weak positive anomaly (27 W/m^2) over Borneo/Celebes.

By August, the anomalies had remained stationary and intensified slightly, with the OLR deficiency over the central Pacific Ocean increasing to -33 W/m^2 and the OLR excess over Indonesia at about the same magnitude.

By September, the positive anomaly over Indonesia extended longitudinally to encompass Sumatra and New Guinea, and intensified to 36 W/m². Over the central Pacific Ocean the OLR deficit reached −36 W/m² and was already extending along the equator toward South America. It was now centered slightly south of the equator at 175 °W, 5 °S.

Intensification of El Nino

The intensification of the OLR response occurred between October 1982 and January 1983. During this period the characteristics of the El Nino response were rapid intensification and expansion.

In October, the Indonesian OLR excess temporarily split into two centers, each of which was more intense than in the preceding month. A large negative anomaly of −50 W/m² was present for the first time over the Arabian Sea. Over the equatorial central Pacific Ocean, the OLR deficit strengthened substantially to −60 W/m², almost doubling in intensity in one month. An eastern extension to 135 °W was evident. An important phenomenon appearing at this time was the doublet of positive anomalies evident to the north and south of the Pacific equatorial rainfall center. This pair of anomalies has important dynamic implications in that it is suggestive of enhanced subsidence caused by a stronger Hadley-type circulation.

In November, the two Indonesian OLR anomalies reemerged over Sumatra/Borneo. A ring of negative centers surrounded the maximum which clearly dominated the region. The primary anomaly, over the equatorial Pacific Ocean, intensified further to −79 W/m² and moved eastward 15 ° to 160 °W relative to the previous month. It, like the Indonesian anomaly, was surrounded by OLR centers of opposite sign. To its north and south were positive anomaly centers; the northern-most center at 135 °W, 15 °N more than doubled in magnitude in one month to match the intensity of its southern partner at 165 °W, 25 °S. Strong quasi-stationary features were becoming evident and persisted throughout the intensification phase. Two mid-latitude centers of special interest are those anomalies which appeared over the southern United States (−29 W/m²) and over central Europe (23 W/m²).

In December, an eastern movement of the two primary anomalies occurred. The Indonesian positive anomaly was centered over New Guinea, while the tropical Pacific OLR deficit continued to intensify, reaching −83 W/m², and moved 20 ° further east to a new position at 140 °W. The accompanying positive regions to the north and south, however, remained stationary, but continued to intensify. The centers noted previously over the southern United States, central Europe, and the Arabian Sea/Indian Ocean persisted. Interestingly, the tropical high/low/high pattern at 140 °W was closely mirrored by a strikingly similar low/high/low pattern at 140 °E.

In January, the peak amplitudes of the OLR anomalies were reached. The negative radiation center in the equatorial Pacific reached −88 W/m². To its north and south, the accompanying positive anomalies averaged half its magnitude. An interesting large-amplitude pattern existed along the equator. The three areas that are normally quite active, convectively, at this time of the year are Indonesia, the Amazon River basin, and the Congo River basin. They now showed positive OLR anomalies indicative of reduced convection. These were replaced with the negative anomalies over the Arabian Sea, the Indian Ocean, and the central equatorial Pacific Ocean. The center over Europe intensified, while the center over the United States moved into the Gulf of Mexico. At this time the true global nature of the El Nino event was evident.

Expansion of El Nino

Between the months of February and May 1983, the negative OLR anomaly over the equatorial Pacific Ocean expanded eastward to the South American coast. At the same time, in the western Pacific Ocean, the anomaly patterns became less stationary.

In February, the OLR minimum over the equatorial Pacific Ocean continued to drift eastward and weaken slightly to −77 W/m². Some oscillation in the magnitudes of the positive anomaly centers to the north and south was evident in this and the next several months. The northernmost intensified to 47 W/m² from 32 W/m², while the southernmost weakened to 28 W/m². The positive OLR anomaly over Indonesia weakened slightly as well to 62 W/m². Two accompanying features are significant with respect to the Australian drought in progress at this time: these are the weakening of the southern tongue of the OLR maximum over Australia and the formation of a (−45 W/m²) negative anomaly to the west (20 °S, 90 °E) of the subcon-

tinent. The positive anomaly over Brazil maintained its intensity, while the center over Africa weakened. The negative anomaly that was centered over the Gulf of Mexico now extended across the Atlantic Ocean to the African coast.

In March, the primary Pacific anomaly weakened slightly to -71 W/m^2 and both moved further eastward and elongated along the equator toward the coast of South America. The accompanying OLR maxima to the north and south intensified. The large positive anomaly that had remained stationary over Indonesia drifted to the east, while in the south an OLR deficit drifted eastward over Australia, signifying the end of the drought. Positive anomalies were still evident over South America and equatorial Africa.

By April the OLR deficit along the eastern Pacific equator clearly extended from the dateline to the coast of South America. It was bounded to the north and south by elongated OLR maxima, to the east by the maximum over South America, and to the west by the large maximum to the northeast of Indonesia/Borneo. A very strong (-55 W/m^2) OLR minimum was present over Australia.

In May, the primary OLR minimum in the eastern Pacific Ocean continued its drift toward South America, reaching 115 °W and intensifying slightly. The four OLR maxima surrounding it decreased in spatial extent. The positive anomaly of 38 W/m^2 in the Arabian Sea was indicative of a late monsoon for which the onset over India appeared to lag one month behind that of other years.

Decay of El Nino

The decay phase of the OLR response occurred between June 1983 and September 1983, at which time the radiative anomalies no longer showed any of the coherent structure present a year before.

In June the weakening OLR minimum approached the equatorial west coast of South America. The OLR maxima on each of its four sides continued to weaken. The late monsoon was evident over the Indian peninsula. It is interesting to note that the anomaly pair (the deficit of -54 W/m^2 off the South American coast and the excess of 48 W/m^2 now over the Philippines) was still, after 1 year, the largest amplitude perturbation in the global OLR field.

In the months of July, August, and September, the Indonesian OLR maximum vanished, while the eastern-equatorial Pacific minimum weakened and moved against the coast of South America. This, in the OLR field, signified the end of the El Nino-induced anomalies.

REFERENCES

Ardanuy, P.E., and J. Rea, 1984: Degradation asymmetries and recovery of the Nimbus-7 Earth radiation budget shortwave radiometer. *J. Geophys. Res., 84,* 5039-5048.

_____ and H.L. Kyle, 1986: El Nino and outgoing longwave radiation: observations from Nimbus-7 ERB. *Mon. Wea. Rev.,* in press (January).

Arkin, P.A., J.D. Kopman, and R.W. Reynolds, 1983: 1982-1983 El Nino/Southern Oscillation event quick look atlas, Climate Analysis Center NOAA/NMC, Washington, D.C.

Bess, T.D., R.N. Green, and G.L. Smith, 1981: Deconvolution of wide field-of-view radiometer measurements of Earth-emitted radiation. Part II: Analysis of first year of Nimbus-6 ERB data. *J. Atmos. Sci, 38,* 474-488.

Hickey, J.R., and A.R. Karoli, 1974: Radiometer calibrations for the Earth radiation budget experiment, *Appl. Opt., 13,* 523-533.

_____ and B.M. Alton, 1983: Extraterrestrial irradiance results from the ERB experiment of Nimbus-7, Preprints of the 5th Conference on Atmospheric Radiation, American Meteorological Society, Baltimore, Md., Oct. 31-Nov 4, pp 444-447.

Jacobowitz, H., L.L. Stowe, and J.R. Hickey, 1978: The Earth radiation budget (ERB) experiment, in the Nimbus-7 User's Guide, NASA Goddard Space Flight Center, Greenbelt, Md.

_____ H.V. Soule, H.L. Kyle, F.B. House, and the Nimbus-7 ERB Experiment Team, 1984: The Earth radiation budget experiment: an overview, *J. Geophys. Res., 89,* 5021-5038.

_____ R.J. Tighe, and the Nimbus-7 ERB Experiment Team, 1984: The Earth radiation budget derived from the Nimbus-7 ERB experiment. *J. Geophys. Res., 89,* 4997-5010.

Julian, P.R., 1984: Objective analysis in the tropics: a proposed scheme. *Mon. Wea. Rev., 112,* 1752-1767.

King, M.D., and R.J. Curran, 1980: The effect of a nonuniform planetary albedo on the interpretation of Earth radiation budget observations. *J. Atmos. Sci, 37,* 1262-1278.

Kyle, H.L., F.B. House, P.E. Ardanuy, H. Jacobowitz, R.H. Maschhoff, and J.R. Hickey, 1984: New in-flight calibration adjustment of the Nimbus-6 and -7 Earth radiation budget wide field-of-view radiometers. *J. Geophys Res., 89,* 5057-5076.

_____ P.E. Ardanuy, and E.J. Hurley, 1985: The status of the Nimbus-7 Earth radiation budget data set. *Bull. Amer. Meteor. Soc., 66,* 1378-1388.

Maschhoff, R., A. Jalink, J. Hickey, and J. Swedberg, 1984: Nimbus-Earth radiation budget sensor characterization for improved data radiation fidelity. *J. Geophys. Res., 89,* 5049-5056.

Minnis, P., and E.F. Harrison, 1984: Diurnal variability of regional cloud and clear-sky radiative parameters derived from GOES data. Part III: November 1978 radiative parameters. *J. Climate Appl. Meteor., 23,* 1032-1051.

Rasmusson, E.M., P.A. Arkin, T.H. Carpenter, J. Kopman, A.F. Krueger, and R.W. Reynolds, 1983a: A warm episode in the eastern equatorial Pacific Ocean. *Tropical Ocean-Atmosphere Newsletter, 16,* 1-3.

_____ A.F. Krueger, R.S. Quiroz, and R.W. Reynolds, 1983b: The equatorial Pacific atmospheric climate during 1982-83. *Tropical Ocean-Atmosphere Newsletter, 21,* 2-3.

_____ and S.M. Hall, 1983: The great equatorial Pacific Ocean warming event of 1982-1983. *Weatherwise, 36,* 166-175.

_____ and J.M. Wallace, 1983: Meteorological aspects of the El Nino/Southern Oscillation. *Science, 222,* 1195-2222.

Smith, G.L., and R.N. Green, 1981: Deconvolution of wide field-of-view radiometer measurements of Earth-emitted radiation. Part I: Theory. *J. Atmos. Sci., 38,* 461-473.

ACKNOWLEDGMENTS

The authors wish to acknowledge the help of Bonnie Cord and Gloria Hoy, of Research and Data Systems (RDS), in the production of this atlas.

MAPS

In this section are the 80 analyses of the OLR fields which comprise this atlas. They are arranged according to time scale from monthly averaged to seasonally averaged to annually averaged fields. In addition, for each averaging period, two kinds of quantities are shown: a flux field and an anomaly flux field. The flux fields represent the average OLR for the given time interval. The anomaly fields, on the other hand, illustrate the deviations in flux from the two-year climatology (June 1980 – May 1982) established for the given time period. Taken together, the three time scales, each with two analyzed parameters, give a total of six groups of displayed maps. The first group is the set of 41 monthly averaged flux fields spanning the period from June 1980 to October 1983. These form a complete basic set in the sense that all other maps portray some algebraic combination of these fields. Following them are the remaining groups presented in order from shortest to longest time scale and, within each, from flux to anomaly field. The contours appearing on all maps represent the fields at the TOA and are given in W/m^2.

MONTHLY AVERAGED FIELDS

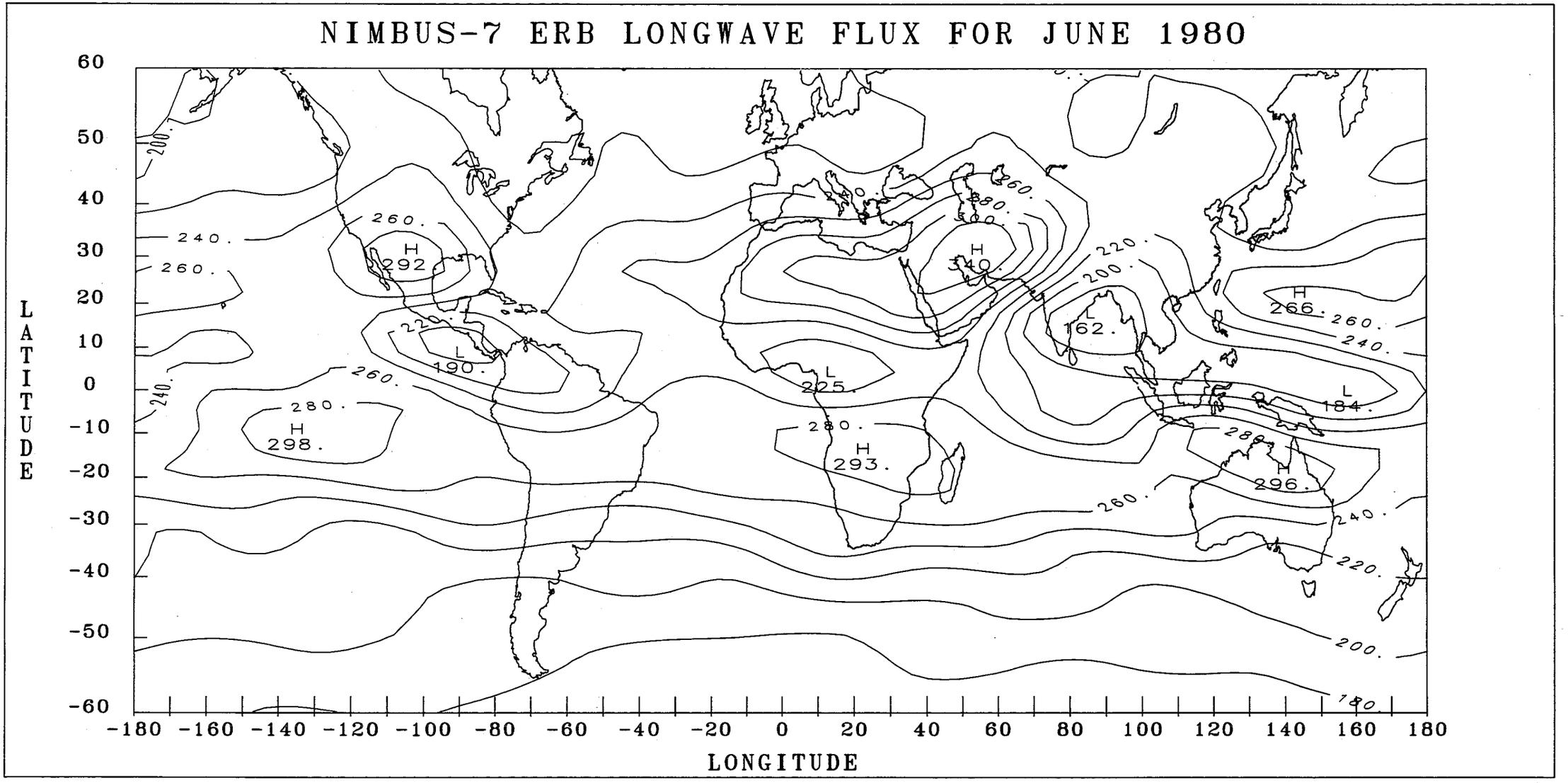
NIMBUS-7 ERB LONGWAVE FLUX FOR JUNE 1980
LATITUDE
LONGITUDE
60
50
40
30
20
10
0
-10
-20
-30
-40
-50
-60
-180 -160 -140 -120 -100 -80 -60 -40 -20 0 20 40 60 80 100 120 140 160 180
H 292
H 298.
H 293.
H 340.
H 296.
H 266.
L 190.
L 225.
L 162.
L 184.
200.
220.
240.
260.
280.
300.
180.

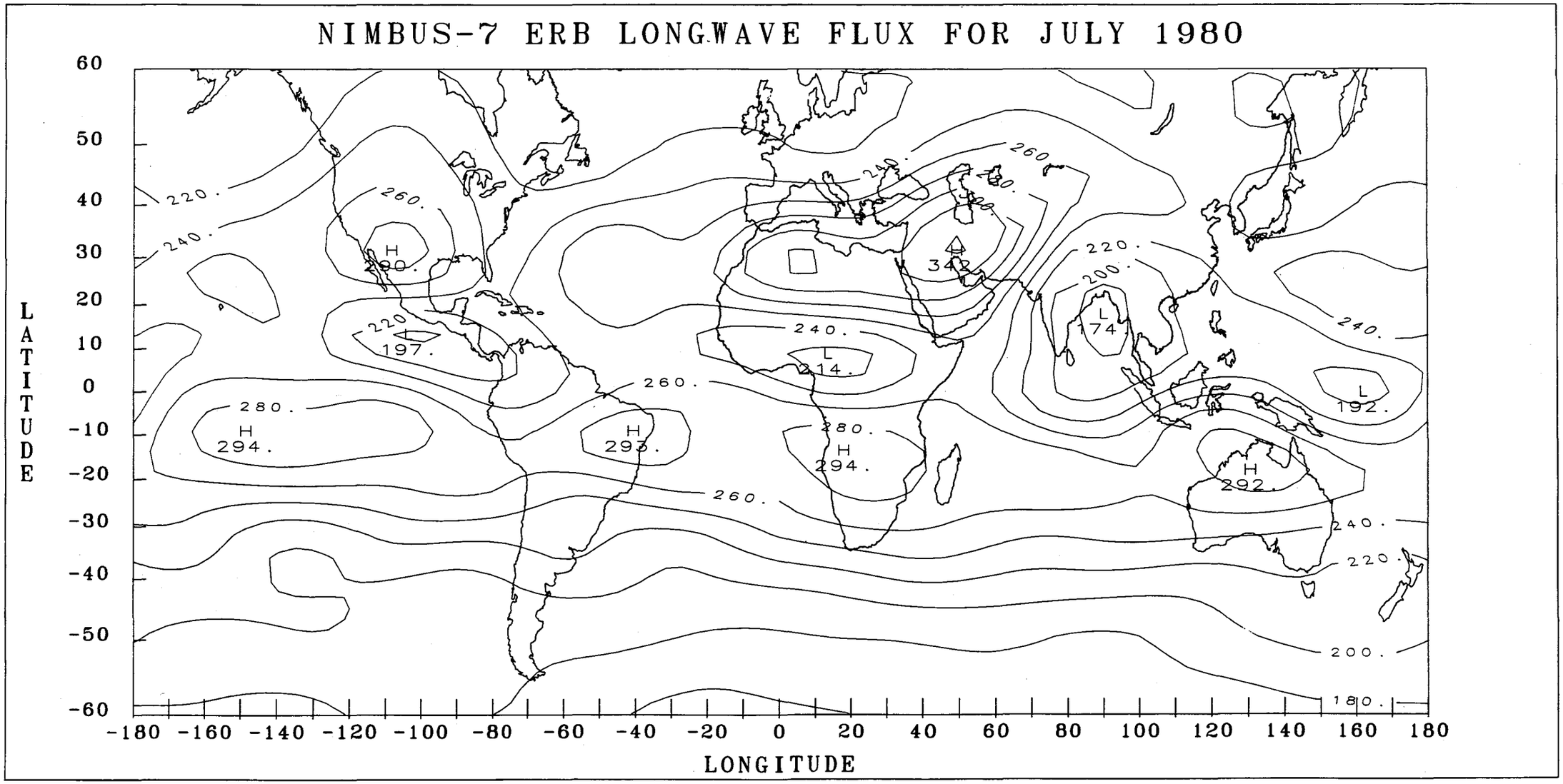
NIMBUS-7 ERB LONGWAVE FLUX FOR JULY 1980
LATITUDE
LONGITUDE
60
50
40
30
20
10
0
-10
-20
-30
-40
-50
-60
-180 -160 -140 -120 -100 -80 -60 -40 -20 0 20 40 60 80 100 120 140 160 180
220.
240.
260.
280.
200.
180.
H
290.
H
294.
H
293.
H
294.
H
292.
L
197.
L
214.
L
343.
L
174.
L
192.

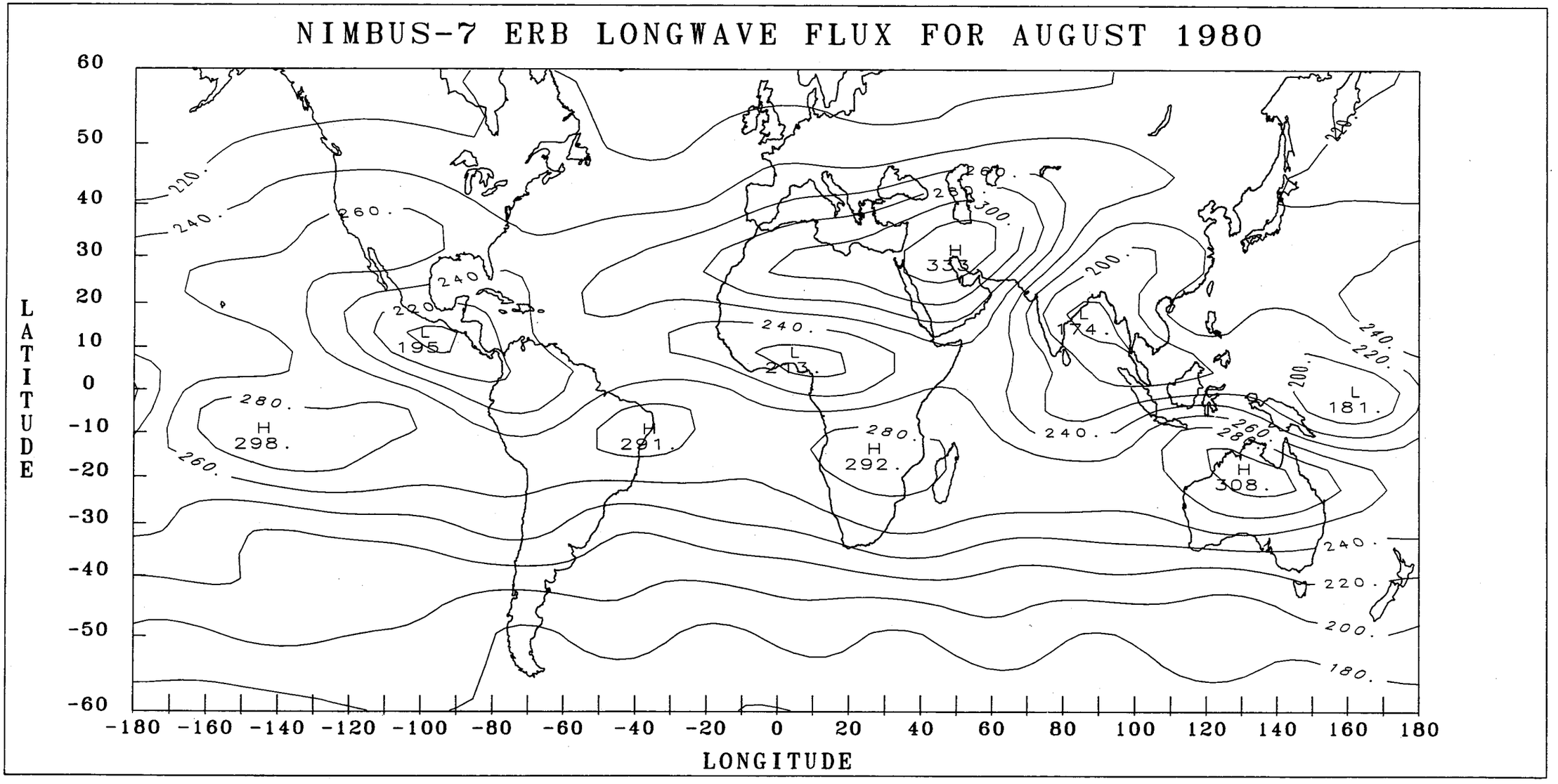
NIMBUS-7 ERB LONGWAVE FLUX FOR AUGUST 1980
LATITUDE
LONGITUDE
60
50
40
30
20
10
0
-10
-20
-30
-40
-50
-60
-180 -160 -140 -120 -100 -80 -60 -40 -20 0 20 40 60 80 100 120 140 160 180
220.
240.
260.
280.
300.
200.
180.
H
298.
H
291.
H
292.
H
308.
L
195
L
213.
L
174.
L
181.

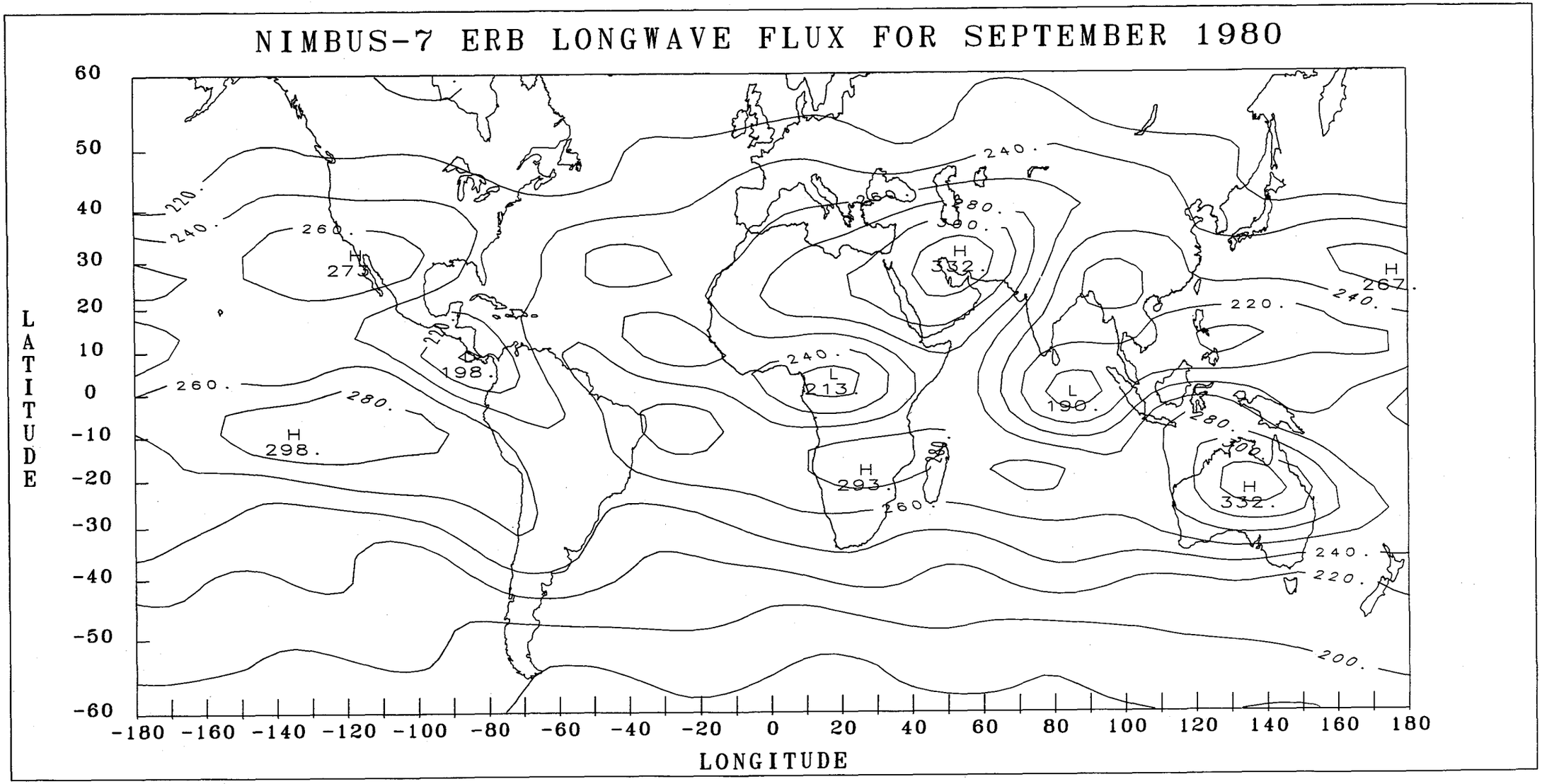
NIMBUS-7 ERB LONGWAVE FLUX FOR SEPTEMBER 1980
LATITUDE
LONGITUDE
60
50
40
30
20
10
0
-10
-20
-30
-40
-50
-60
-180 -160 -140 -120 -100 -80 -60 -40 -20 0 20 40 60 80 100 120 140 160 180
220.
240.
260.
280.
300.
H
273.
198.
H
298.
L
213.
240.
H
293.
260.
H
332.
L
190.
H
267.
220.
240.
280.
300.
240.
220.
200.

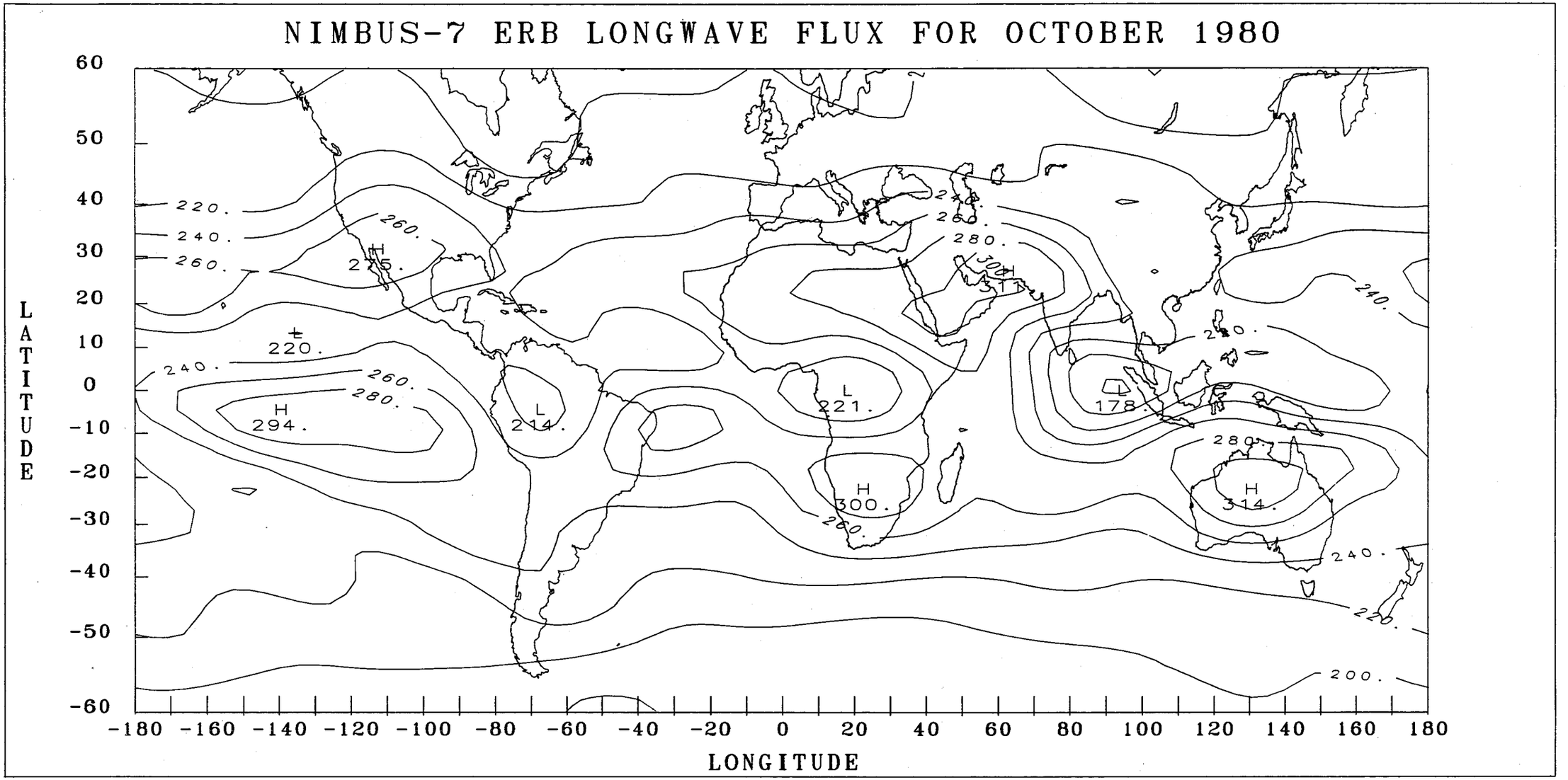
NIMBUS-7 ERB LONGWAVE FLUX FOR OCTOBER 1980
LATITUDE
LONGITUDE
60
50
40
30
20
10
0
-10
-20
-30
-40
-50
-60
-180 -160 -140 -120 -100 -80 -60 -40 -20 0 20 40 60 80 100 120 140 160 180
220.
240.
260.
280.
300.
H
294.
H
275.
H
317.
L
214.
L
221.
L
178.
H
300.
H
314.
200.

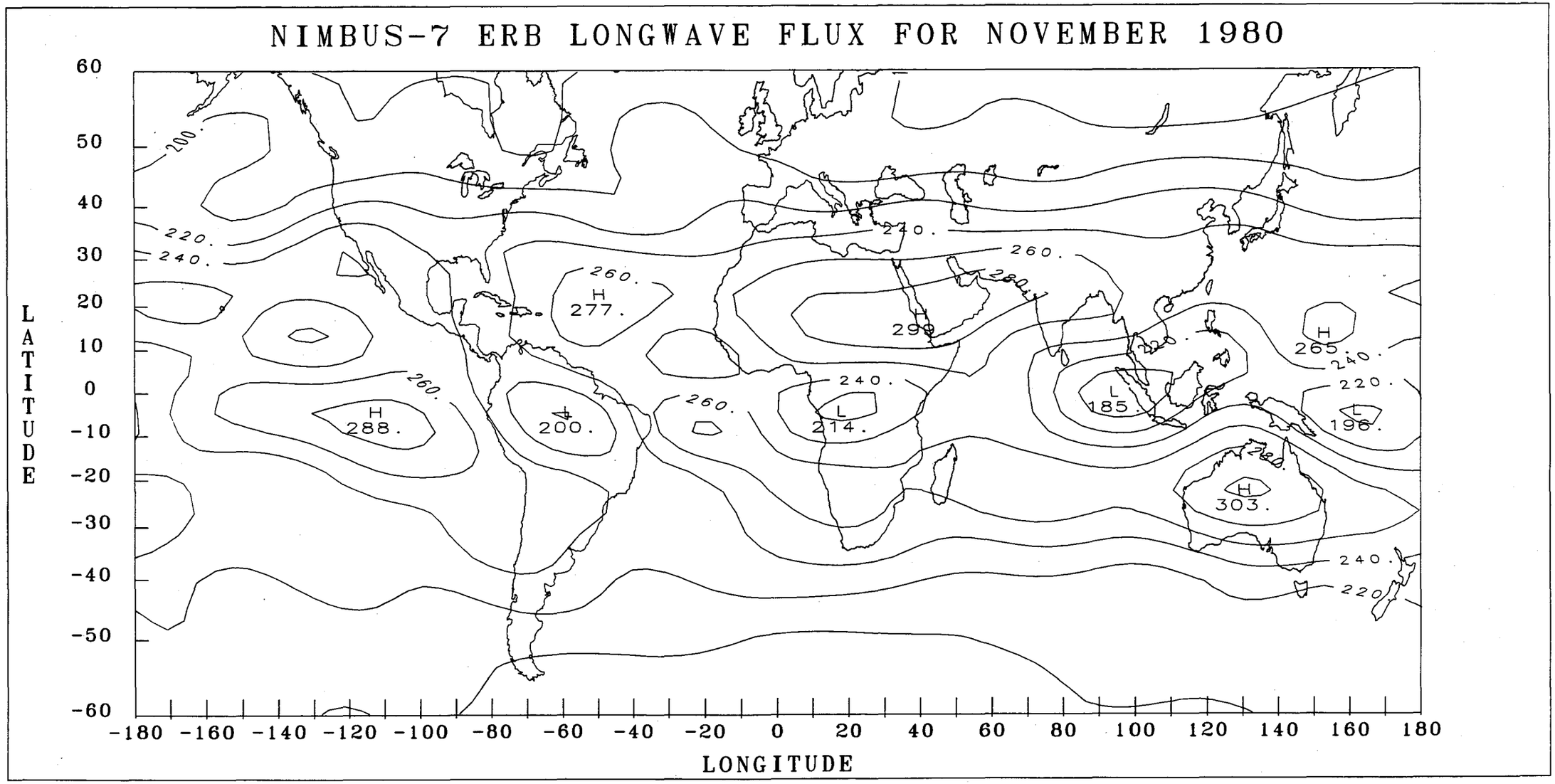
NIMBUS-7 ERB LONGWAVE FLUX FOR NOVEMBER 1980
LATITUDE
LONGITUDE
60
50
40
30
20
10
0
-10
-20
-30
-40
-50
-60
-180 -160 -140 -120 -100 -80 -60 -40 -20 0 20 40 60 80 100 120 140 160 180
200.
220.
240.
260.
H
277.
299
H
265.
L
185.
L
214.
H
288.
200.
L
196.
H
303.

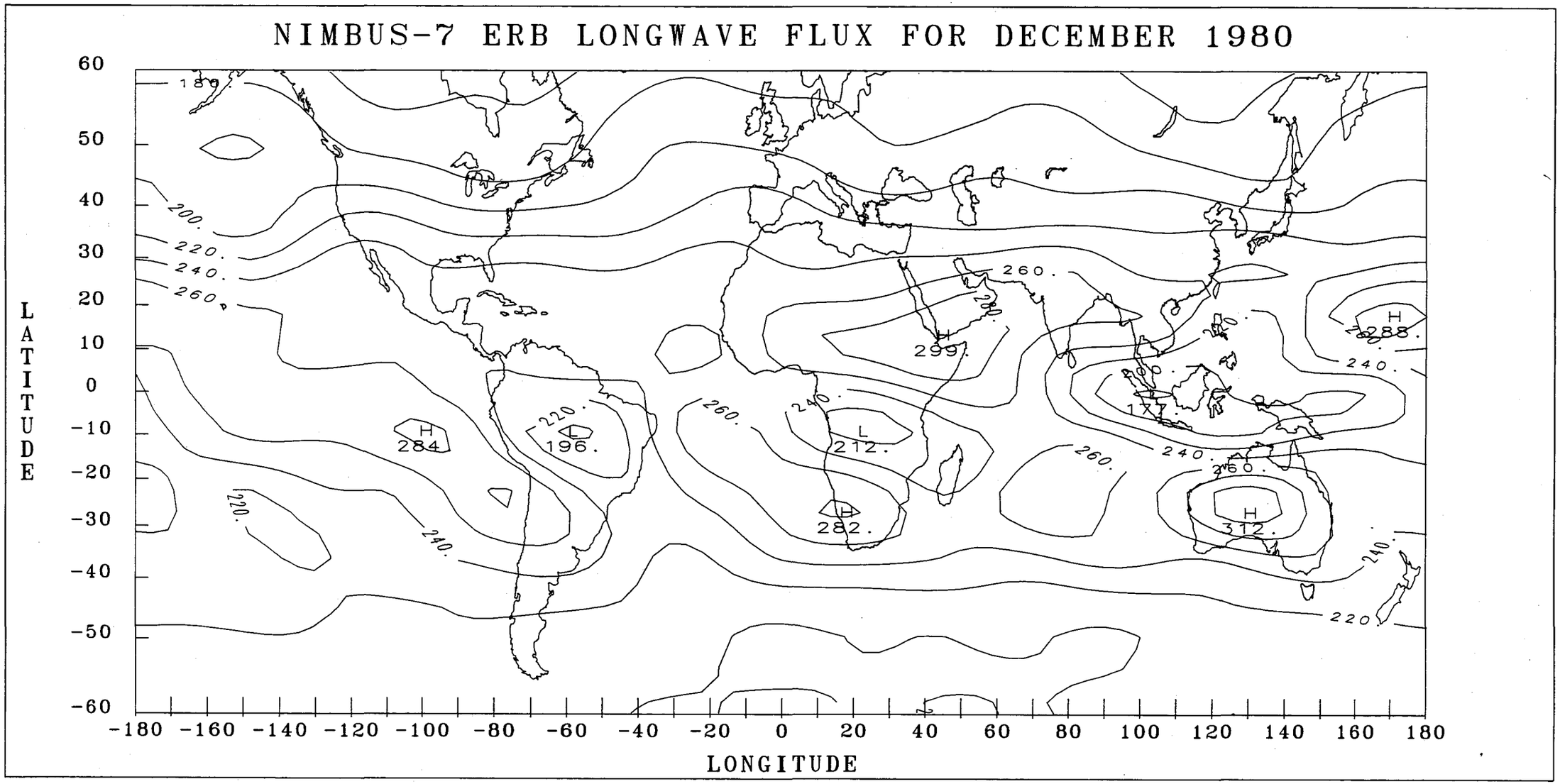
NIMBUS-7 ERB LONGWAVE FLUX FOR DECEMBER 1980
LATITUDE
LONGITUDE
60
50
40
30
20
10
0
-10
-20
-30
-40
-50
-60
-180 -160 -140 -120 -100 -80 -60 -40 -20 0 20 40 60 80 100 120 140 160 180
180.
200.
220.
240.
260.
H
284
220.
196.
L
260.
240.
212.
H
282.
299.
260.
240.
H
312.
240.
220.
H
288.
240.

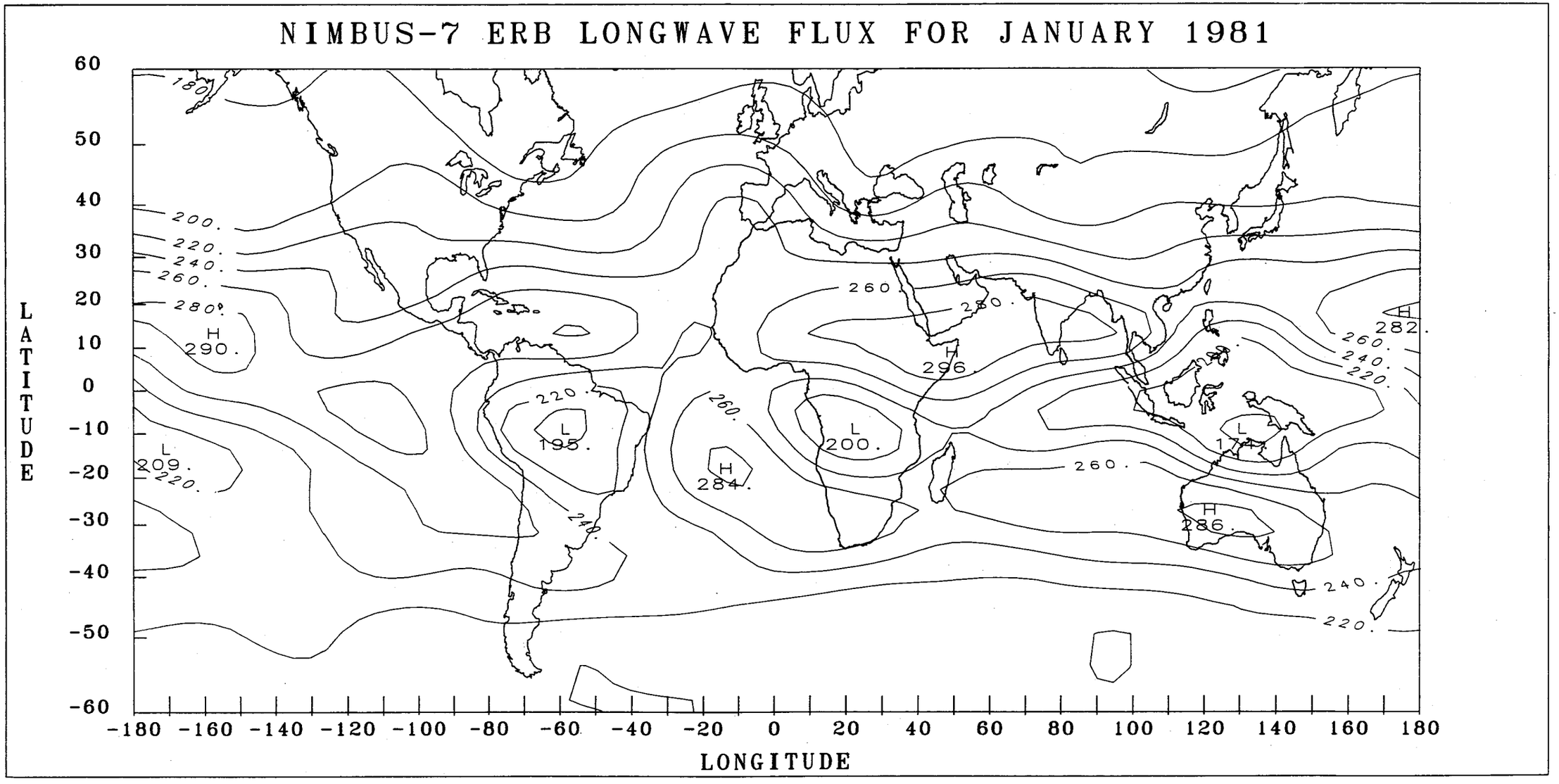
NIMBUS-7 ERB LONGWAVE FLUX FOR JANUARY 1981
LATITUDE
LONGITUDE
60
50
40
30
20
10
0
-10
-20
-30
-40
-50
-60
-180 -160 -140 -120 -100 -80 -60 -40 -20 0 20 40 60 80 100 120 140 160 180
180.
200.
220.
240.
260.
280.
H
290.
L
209.
220.
220.
L
195.
260.
H
284.
240.
260
250.
H
296.
L
200.
260.
H
282.
260.
240.
220.
L
174.
260.
H
286.
240.
220.

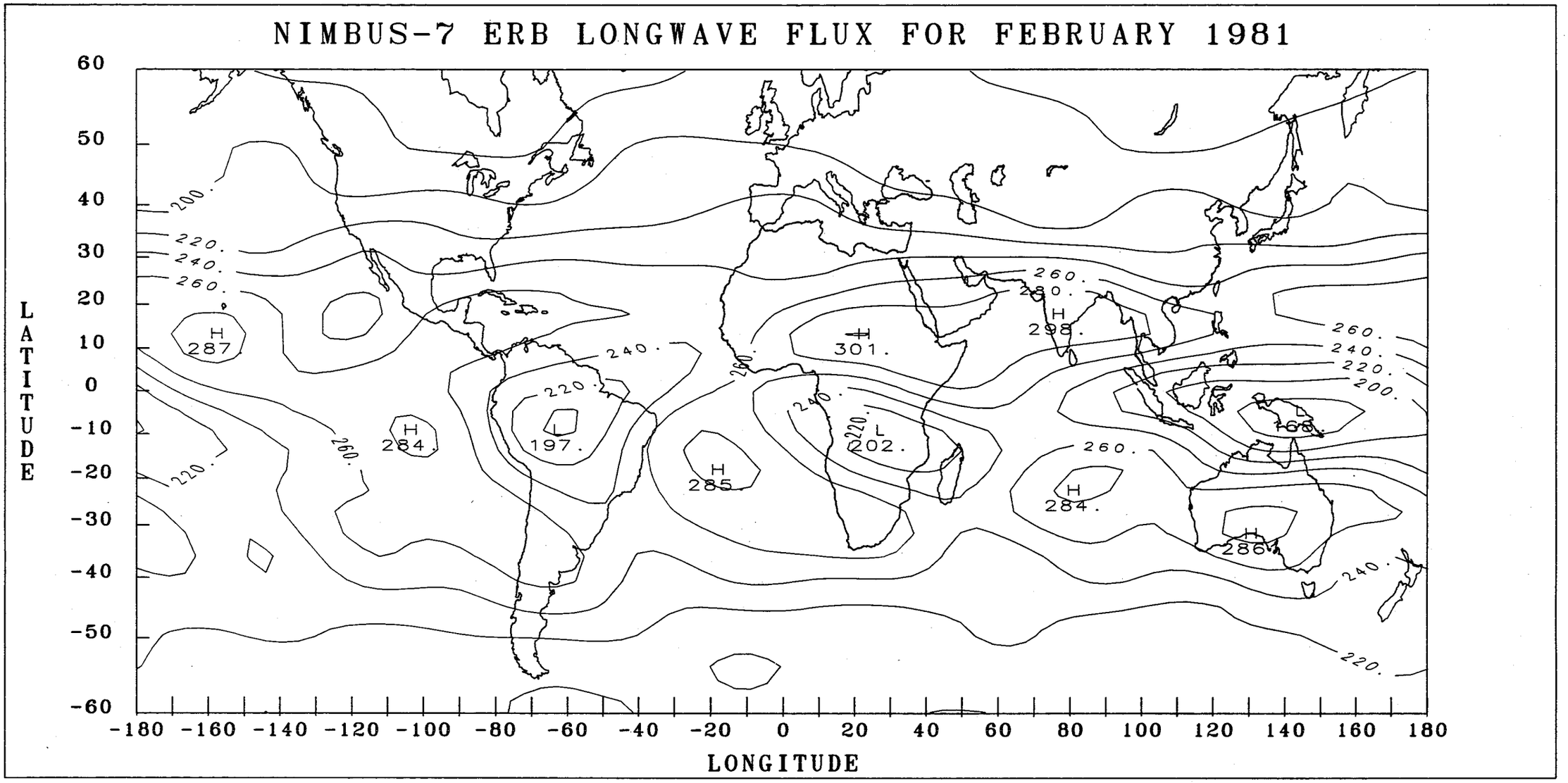
NIMBUS-7 ERB LONGWAVE FLUX FOR FEBRUARY 1981
LATITUDE
LONGITUDE
60
50
40
30
20
10
0
-10
-20
-30
-40
-50
-60
-180 -160 -140 -120 -100 -80 -60 -40 -20 0 20 40 60 80 100 120 140 160 180
200.
220.
240.
260.
280.
H 287
H 284.
L 197.
H 285
L 202.
H 301.
H 298.
H 284.
H 286
L 166.

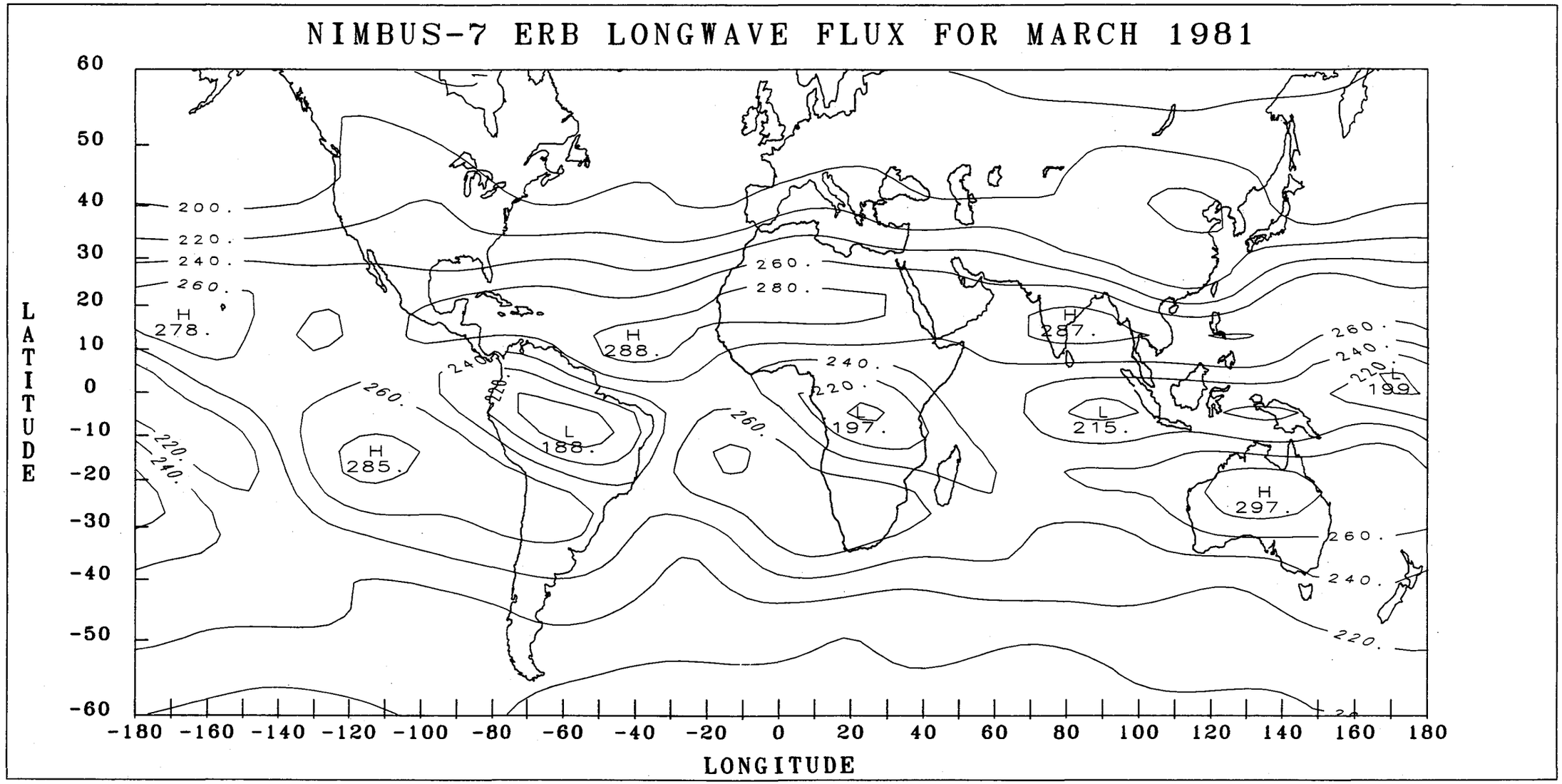
NIMBUS-7 ERB LONGWAVE FLUX FOR MARCH 1981
LATITUDE
LONGITUDE
60
50
40
30
20
10
0
-10
-20
-30
-40
-50
-60
-180 -160 -140 -120 -100 -80 -60 -40 -20 0 20 40 60 80 100 120 140 160 180
200.
220.
240.
260.
280.
H
278.
H
288.
H
287.
H
285.
H
297.
L
188.
L
197.
L
215.
L
199.

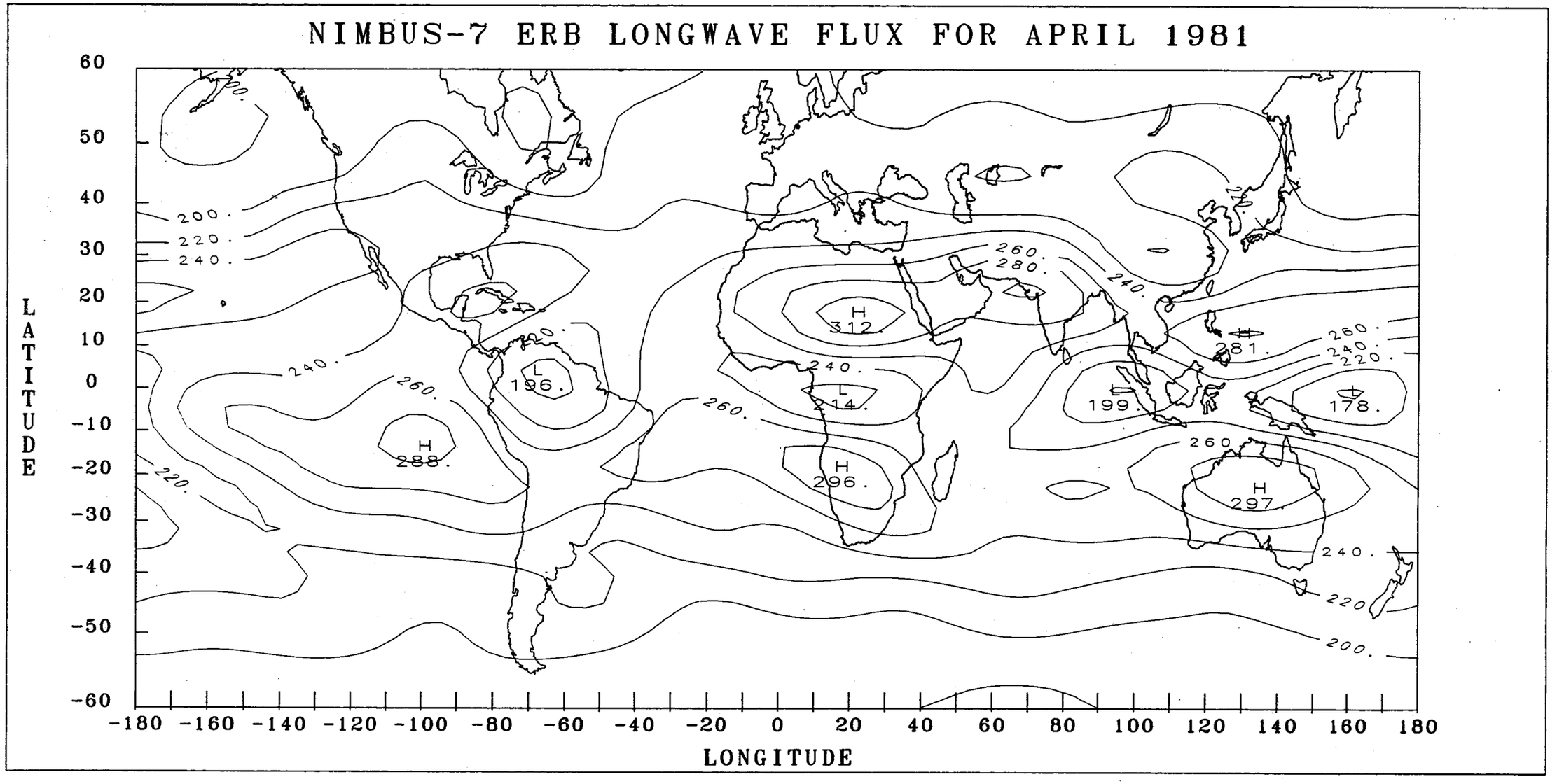
NIMBUS-7 ERB LONGWAVE FLUX FOR APRIL 1981
LATITUDE
LONGITUDE
60
50
40
30
20
10
0
-10
-20
-30
-40
-50
-60
-180 -160 -140 -120 -100 -80 -60 -40 -20 0 20 40 60 80 100 120 140 160 180
200.
220.
240.
260.
280.
H
312.
L
196.
L
214.
H
288.
H
296.
199.
281.
178.
H
297.

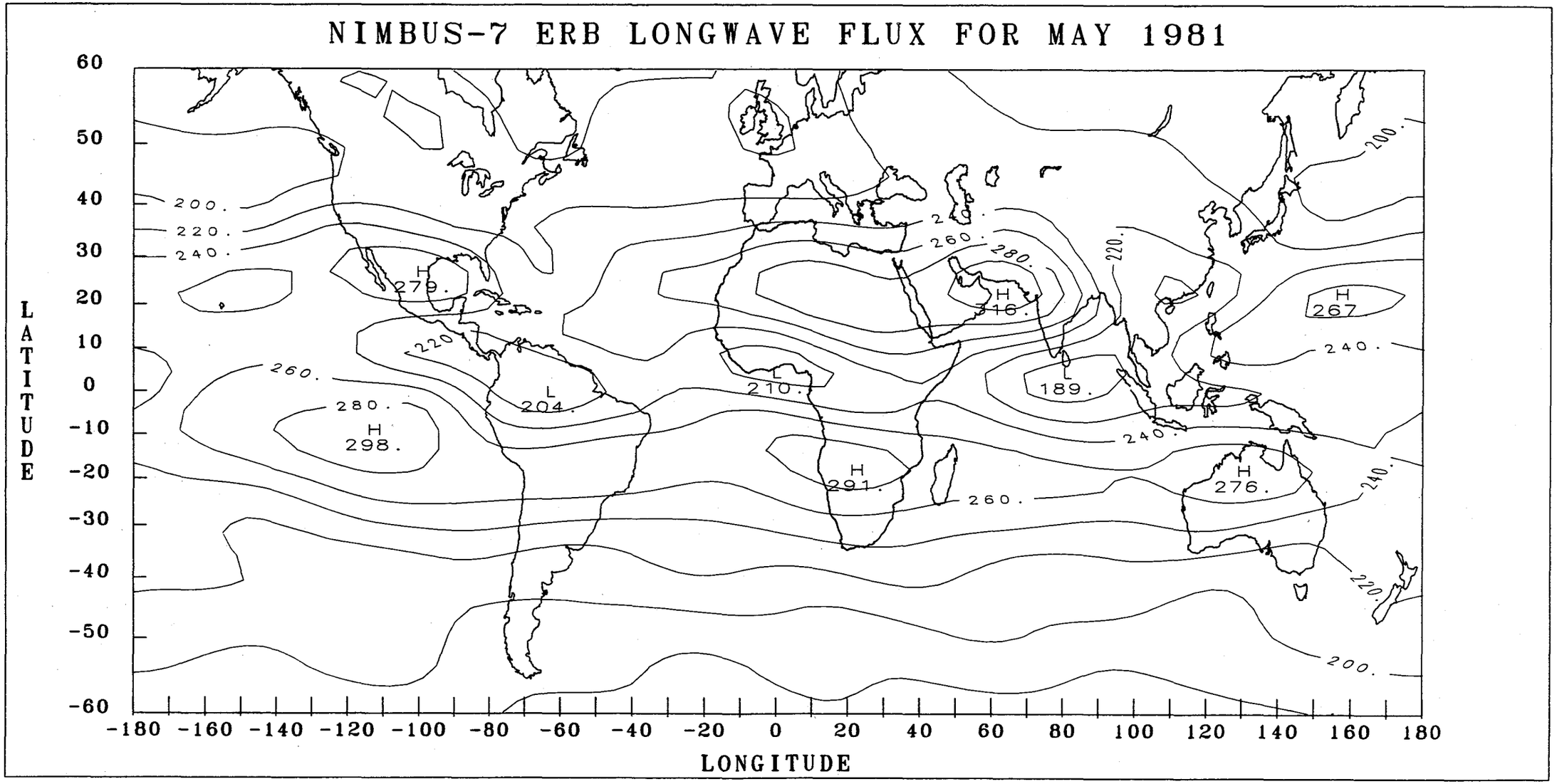
NIMBUS-7 ERB LONGWAVE FLUX FOR MAY 1981
LATITUDE
LONGITUDE
60
50
40
30
20
10
0
-10
-20
-30
-40
-50
-60
-180 -160 -140 -120 -100 -80 -60 -40 -20 0 20 40 60 80 100 120 140 160 180
200.
220.
240.
260.
280.
H
279.
H
298.
L
204.
220
L
210.
H
291.
H
316.
L
189.
H
276.
H
267
240.
260.
220.
200.

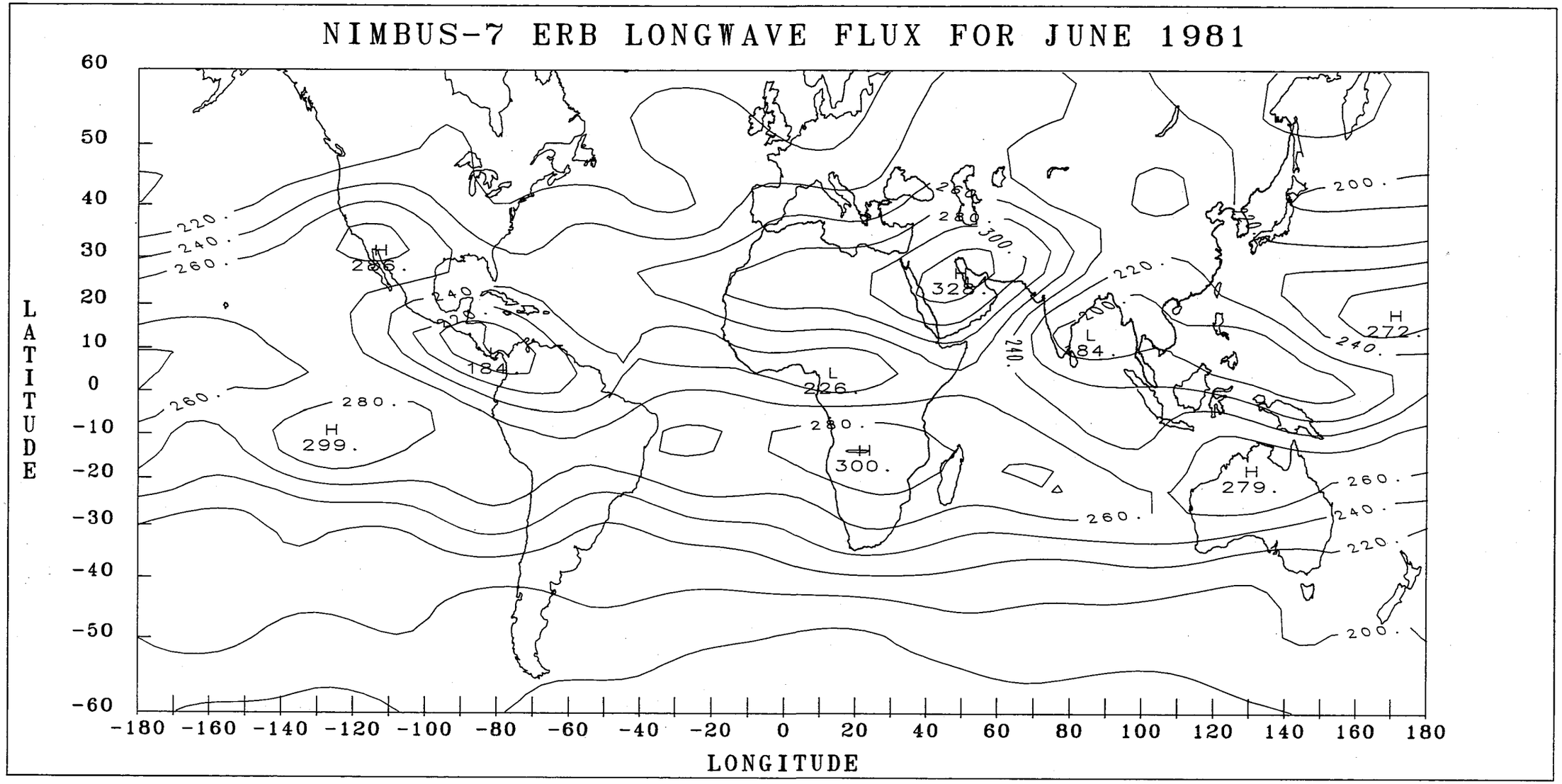
NIMBUS-7 ERB LONGWAVE FLUX FOR JUNE 1981
LATITUDE
LONGITUDE
60
50
40
30
20
10
0
-10
-20
-30
-40
-50
-60
-180 -160 -140 -120 -100 -80 -60 -40 -20 0 20 40 60 80 100 120 140 160 180
220.
240.
260.
280.
300.
200.
H
286.
328.
272.
L
184.
226.
H
299.
H
300.
H
279.

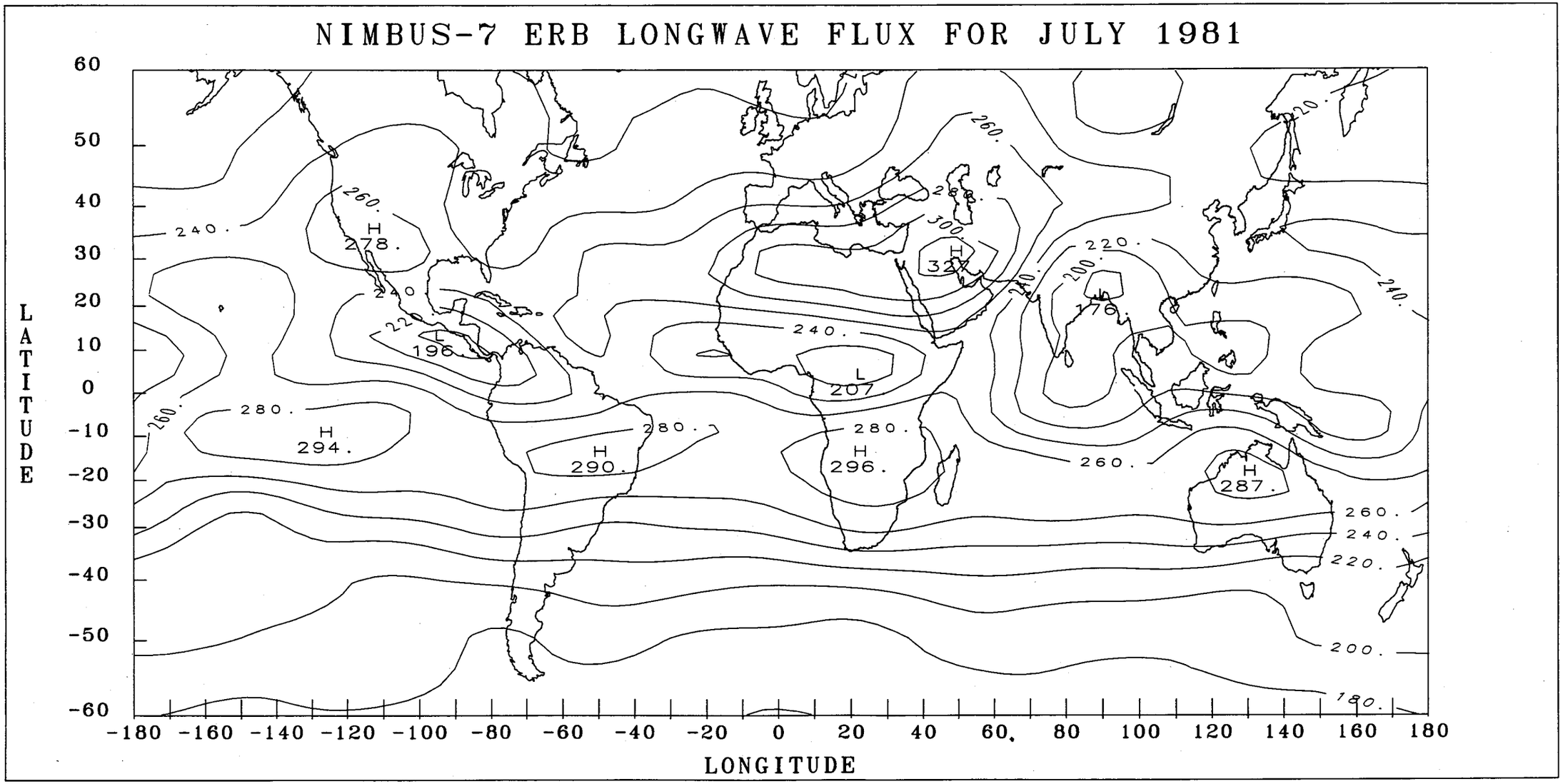
NIMBUS-7 ERB LONGWAVE FLUX FOR JULY 1981
LATITUDE
60
50
40
30
20
10
0
-10
-20
-30
-40
-50
-60
-180 -160 -140 -120 -100 -80 -60 -40 -20 0 20 40 60 80 100 120 140 160 180
LONGITUDE
260.
240.
H
278.
240.
220.
196
240.
L
207
280.
H
294.
280.
H
290.
280.
H
296.
260.
H
287.
260.
240.
220.
200.
190.
300.
H
320
220.
200.
240.
176.

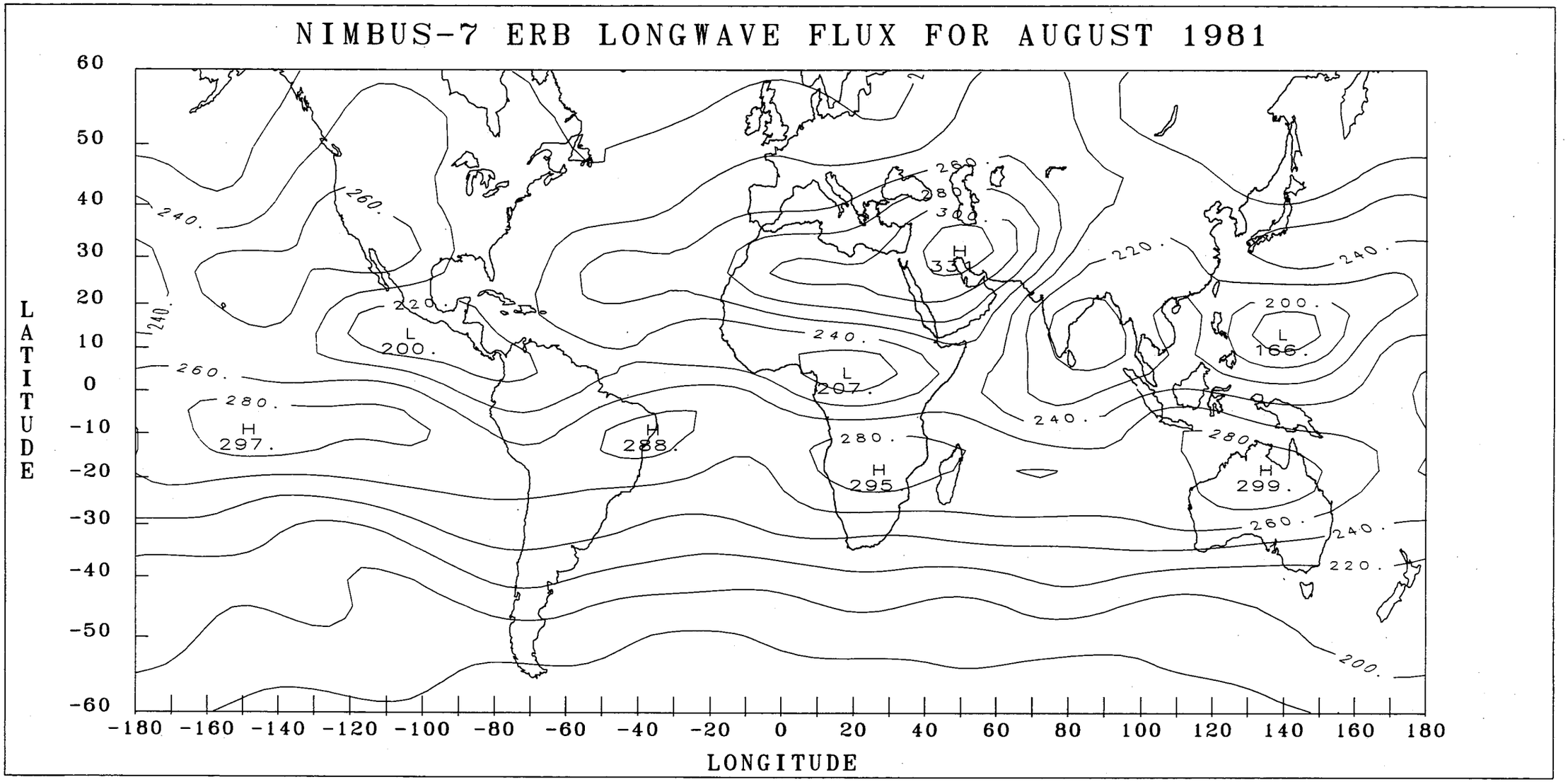
NIMBUS-7 ERB LONGWAVE FLUX FOR AUGUST 1981
LATITUDE
60
50
40
30
20
10
0
-10
-20
-30
-40
-50
-60
-180 -160 -140 -120 -100 -80 -60 -40 -20 0 20 40 60 80 100 120 140 160 180
LONGITUDE
240.
260.
220.
L
200.
280.
H
297.
H
288.
240.
L
207.
280.
H
295
300.
H
33
220.
240.
200.
L
166.
240.
280.
H
299.
260.
240.
220.
200.

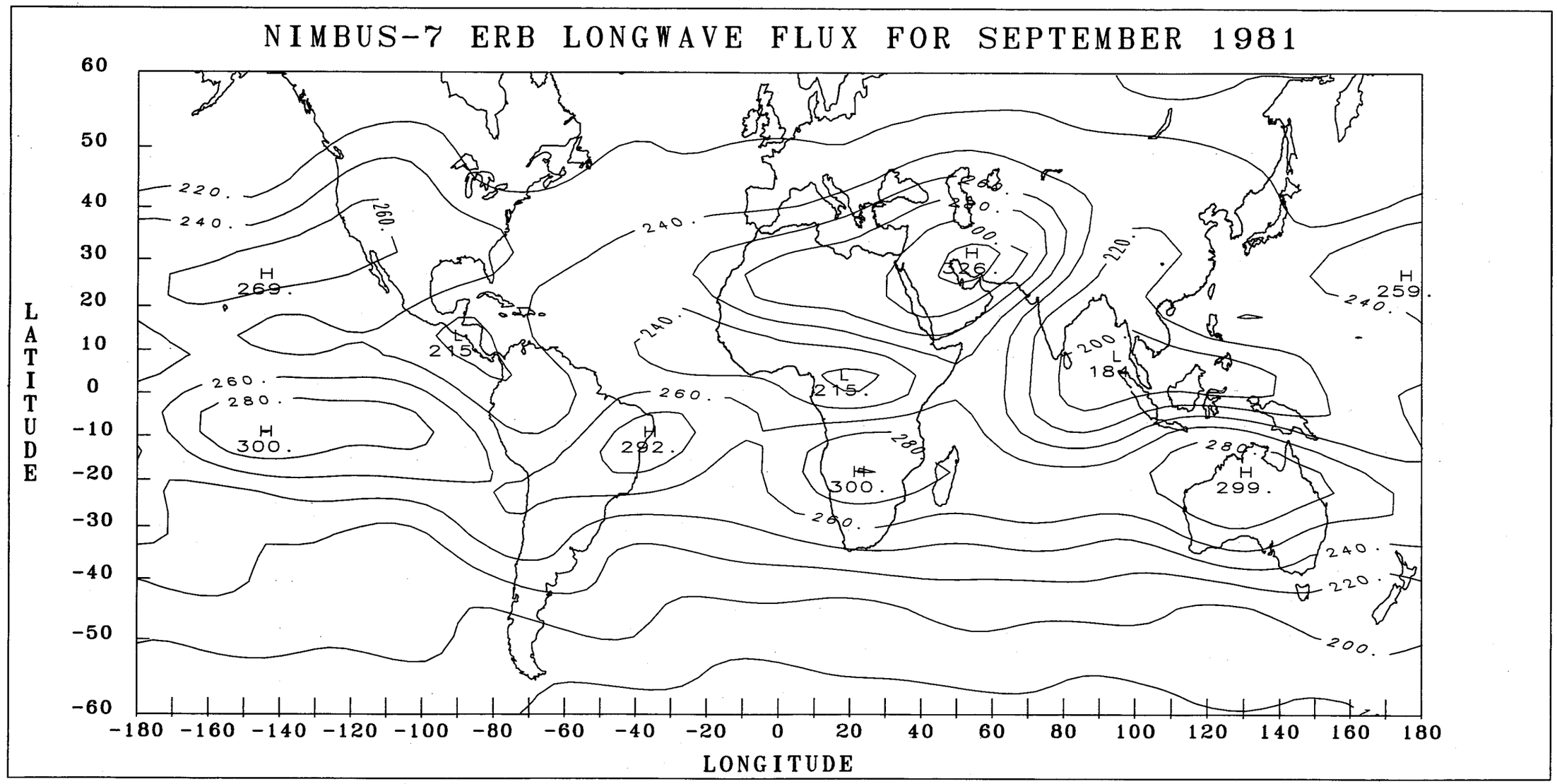
NIMBUS-7 ERB LONGWAVE FLUX FOR SEPTEMBER 1981
LATITUDE
LONGITUDE
60
50
40
30
20
10
0
-10
-20
-30
-40
-50
-60
-180 -160 -140 -120 -100 -80 -60 -40 -20 0 20 40 60 80 100 120 140 160 180
220.
240.
260.
H
269.
L
215.
260.
280.
H
300.
240.
260.
H
292.
L
215.
280.
H
300.
260.
H
H
259.
240.
200.
L
184.
280.
H
299.
240.
220.
200.

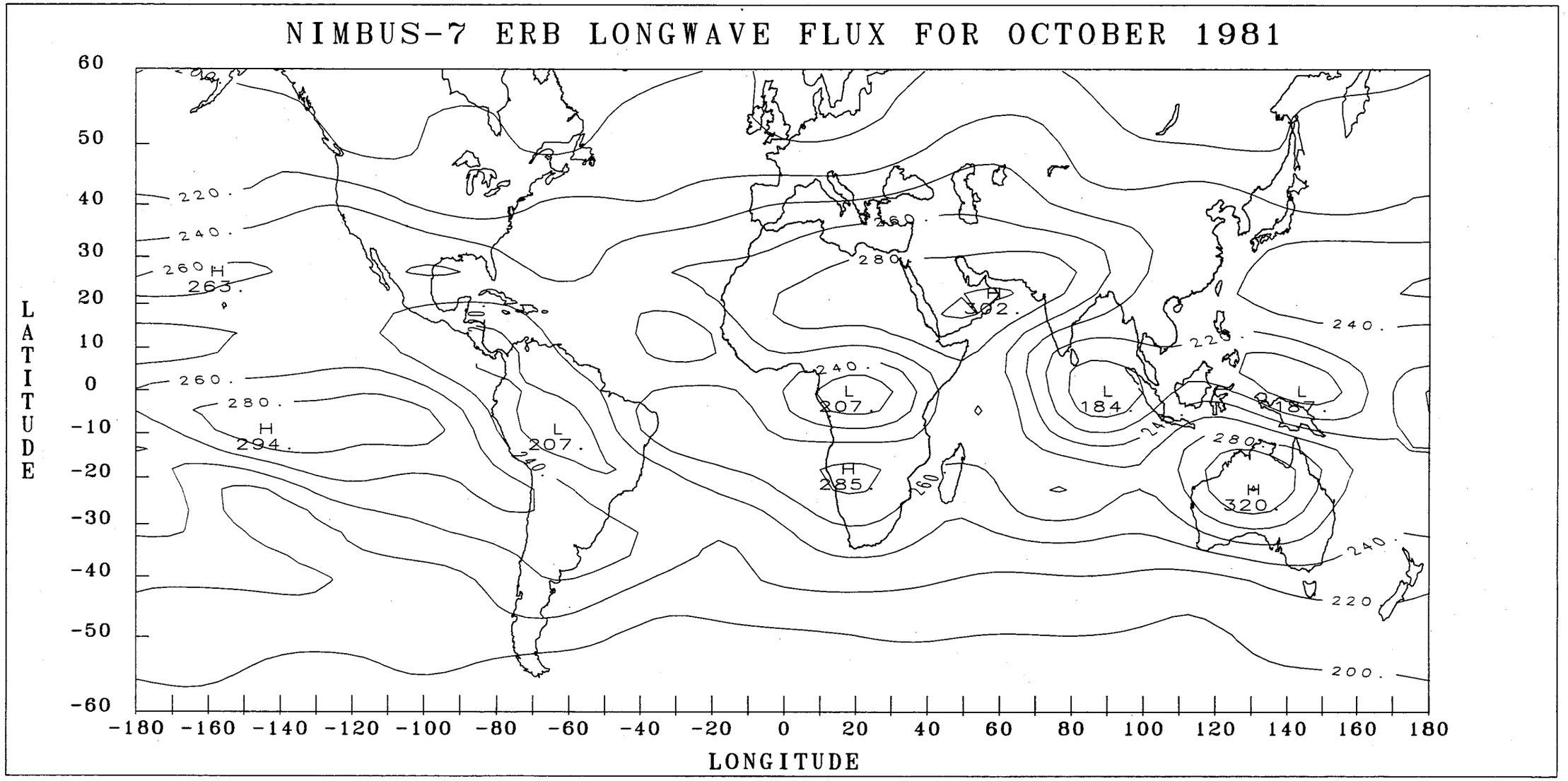
NIMBUS-7 ERB LONGWAVE FLUX FOR OCTOBER 1981
LATITUDE
LONGITUDE
60
50
40
30
20
10
0
-10
-20
-30
-40
-50
-60
-180 -160 -140 -120 -100 -80 -60 -40 -20 0 20 40 60 80 100 120 140 160 180
220.
240.
260
H
263.
260.
280.
H
294.
L
207.
240.
280
H
302.
240.
L
207.
H
285.
260
L
184.
240.
L
218.
280.
H
320
240.
220
200.

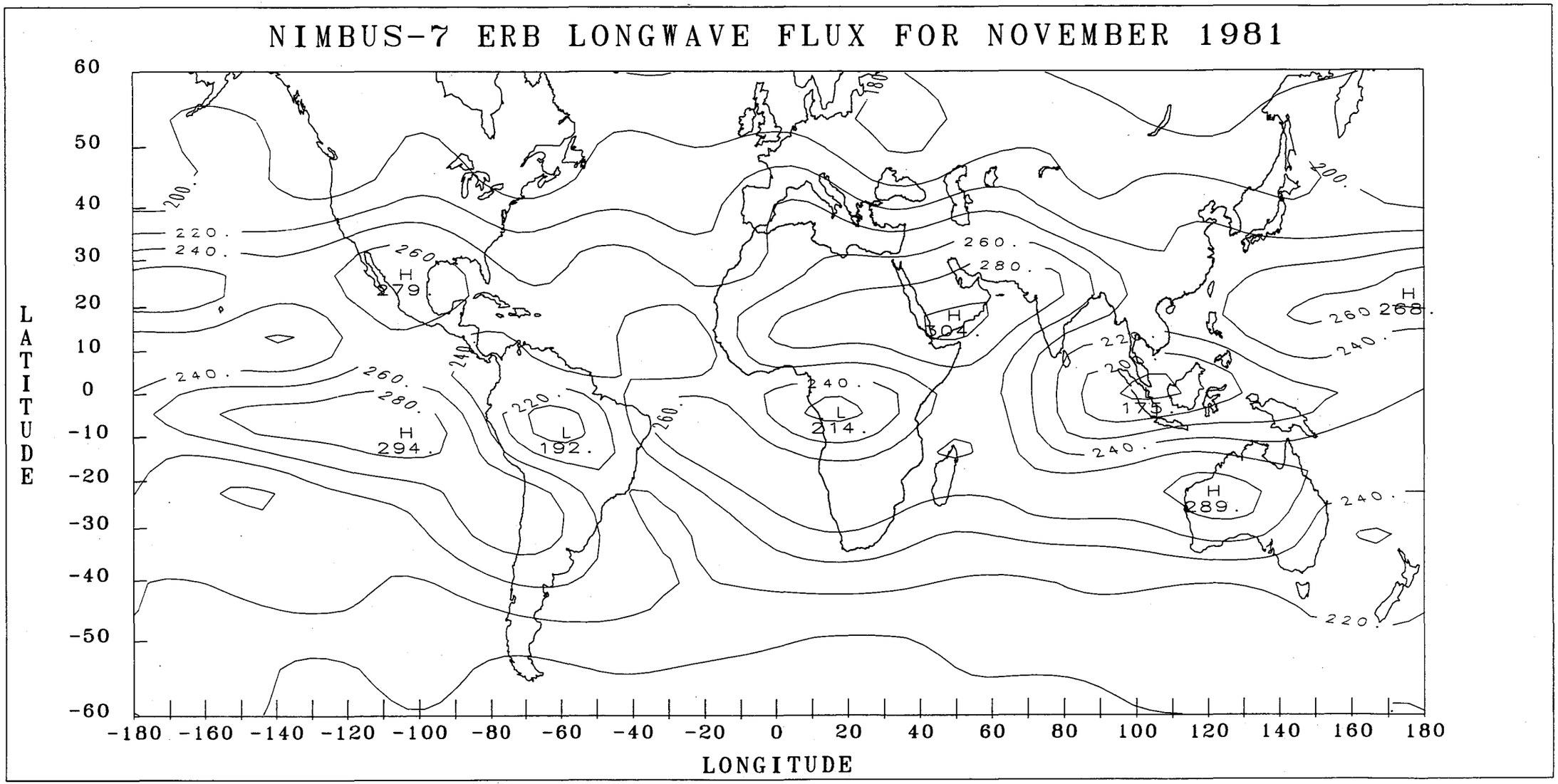
NIMBUS-7 ERB LONGWAVE FLUX FOR NOVEMBER 1981
LATITUDE
LONGITUDE
60
50
40
30
20
10
0
-10
-20
-30
-40
-50
-60
-180 -160 -140 -120 -100 -80 -60 -40 -20 0 20 40 60 80 100 120 140 160 180
200.
220.
240.
260.
280.
H
279.
H
294.
L
192.
L
214.
H
304.
H
289.
175.
H
268.

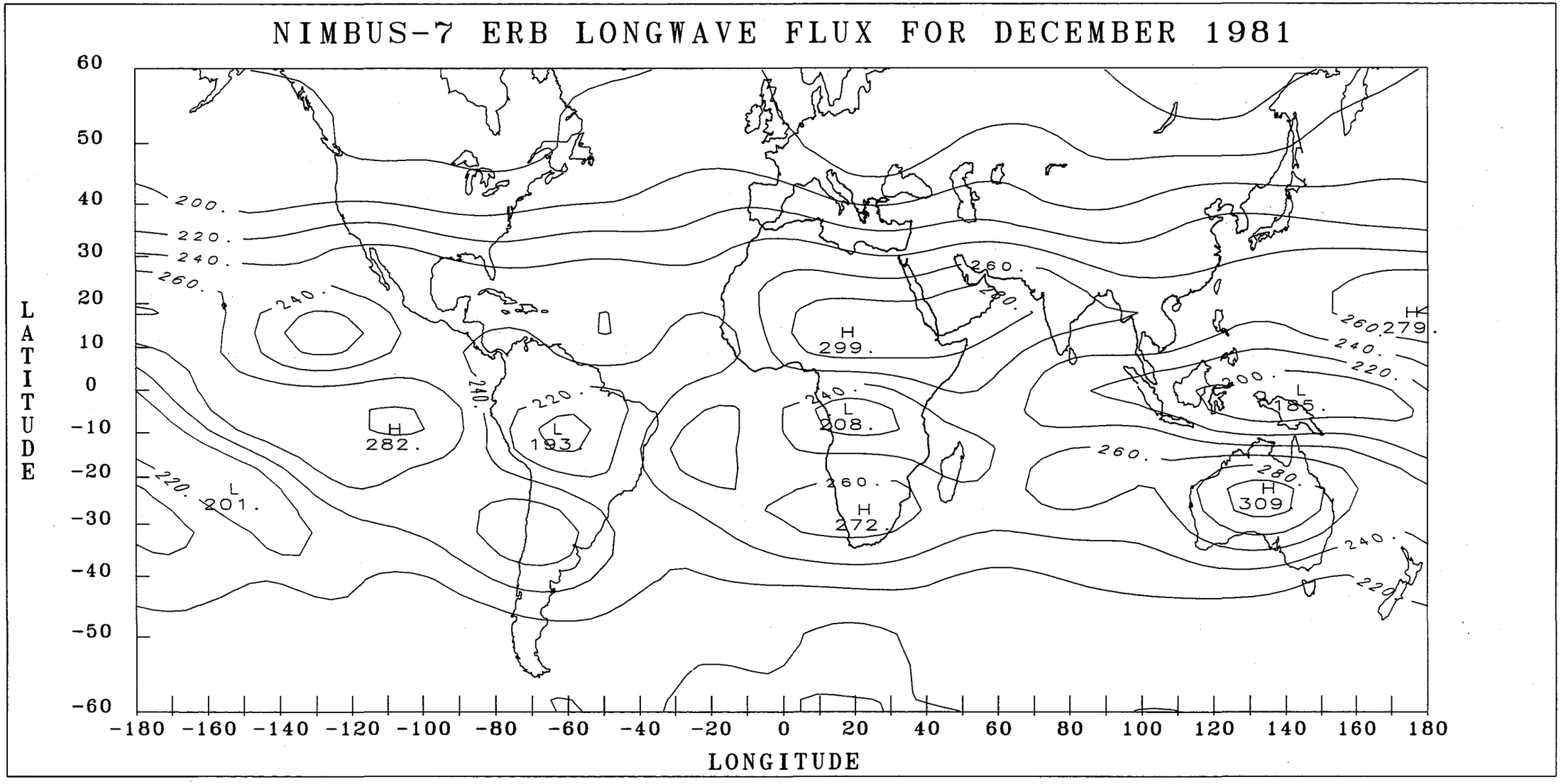
NIMBUS-7 ERB LONGWAVE FLUX FOR DECEMBER 1981
LATITUDE
LONGITUDE
60
50
40
30
20
10
0
-10
-20
-30
-40
-50
-60
-180 -160 -140 -120 -100 -80 -60 -40 -20 0 20 40 60 80 100 120 140 160 180
200.
220.
240.
260.
H
299.
H
282.
L
193.
L
208.
H
272.
L
201.
H
309.
L
185.
H
279.

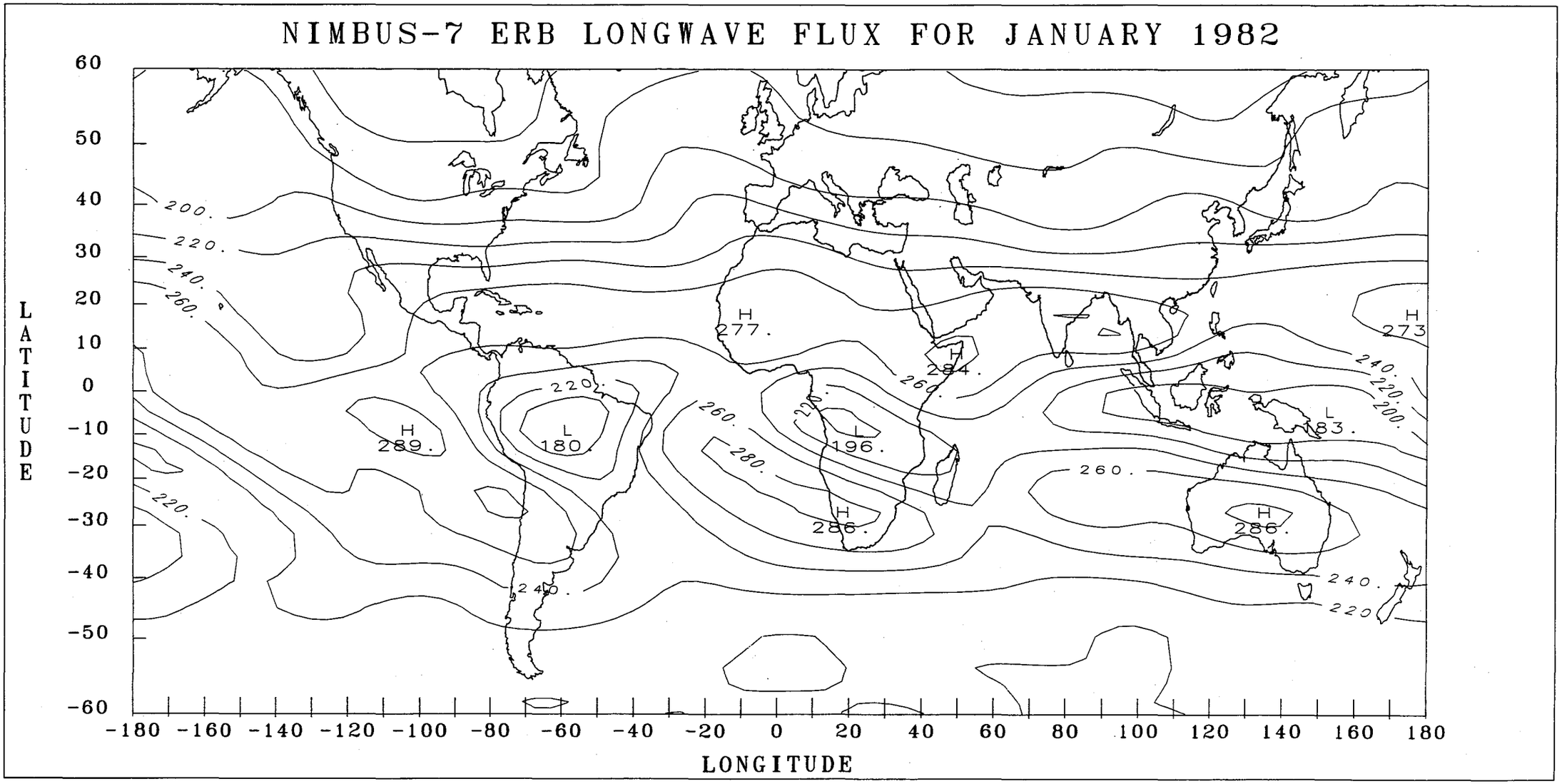
NIMBUS-7 ERB LONGWAVE FLUX FOR JANUARY 1982
LATITUDE
60
50
40
30
20
10
0
-10
-20
-30
-40
-50
-60
-180 -160 -140 -120 -100 -80 -60 -40 -20 0 20 40 60 80 100 120 140 160 180
LONGITUDE
200.
220.
240.
260.
H
277.
H
284.
H
273
240.
220.
200.
220
260.
H
289.
L
180.
260.
220
L
196.
280.
H
286.
260.
L
183.
H
286.
240.
220
240.

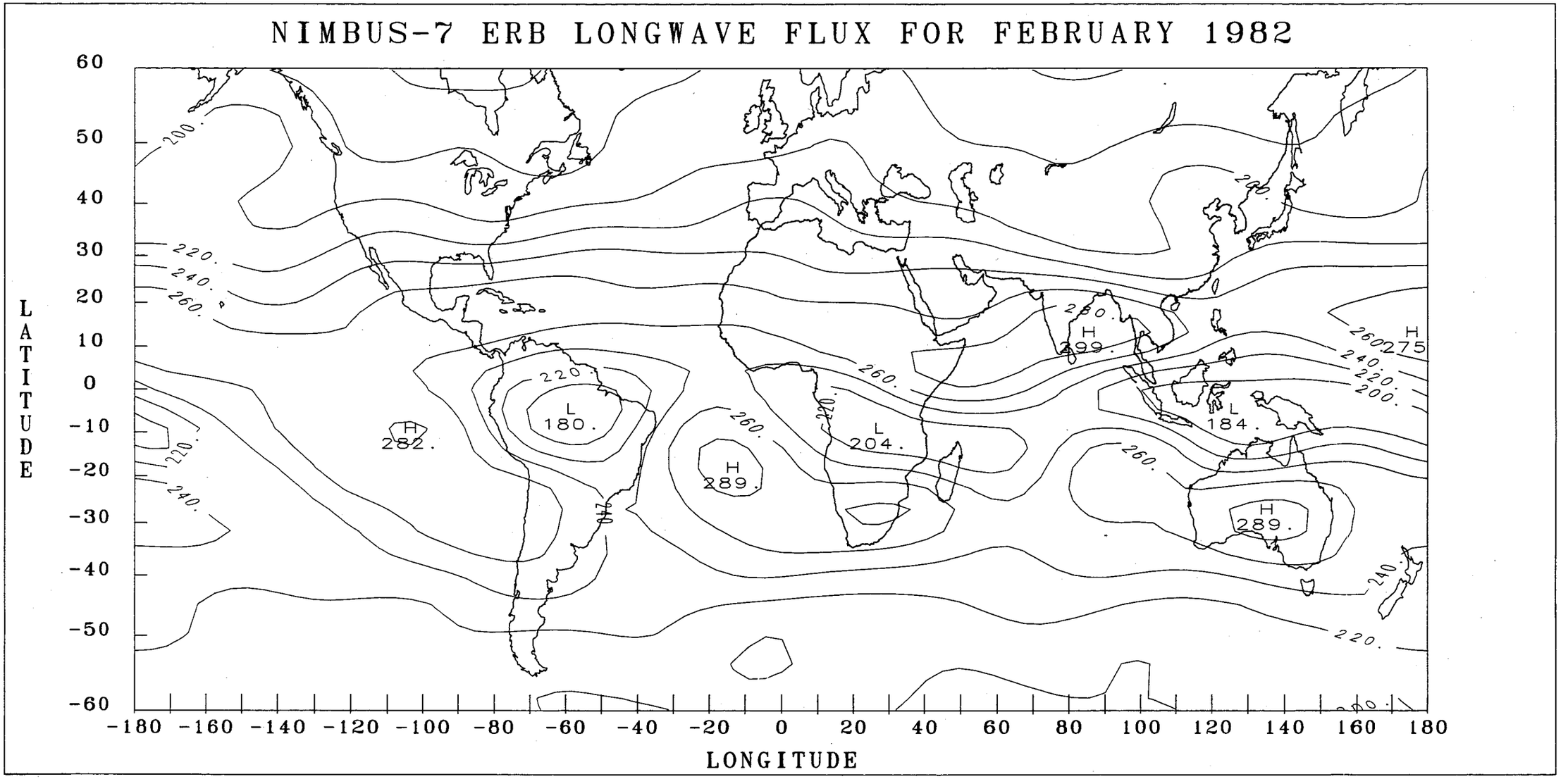
NIMBUS-7 ERB LONGWAVE FLUX FOR FEBRUARY 1982
LATITUDE
60
50
40
30
20
10
0
-10
-20
-30
-40
-50
-60
-180 -160 -140 -120 -100 -80 -60 -40 -20 0 20 40 60 80 100 120 140 160 180
LONGITUDE
200.
220.
240.
260.
H
282.
L
180.
H
289.
L
204.
H
299.
H
275
L
184.
H
289.

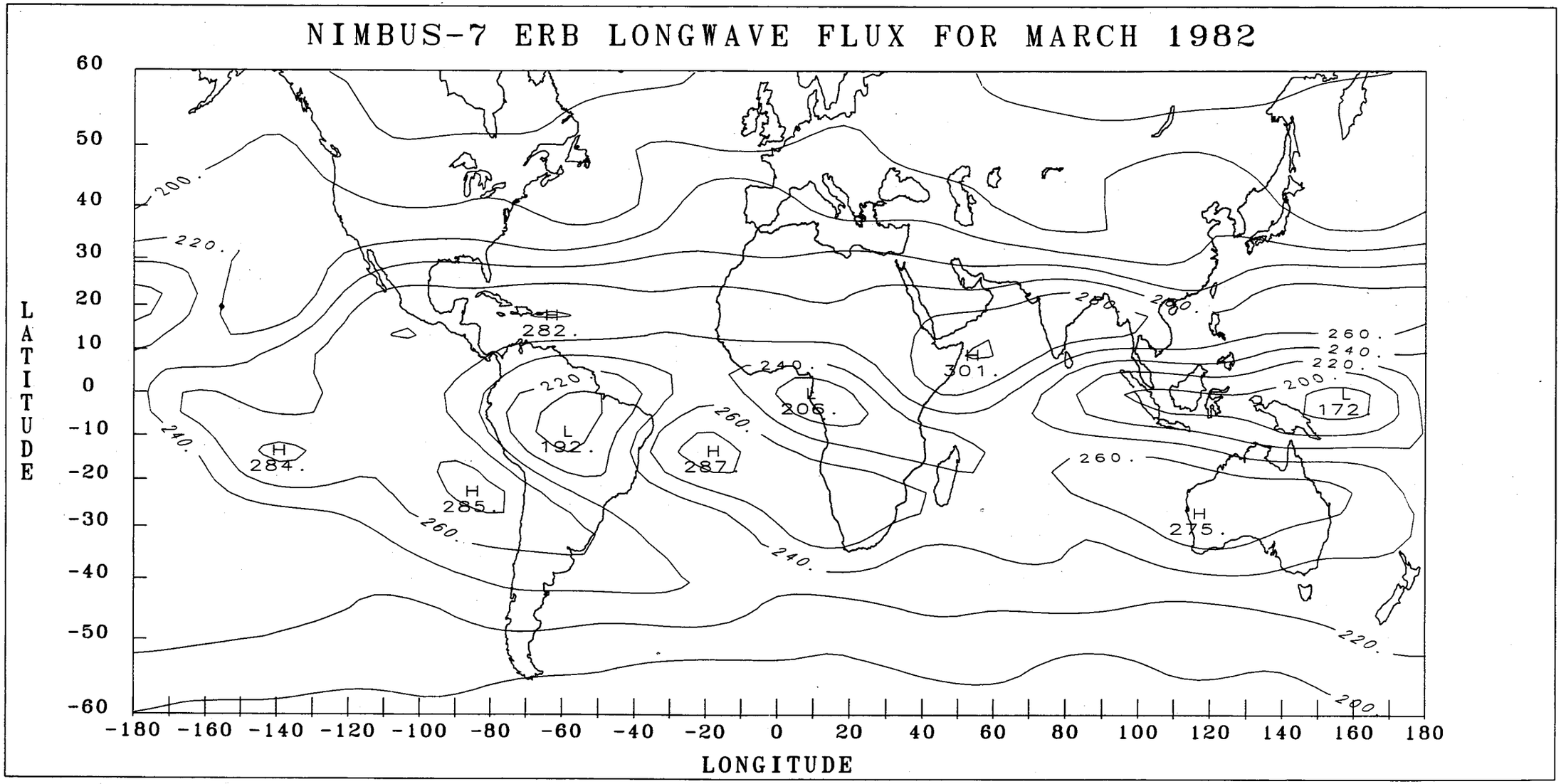
NIMBUS-7 ERB LONGWAVE FLUX FOR MARCH 1982
LATITUDE
60
50
40
30
20
10
0
-10
-20
-30
-40
-50
-60
-180 -160 -140 -120 -100 -80 -60 -40 -20 0 20 40 60 80 100 120 140 160 180
LONGITUDE
200.
220.
240.
260.
280.
H 282.
H 284.
H 285.
L 192.
H 287
L 206.
H 301.
L 172
H 275.

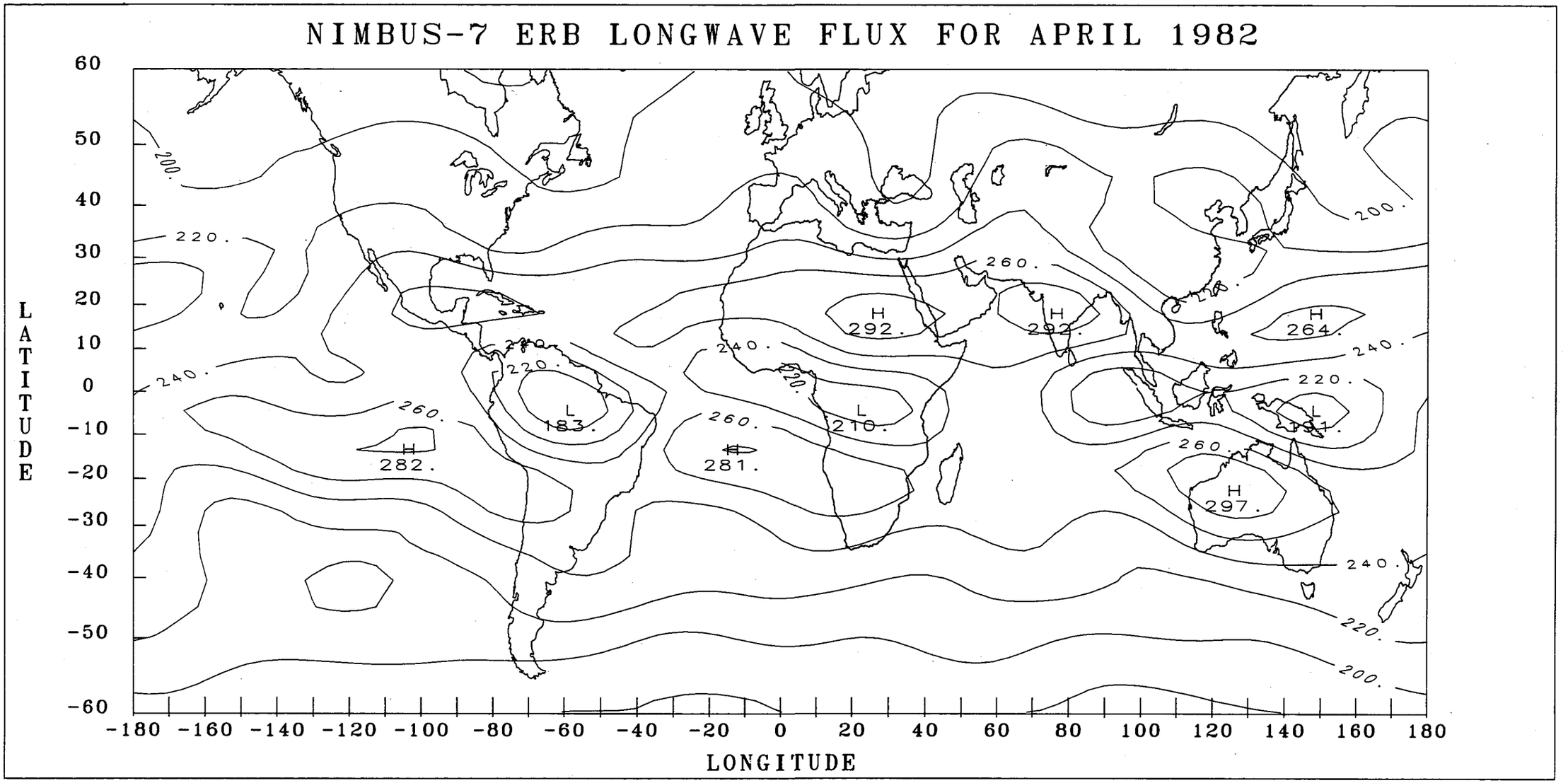
NIMBUS-7 ERB LONGWAVE FLUX FOR APRIL 1982
LATITUDE
LONGITUDE
60
50
40
30
20
10
0
-10
-20
-30
-40
-50
-60
-180 -160 -140 -120 -100 -80 -60 -40 -20 0 20 40 60 80 100 120 140 160 180
200.
220.
240.
260.
H
282.
L
183.
H
281.
L
210.
H
292.
H
292.
H
264.
L
H
297.

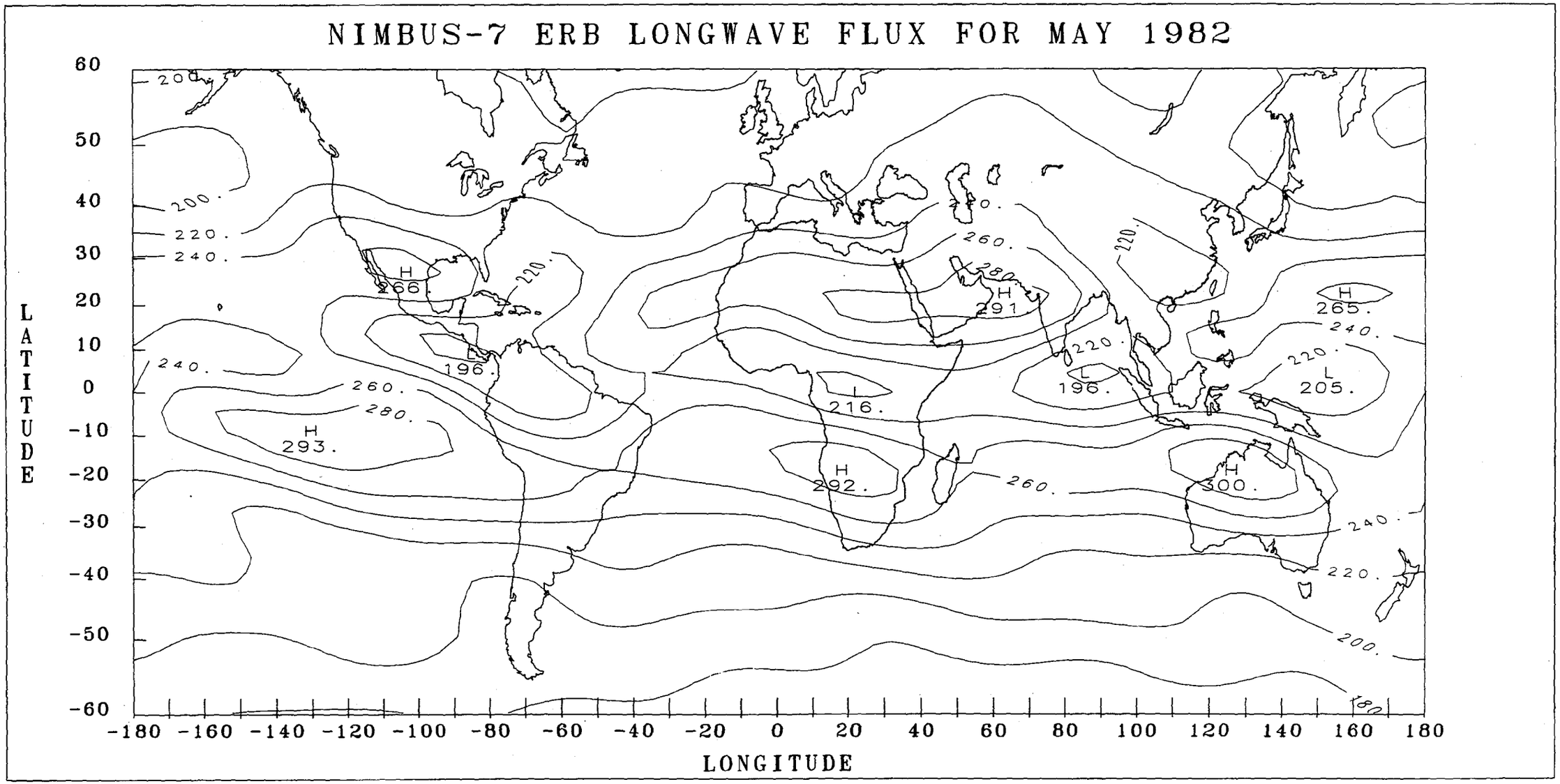
NIMBUS-7 ERB LONGWAVE FLUX FOR MAY 1982
LATITUDE
LONGITUDE
60
50
40
30
20
10
0
-10
-20
-30
-40
-50
-60
-180 -160 -140 -120 -100 -80 -60 -40 -20 0 20 40 60 80 100 120 140 160 180
200.
220.
240.
260.
280.
H 266.
H 291.
H 265.
L 196.
L 216.
L 196.
L 205.
H 293.
H 292.
H 300.

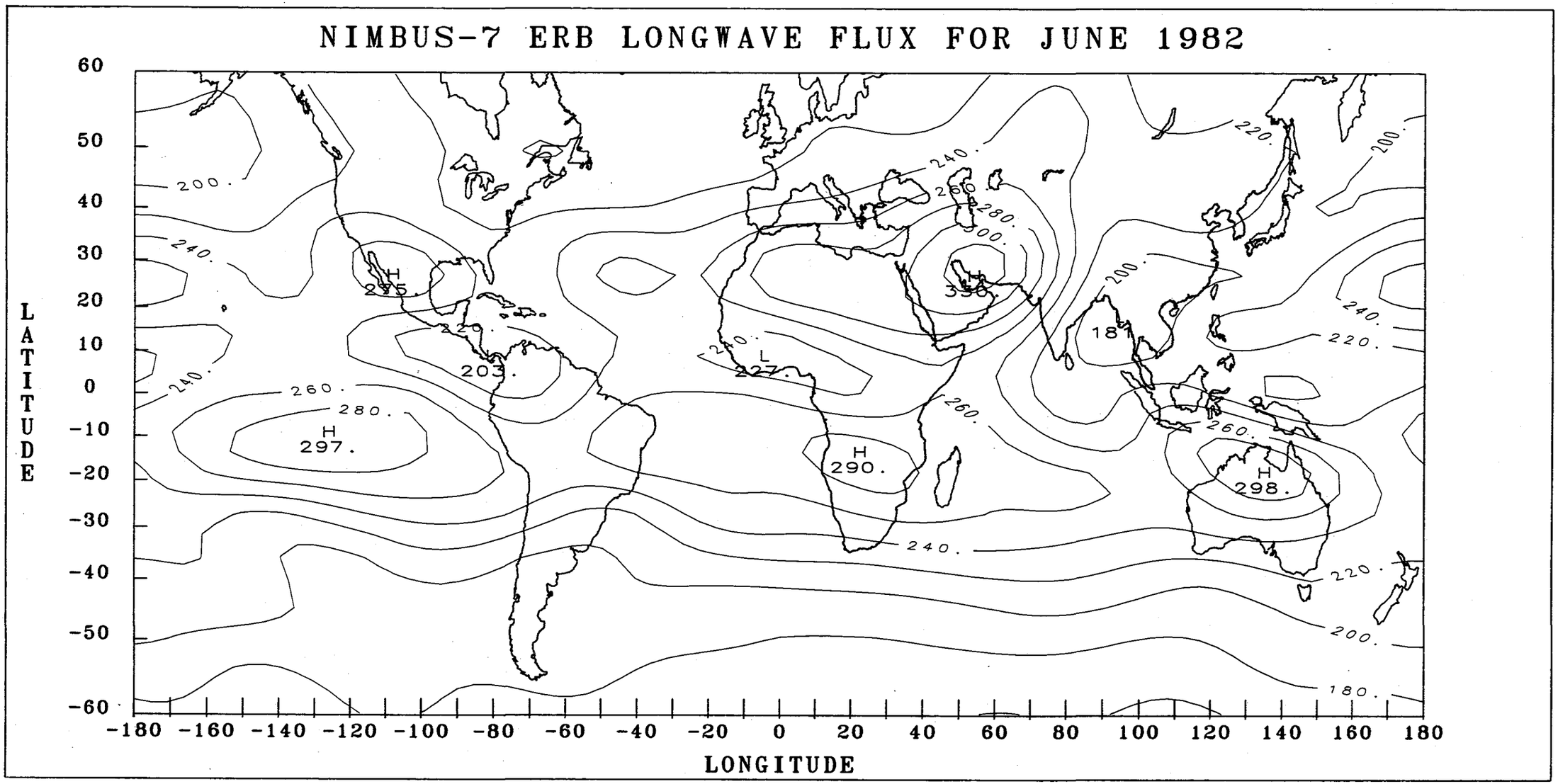
NIMBUS-7 ERB LONGWAVE FLUX FOR JUNE 1982
LATITUDE
LONGITUDE
60
50
40
30
20
10
0
-10
-20
-30
-40
-50
-60
-180 -160 -140 -120 -100 -80 -60 -40 -20 0 20 40 60 80 100 120 140 160 180
200.
240.
260.
280.
300.
220.
180.
H
297.
H
290.
H
298.
H
356.
L
227.
203.
18

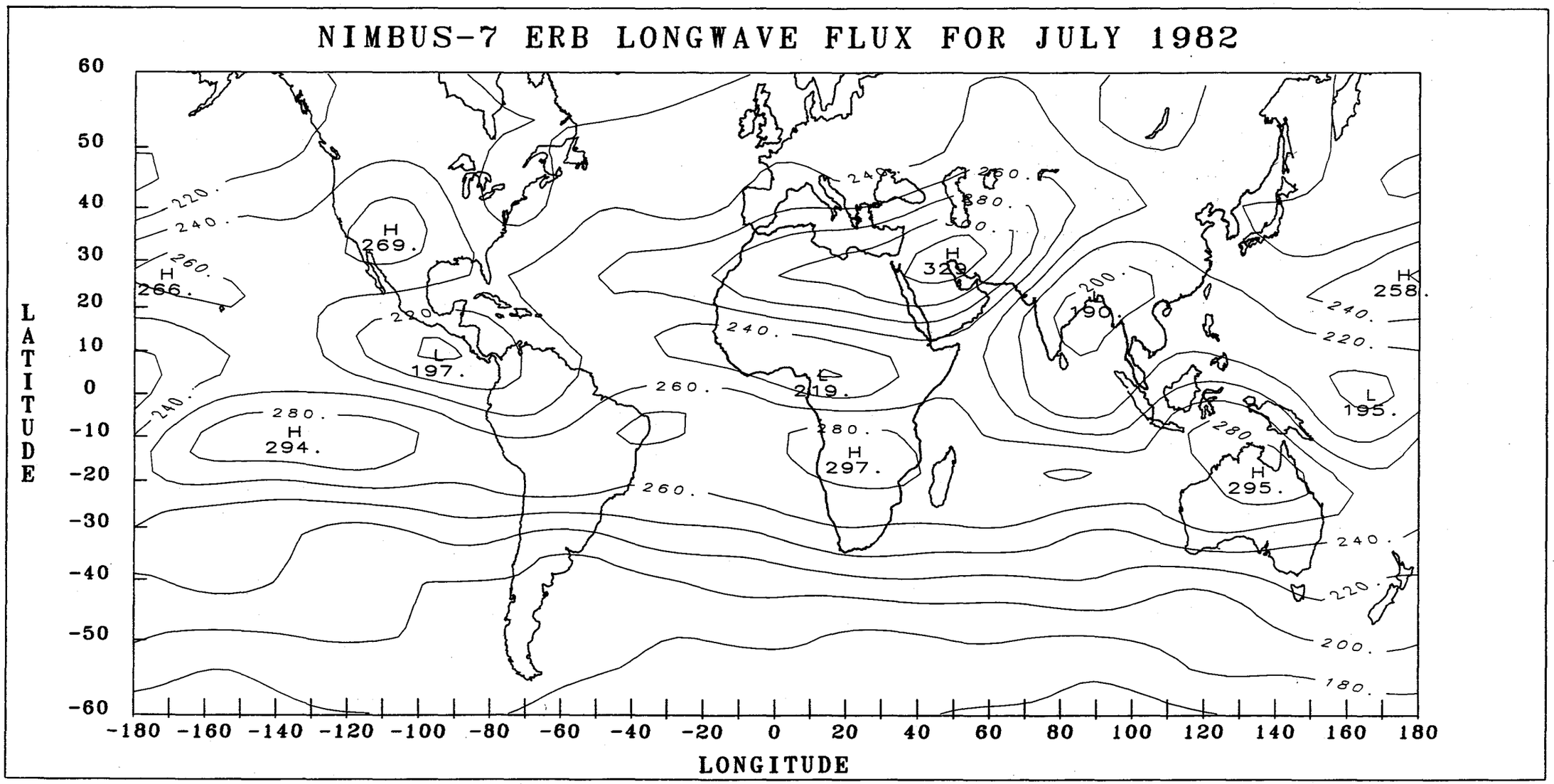
NIMBUS-7 ERB LONGWAVE FLUX FOR JULY 1982
LATITUDE
LONGITUDE
60
50
40
30
20
10
0
-10
-20
-30
-40
-50
-60
-180 -160 -140 -120 -100 -80 -60 -40 -20 0 20 40 60 80 100 120 140 160 180
H 269.
H 266.
H 329.
H 258.
L 197.
L 219.
L 195.
H 294.
H 297.
H 295.
220.
240.
260.
280.
200.
180.

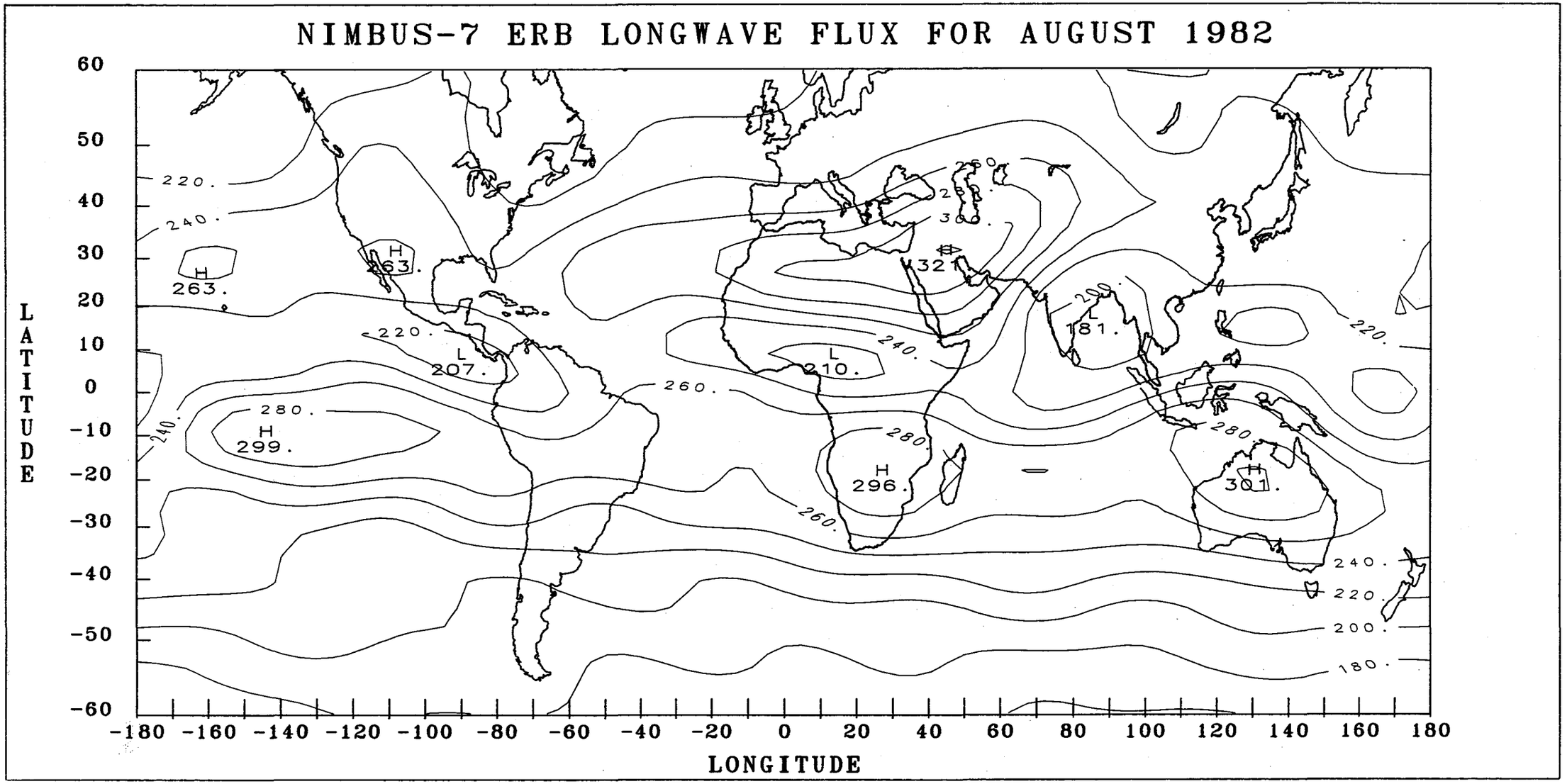
NIMBUS-7 ERB LONGWAVE FLUX FOR AUGUST 1982
LATITUDE
LONGITUDE
60
50
40
30
20
10
0
-10
-20
-30
-40
-50
-60
-180 -160 -140 -120 -100 -80 -60 -40 -20 0 20 40 60 80 100 120 140 160 180
220.
240.
260.
280.
300.
320
200.
180.
H
263.
H
263.
L
207.
H
299.
L
210.
H
296.
L
181.
H
301.

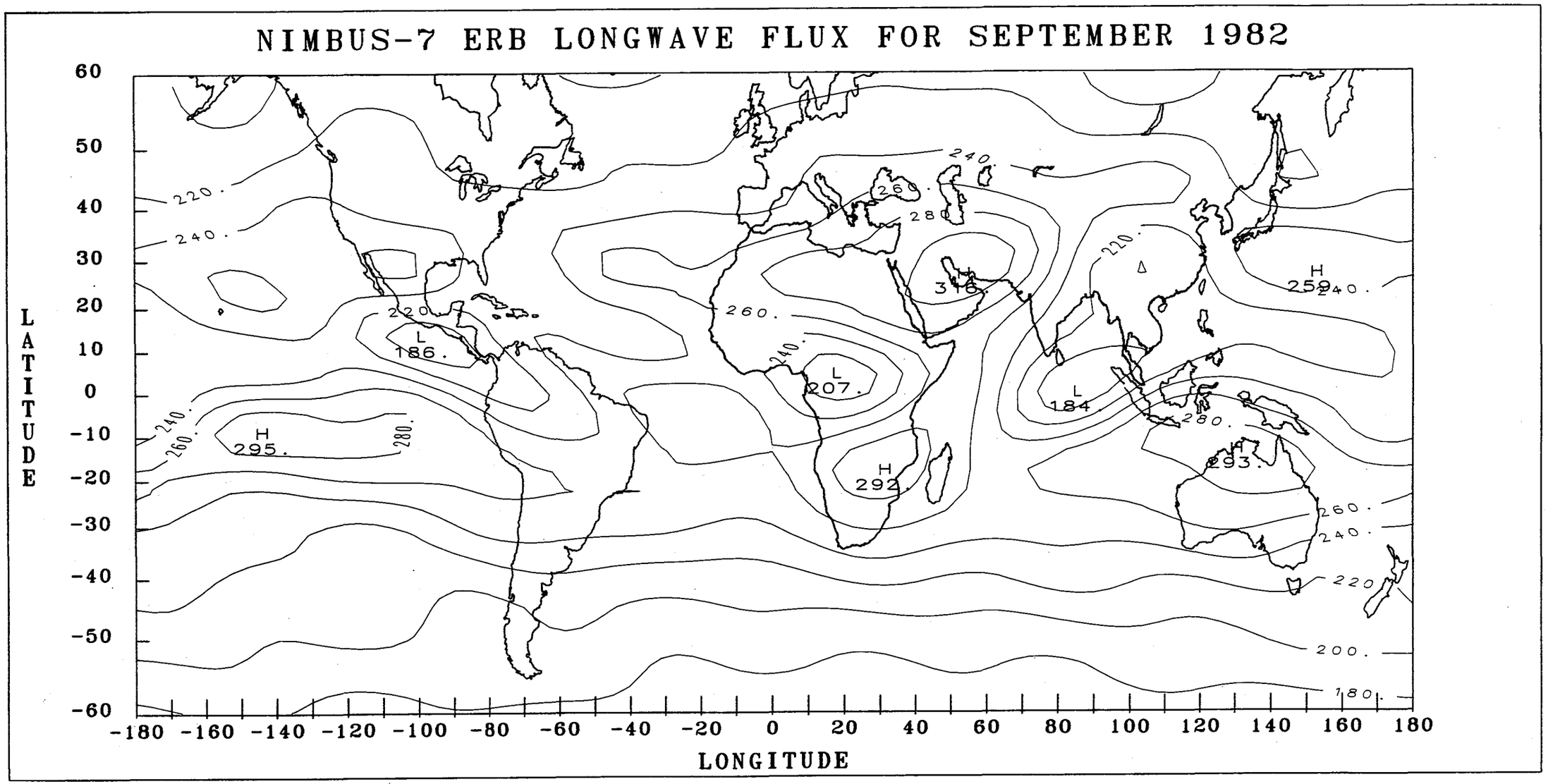
NIMBUS-7 ERB LONGWAVE FLUX FOR SEPTEMBER 1982
LATITUDE
LONGITUDE
60
50
40
30
20
10
0
-10
-20
-30
-40
-50
-60
-180 -160 -140 -120 -100 -80 -60 -40 -20 0 20 40 60 80 100 120 140 160 180
220.
240.
260.
280.
H
295.
L
186.
L
207.
H
292.
316.
H
259.
L
184.
293.
200.
180.

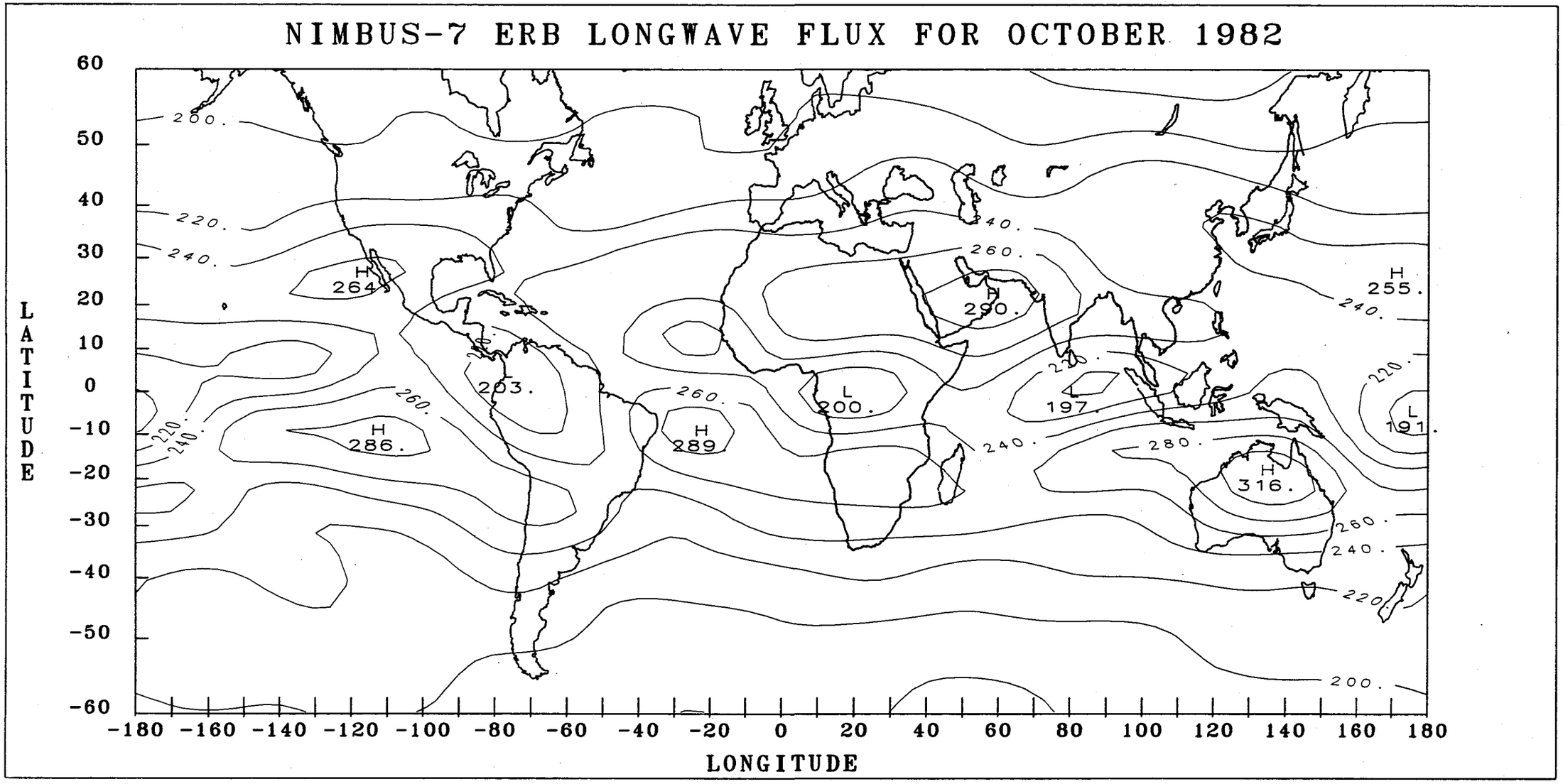
NIMBUS-7 ERB LONGWAVE FLUX FOR OCTOBER 1982
LATITUDE
LONGITUDE
60
50
40
30
20
10
0
-10
-20
-30
-40
-50
-60
-180 -160 -140 -120 -100 -80 -60 -40 -20 0 20 40 60 80 100 120 140 160 180
200.
220.
240.
260.
280.
H 264
H 286.
H 289
H 290.
H 316.
H 255.
L 200.
L 191.
203.
197.

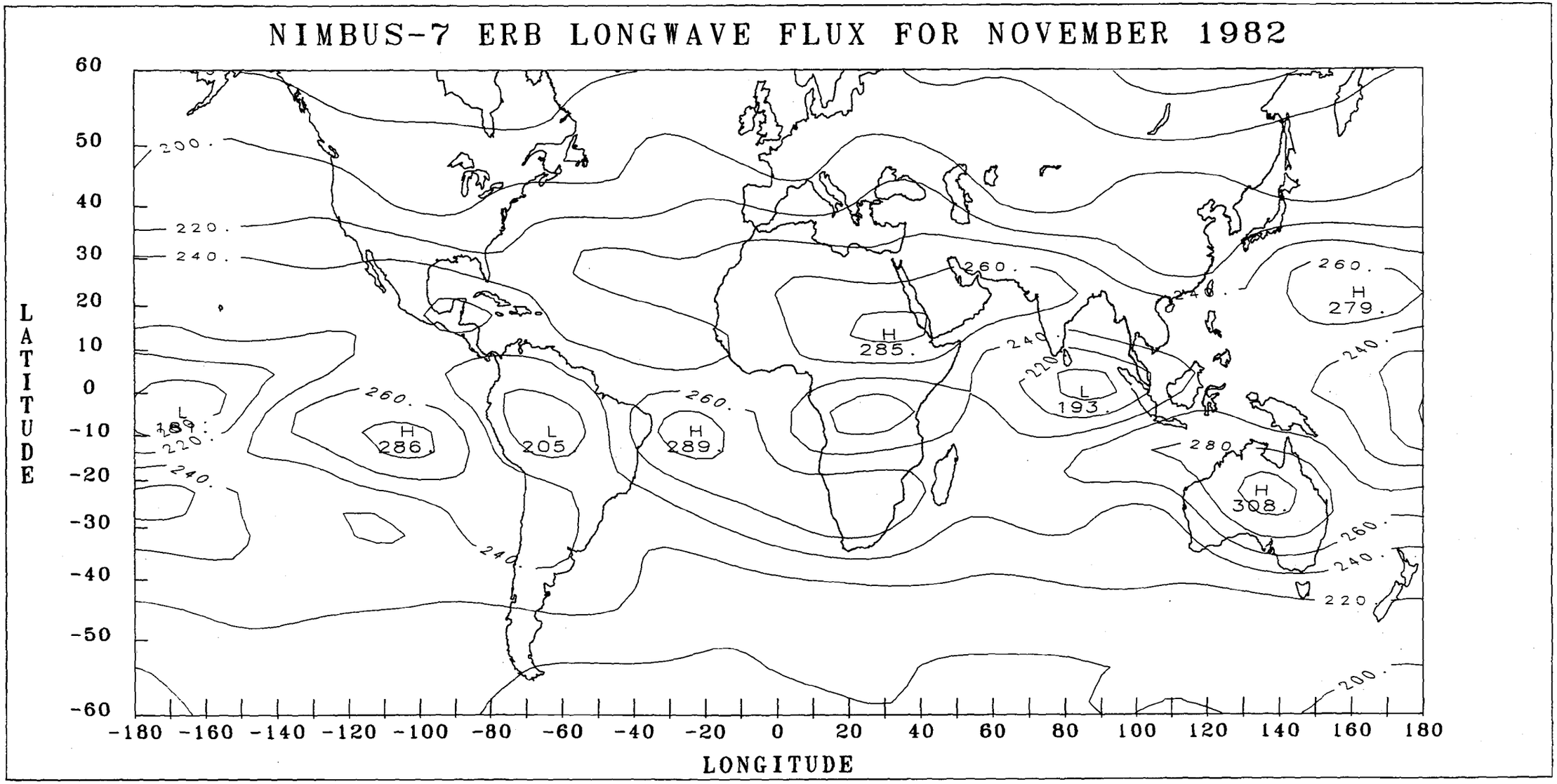
NIMBUS-7 ERB LONGWAVE FLUX FOR NOVEMBER 1982
LATITUDE
LONGITUDE
60
50
40
30
20
10
0
-10
-20
-30
-40
-50
-60
-180 -160 -140 -120 -100 -80 -60 -40 -20 0 20 40 60 80 100 120 140 160 180
200.
220.
240.
260.
280
H 286.
L 205
H 289.
H 285.
L 193.
H 279.
H 308.

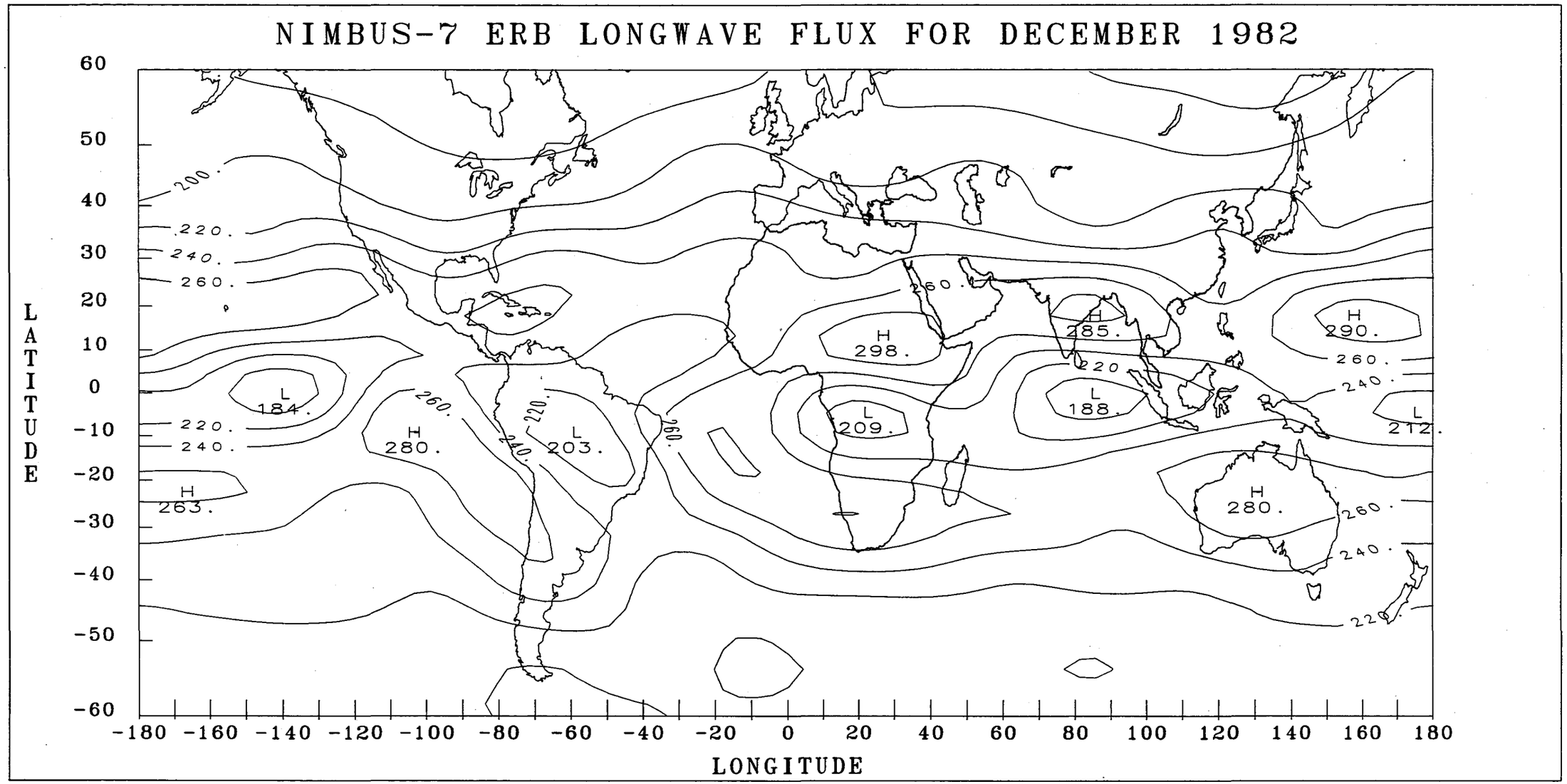
NIMBUS-7 ERB LONGWAVE FLUX FOR DECEMBER 1982
LATITUDE
LONGITUDE
60
50
40
30
20
10
0
-10
-20
-30
-40
-50
-60
-180 -160 -140 -120 -100 -80 -60 -40 -20 0 20 40 60 80 100 120 140 160 180
200.
220.
240.
260.
H 263.
L 184.
H 280.
L 203.
H 298.
L 209.
H 285.
L 188.
H 290.
L 212.
H 280.

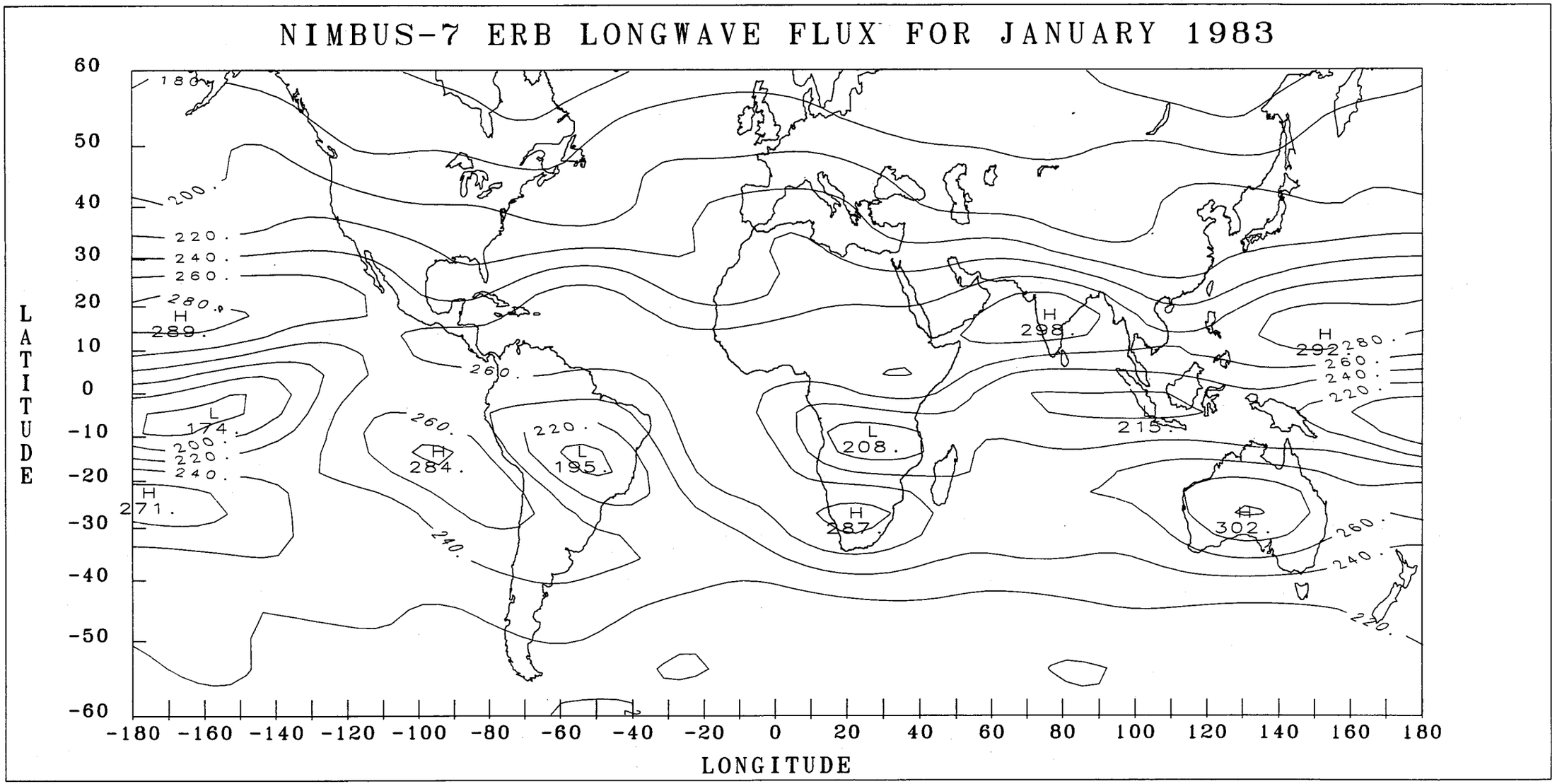
NIMBUS-7 ERB LONGWAVE FLUX FOR JANUARY 1983
LATITUDE
LONGITUDE
60
50
40
30
20
10
0
-10
-20
-30
-40
-50
-60
-180 -160 -140 -120 -100 -80 -60 -40 -20 0 20 40 60 80 100 120 140 160 180
180
200.
220.
240.
260.
280.
H
289.
L
174.
200.
220.
240.
H
271.
260.
260.
H
284.
220.
L
195.
240.
L
208.
H
298.
H
287.
215.
H
292.
280.
260.
240.
220.
H
302.
260.
240.
220.

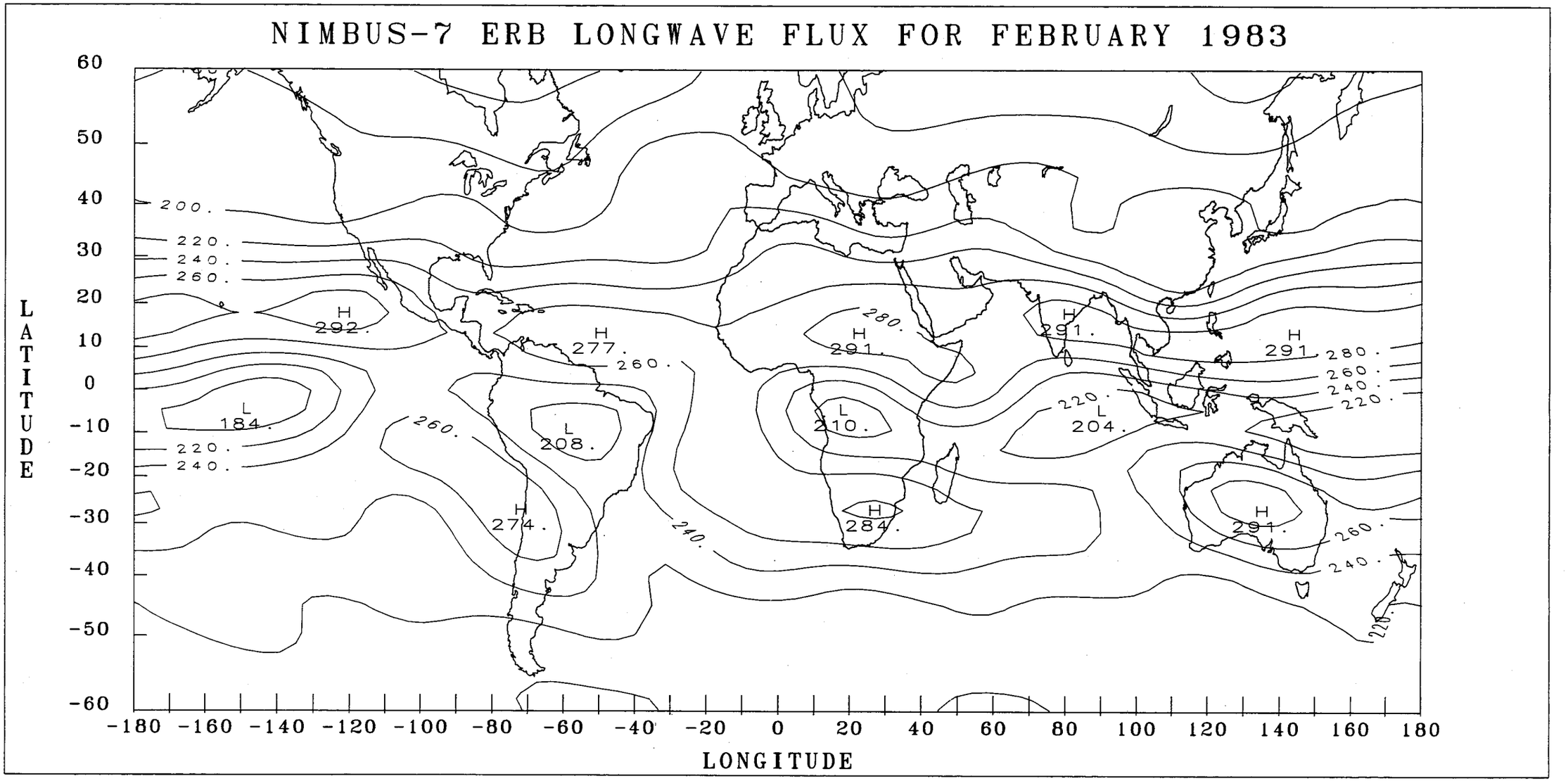
NIMBUS-7 ERB LONGWAVE FLUX FOR FEBRUARY 1983
LATITUDE
LONGITUDE
60
50
40
30
20
10
0
-10
-20
-30
-40
-50
-60
-180 -160 -140 -120 -100 -80 -60 -40 -20 0 20 40 60 80 100 120 140 160 180
200.
220.
240.
260.
280.
H 292.
H 277.
H 291.
H 291.
H 291.
L 184.
L 208.
L 210.
L 204.
H 274.
H 284.
H 291.

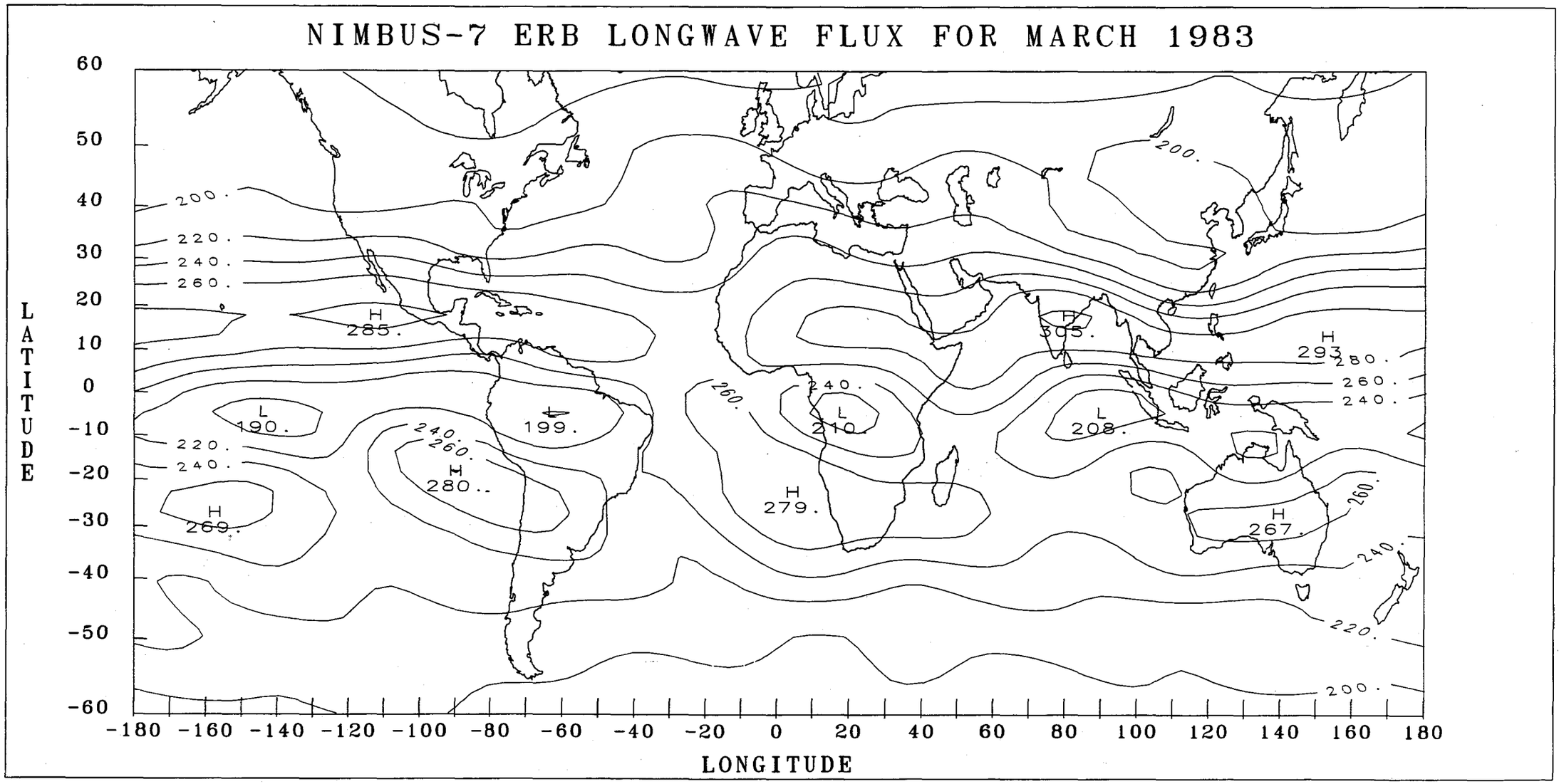
NIMBUS-7 ERB LONGWAVE FLUX FOR MARCH 1983
LATITUDE
LONGITUDE
60
50
40
30
20
10
0
-10
-20
-30
-40
-50
-60
-180 -160 -140 -120 -100 -80 -60 -40 -20 0 20 40 60 80 100 120 140 160 180
200.
220.
240.
260.
280.
H 285.
H 305.
H 293
L 190.
199.
L 210
L 208.
H 280..
H 279.
H 269.
H 267.

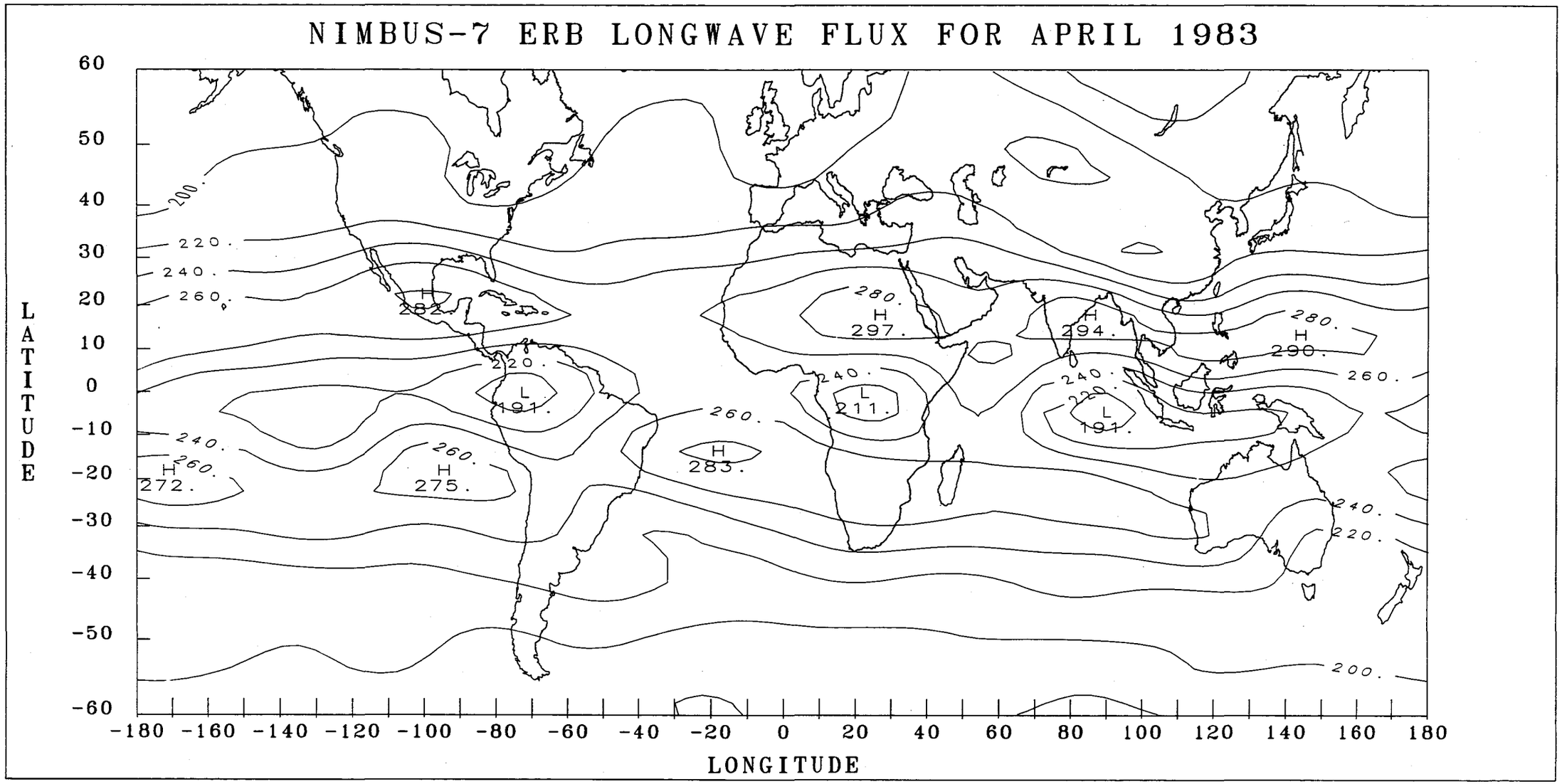
NIMBUS-7 ERB LONGWAVE FLUX FOR APRIL 1983
LATITUDE
LONGITUDE
60
50
40
30
20
10
0
-10
-20
-30
-40
-50
-60
-180 -160 -140 -120 -100 -80 -60 -40 -20 0 20 40 60 80 100 120 140 160 180
200.
220.
240.
260.
280.
H 282.
H 272.
H 275.
H 283.
H 297.
H 294.
H 290.
L 191.
L 211.
L 191.

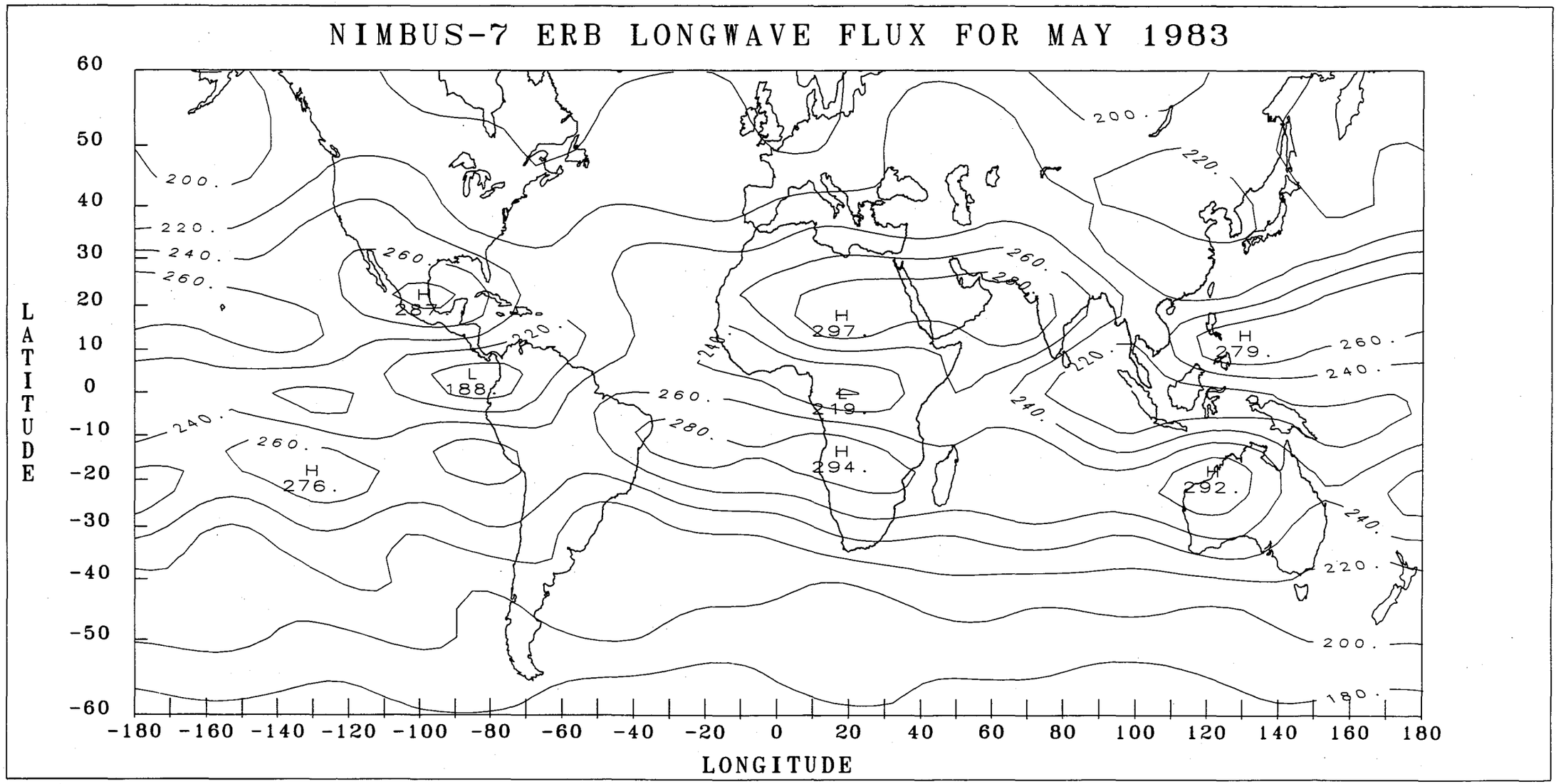
NIMBUS-7 ERB LONGWAVE FLUX FOR MAY 1983
LATITUDE
LONGITUDE
60
50
40
30
20
10
0
-10
-20
-30
-40
-50
-60
-180 -160 -140 -120 -100 -80 -60 -40 -20 0 20 40 60 80 100 120 140 160 180
200.
220.
240.
260.
280.
H 287.
L 188.
H 276.
H 297.
219.
H 294.
H 279.
H 292.
180.

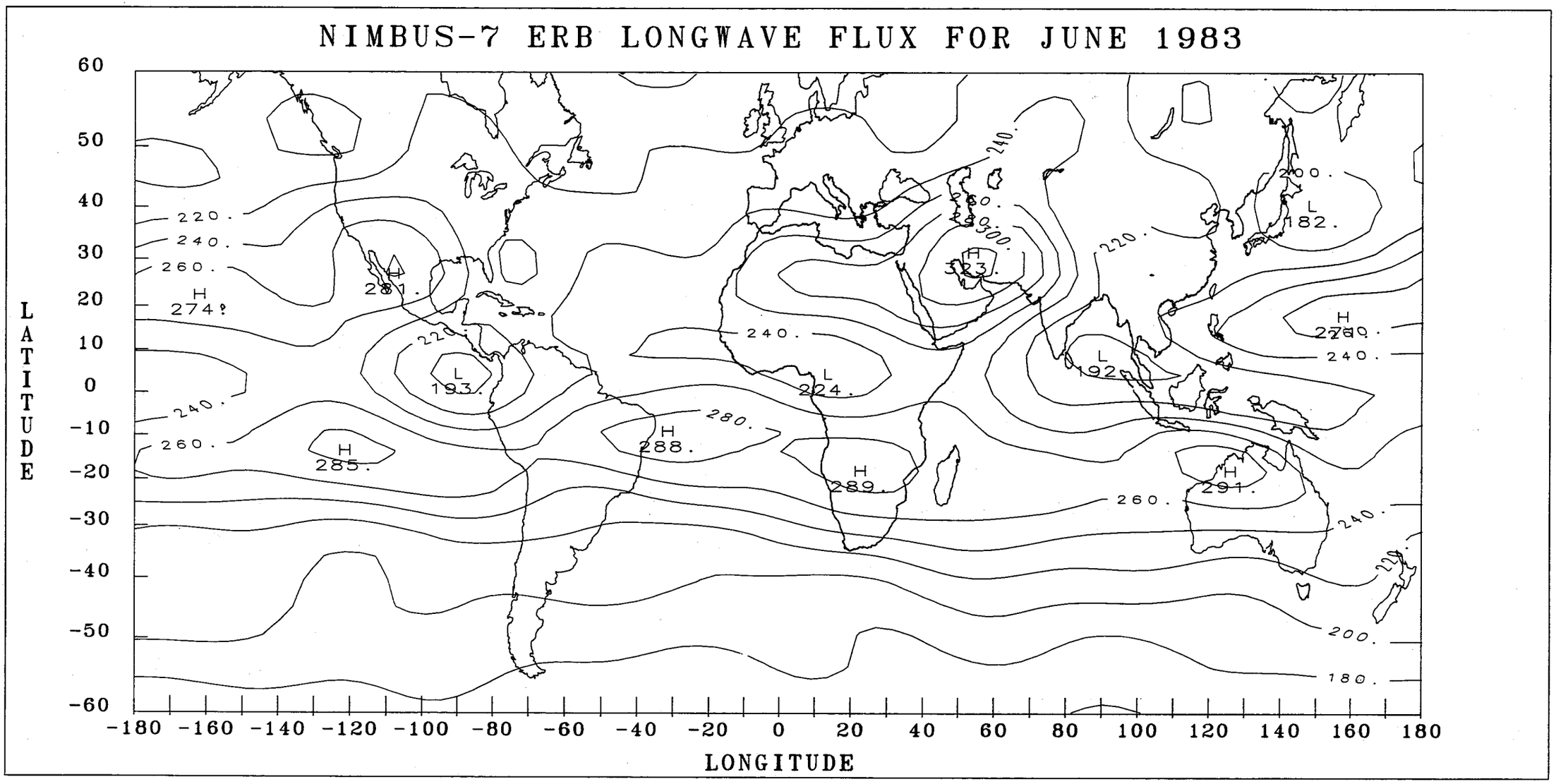
NIMBUS-7 ERB LONGWAVE FLUX FOR JUNE 1983
LATITUDE
LONGITUDE
60
50
40
30
20
10
0
-10
-20
-30
-40
-50
-60
-180 -160 -140 -120 -100 -80 -60 -40 -20 0 20 40 60 80 100 120 140 160 180
220.
240.
260.
H
274.
H
281.
L
193.
240.
260.
H
285.
280.
H
288.
240.
L
224.
H
289.
240.
H
323.
300.
240.
220.
200.
L
182.
L
192.
H
291.
260.
240.
220.
200.
180.

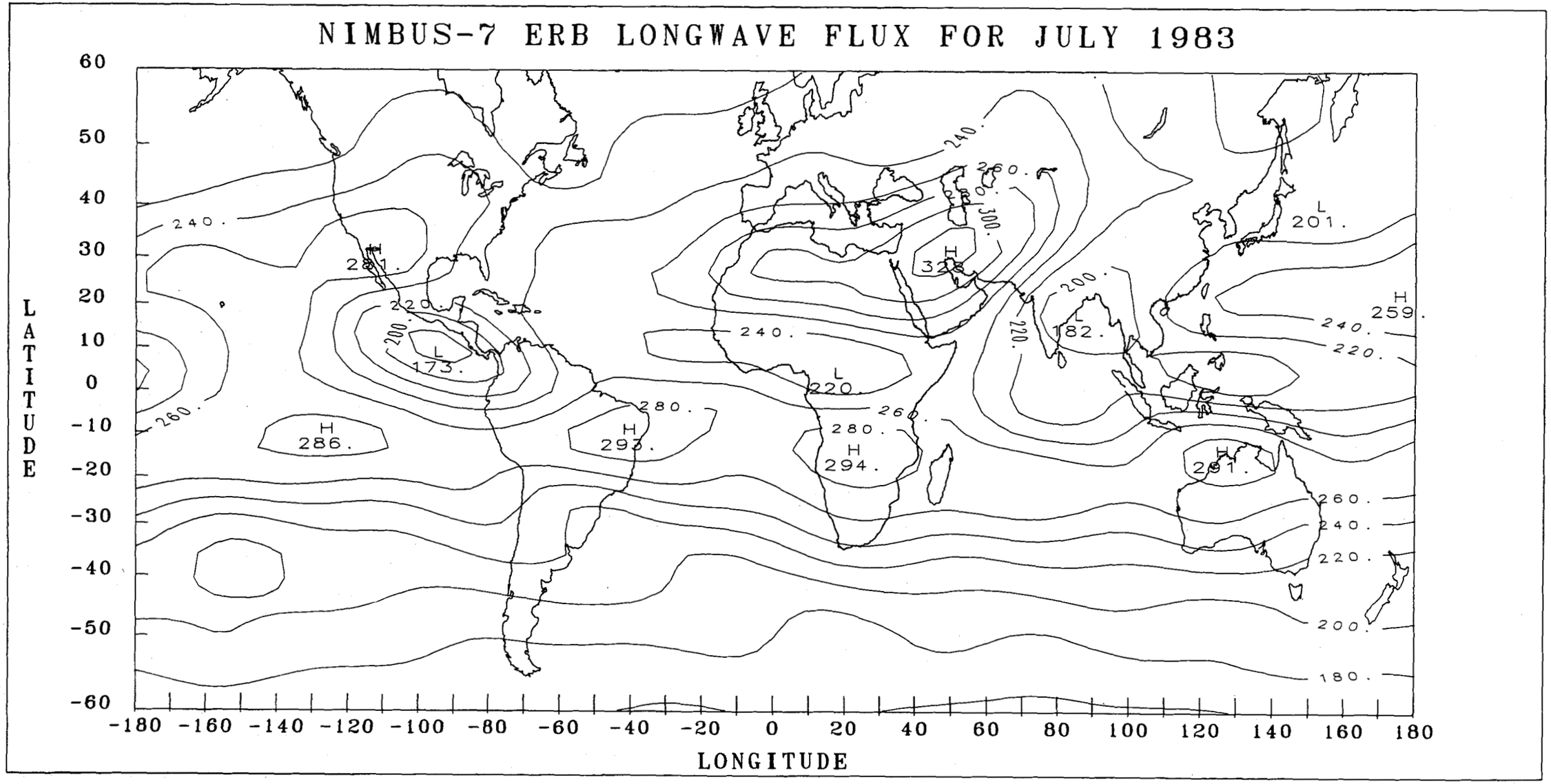
NIMBUS-7 ERB LONGWAVE FLUX FOR JULY 1983
LATITUDE
LONGITUDE
60
50
40
30
20
10
0
-10
-20
-30
-40
-50
-60
-180 -160 -140 -120 -100 -80 -60 -40 -20 0 20 40 60 80 100 120 140 160 180
240.
260.
300.
200.
220.
280.
H 286.
H 293.
H 294.
H 291.
H 259.
H 328.
L 173.
L 220.
L 182.
L 201.

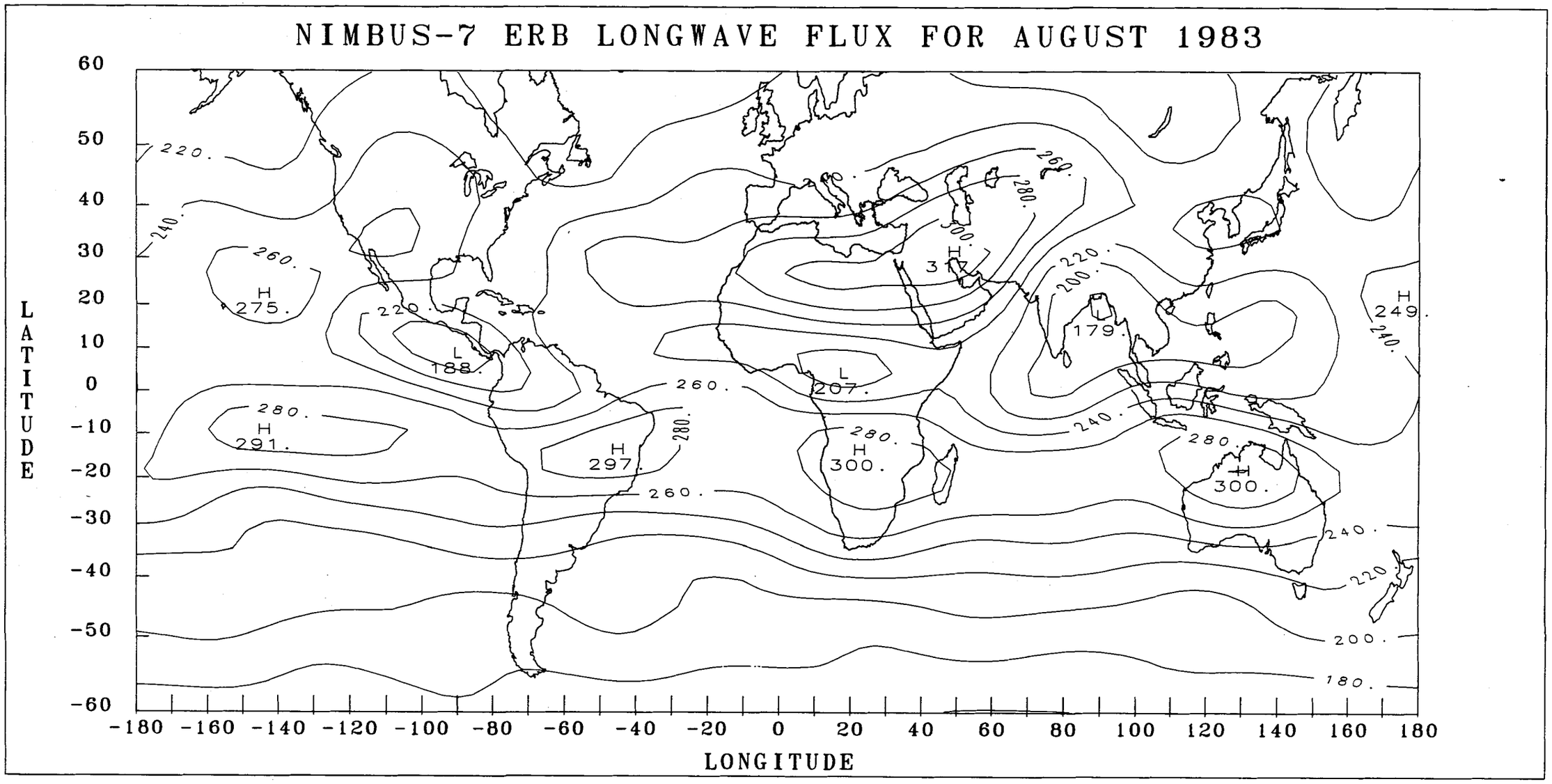
NIMBUS-7 ERB LONGWAVE FLUX FOR AUGUST 1983
LATITUDE
LONGITUDE
60
50
40
30
20
10
0
-10
-20
-30
-40
-50
-60
-180 -160 -140 -120 -100 -80 -60 -40 -20 0 20 40 60 80 100 120 140 160 180
220.
240.
260.
H
275.
220.
L
188.
280.
H
291.
260.
280.
H
297.
260.
300.
H
31
260.
280.
L
207.
280.
H
300.
220.
200.
179.
240.
280.
H
300.
H
249.
240.
240.
220.
200.
180.

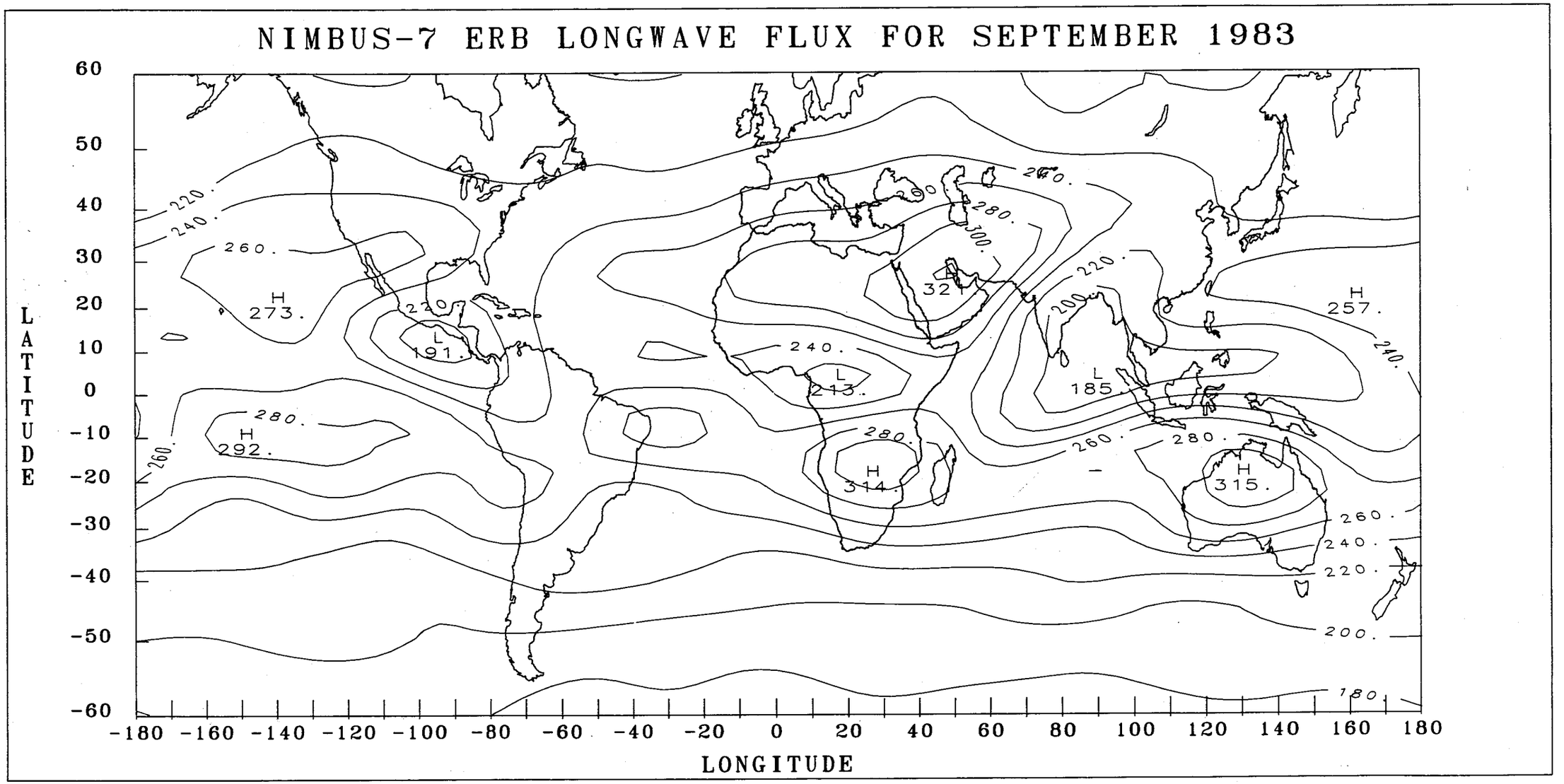
NIMBUS-7 ERB LONGWAVE FLUX FOR SEPTEMBER 1983
LATITUDE
LONGITUDE
60
50
40
30
20
10
0
-10
-20
-30
-40
-50
-60
-180 -160 -140 -120 -100 -80 -60 -40 -20 0 20 40 60 80 100 120 140 160 180
H 273.
L 191.
H 292.
L 321.
L 213.
H 314.
L 185.
H 257.
H 315.
220.
240.
260.
280.
300.
200.
180.

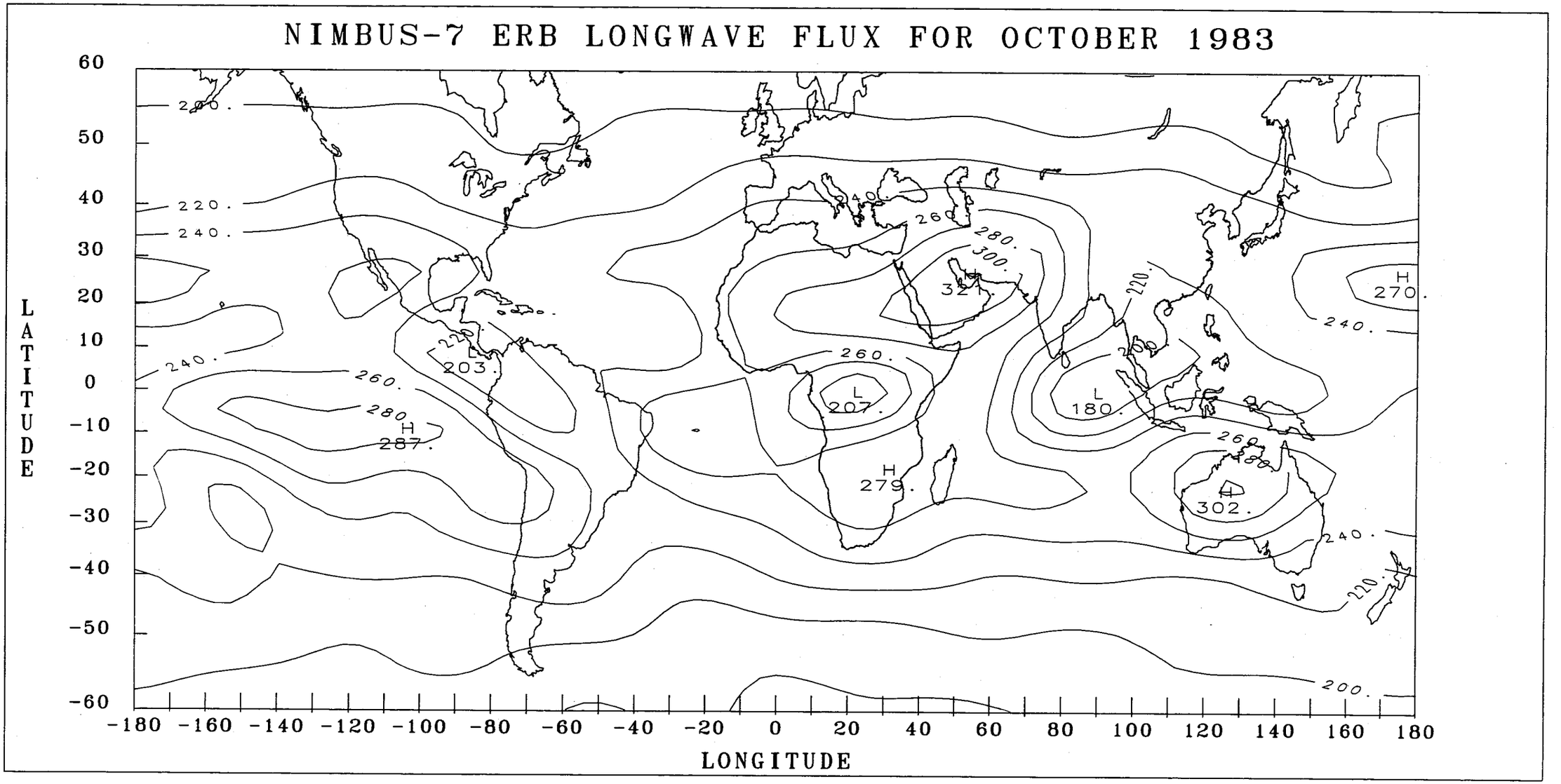
NIMBUS-7 ERB LONGWAVE FLUX FOR OCTOBER 1983
LATITUDE
LONGITUDE
60
50
40
30
20
10
0
-10
-20
-30
-40
-50
-60
-180 -160 -140 -120 -100 -80 -60 -40 -20 0 20 40 60 80 100 120 140 160 180
200.
220.
240.
260.
280.
300.
320.
203.
H
287.
L
207.
H
279.
L
180.
H
302.
H
270.

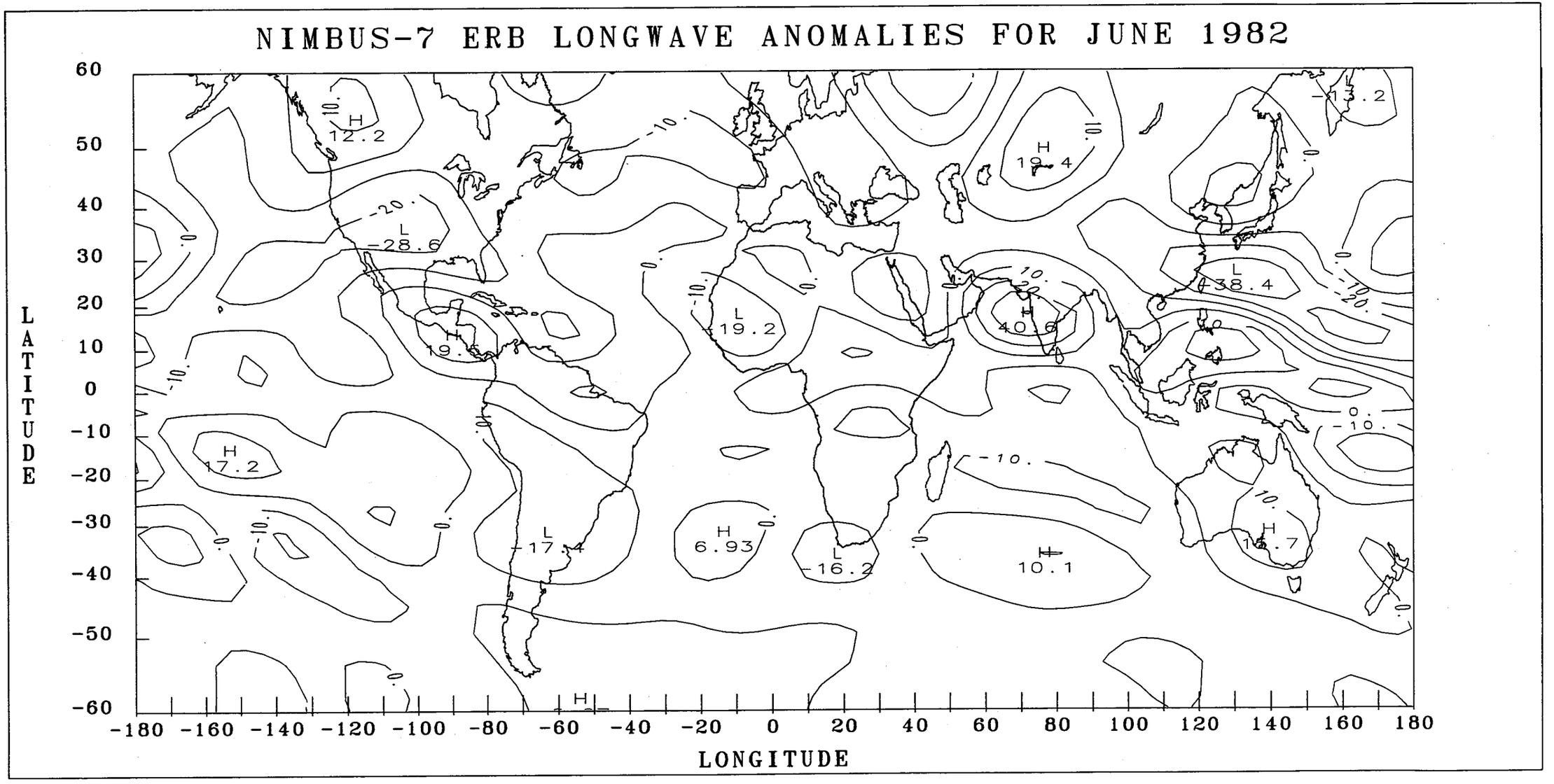
NIMBUS-7 ERB LONGWAVE ANOMALIES FOR JUNE 1982
LATITUDE
LONGITUDE
60
50
40
30
20
10
0
-10
-20
-30
-40
-50
-60
-180 -160 -140 -120 -100 -80 -60 -40 -20 0 20 40 60 80 100 120 140 160 180
H 12.2
L -28.6
H 19.4
L 19.2
H 40.6
L 38.4
H 17.2
L -17.4
H 6.93
L -16.2
H 10.1
H 15.7
-17.2

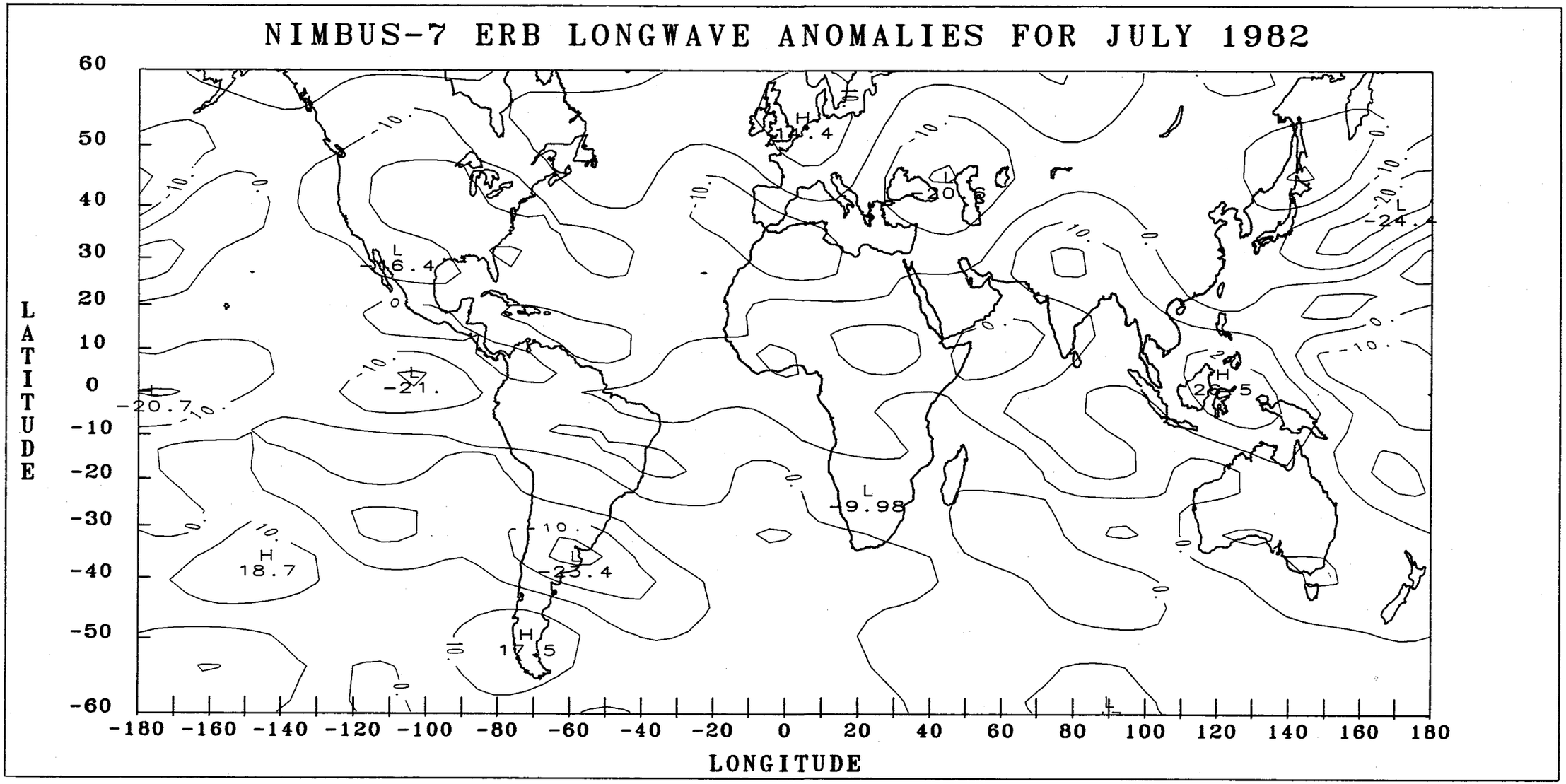
NIMBUS-7 ERB LONGWAVE ANOMALIES FOR JULY 1982
LATITUDE
LONGITUDE
60
50
40
30
20
10
0
-10
-20
-30
-40
-50
-60
-180 -160 -140 -120 -100 -80 -60 -40 -20 0 20 40 60 80 100 120 140 160 180
L 6.4
-21.
-20.7
H 18.7
-23.4
H 17.5
L -9.98
H 14.4
L -20.6
L -24.4
H 26.5

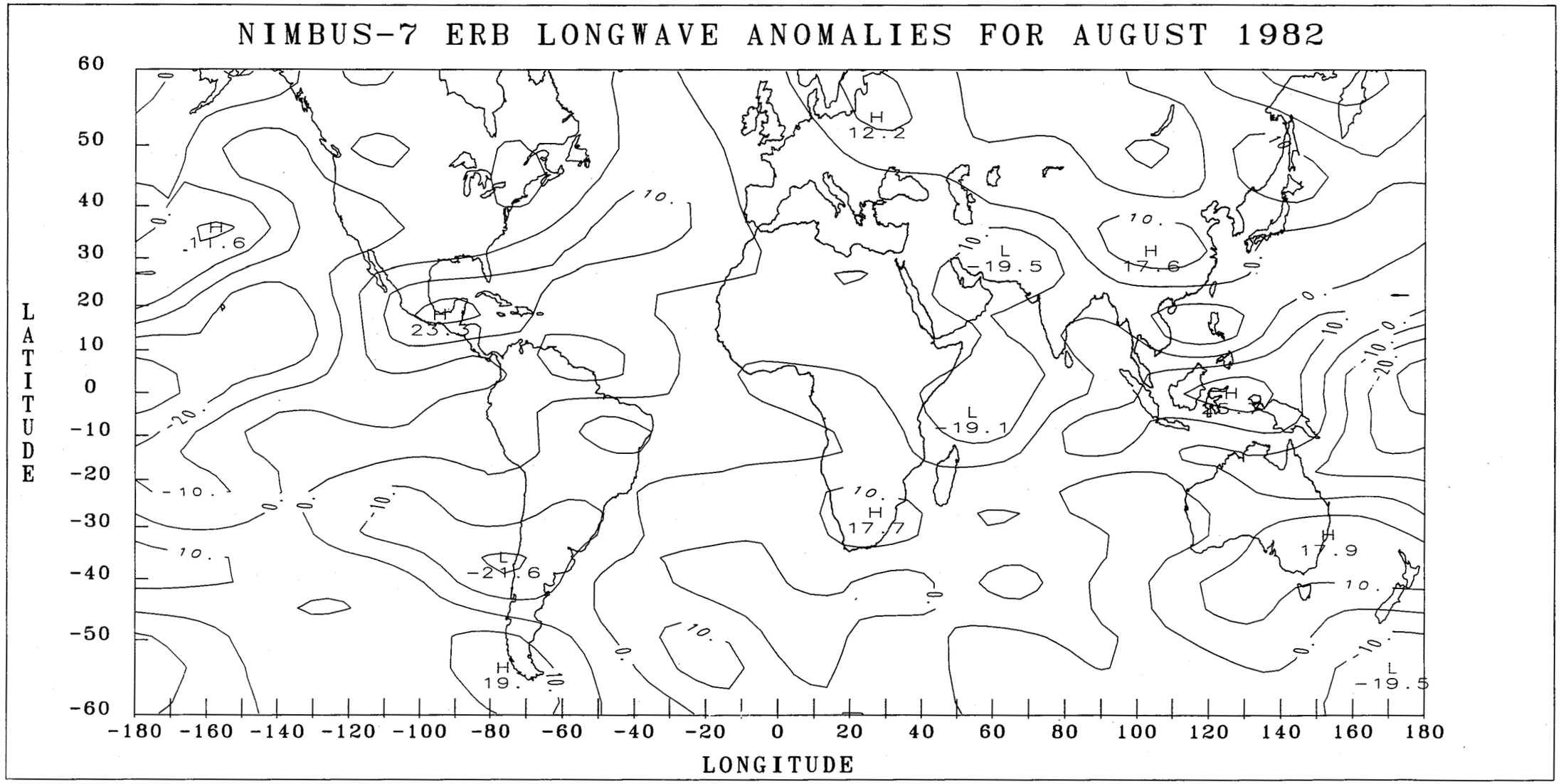
NIMBUS-7 ERB LONGWAVE ANOMALIES FOR AUGUST 1982
LATITUDE
LONGITUDE
60
50
40
30
20
10
0
-10
-20
-30
-40
-50
-60
-180 -160 -140 -120 -100 -80 -60 -40 -20 0 20 40 60 80 100 120 140 160 180
H 12.2
H -11.6
H 23.5
L -19.5
H 17.6
L -19.1
H 17.7
L -21.6
H 19.
H 17.9
L -19.5
10.
0.
-10.
-20.

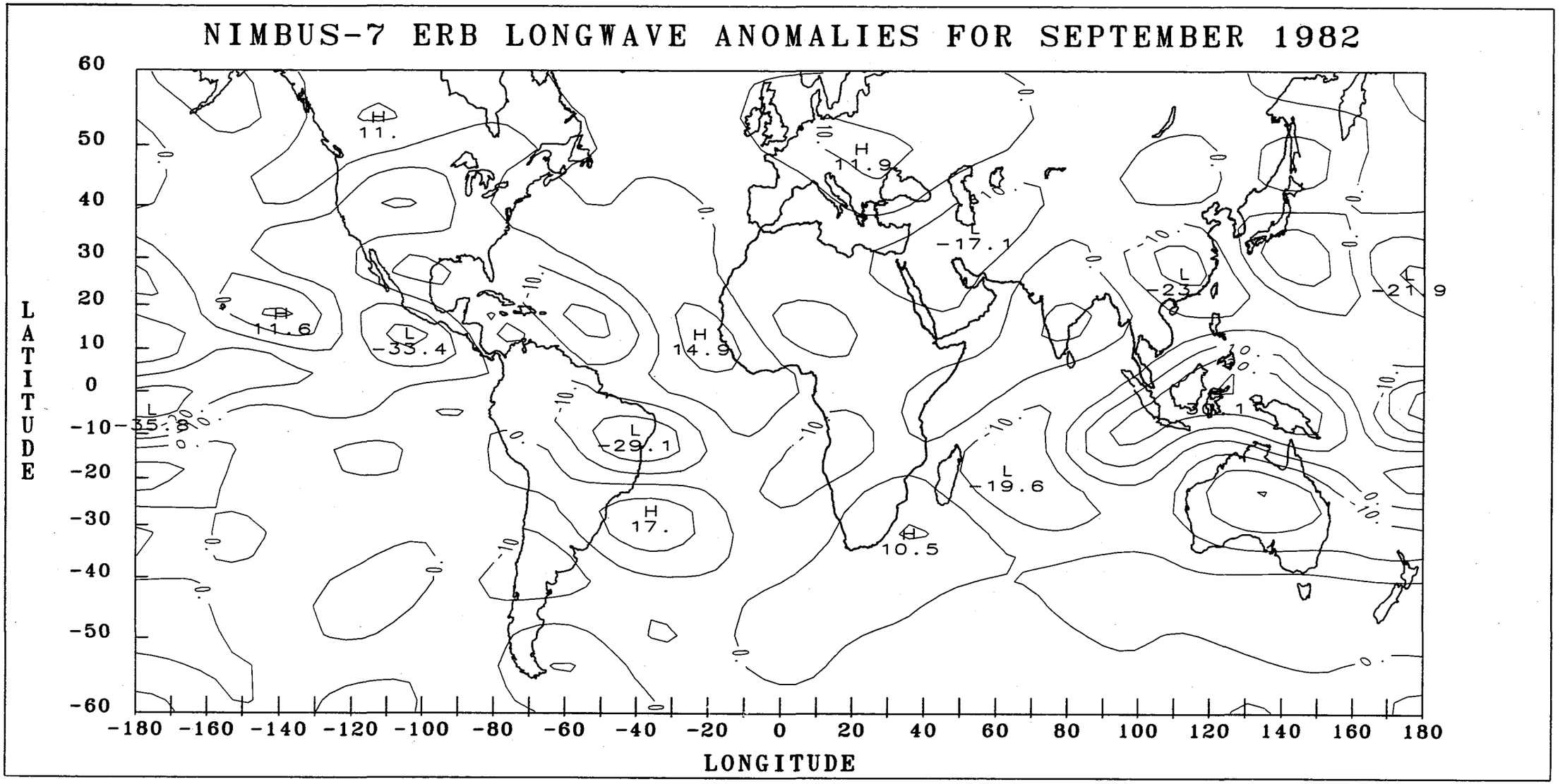
NIMBUS-7 ERB LONGWAVE ANOMALIES FOR SEPTEMBER 1982
LATITUDE
LONGITUDE
60
50
40
30
20
10
0
-10
-20
-30
-40
-50
-60
-180 -160 -140 -120 -100 -80 -60 -40 -20 0 20 40 60 80 100 120 140 160 180
H 11.
H 11.9
L -17.1
L -23
L -21.9
H 11.6
L -33.4
H 14.9
L -35.8
L -29.1
L -19.6
H 17.
H 10.5

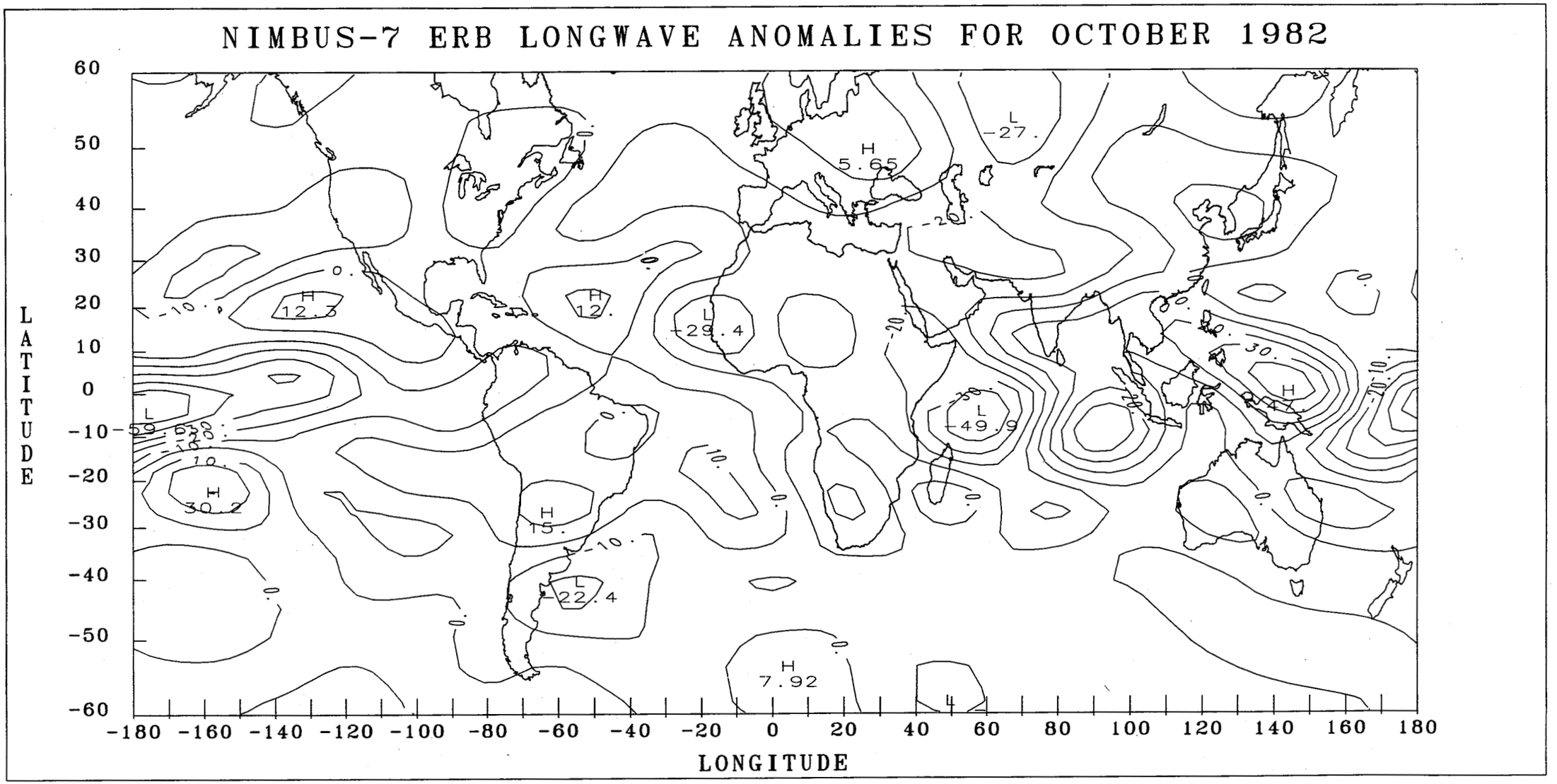
NIMBUS-7 ERB LONGWAVE ANOMALIES FOR OCTOBER 1982
LATITUDE
LONGITUDE
60
50
40
30
20
10
0
-10
-20
-30
-40
-50
-60
-180 -160 -140 -120 -100 -80 -60 -40 -20 0 20 40 60 80 100 120 140 160 180
H 5.65
L -27.
H 12.3
H 12.
L -29.4
L -49.9
H 30.2
H 15.
L -22.4
H 7.92

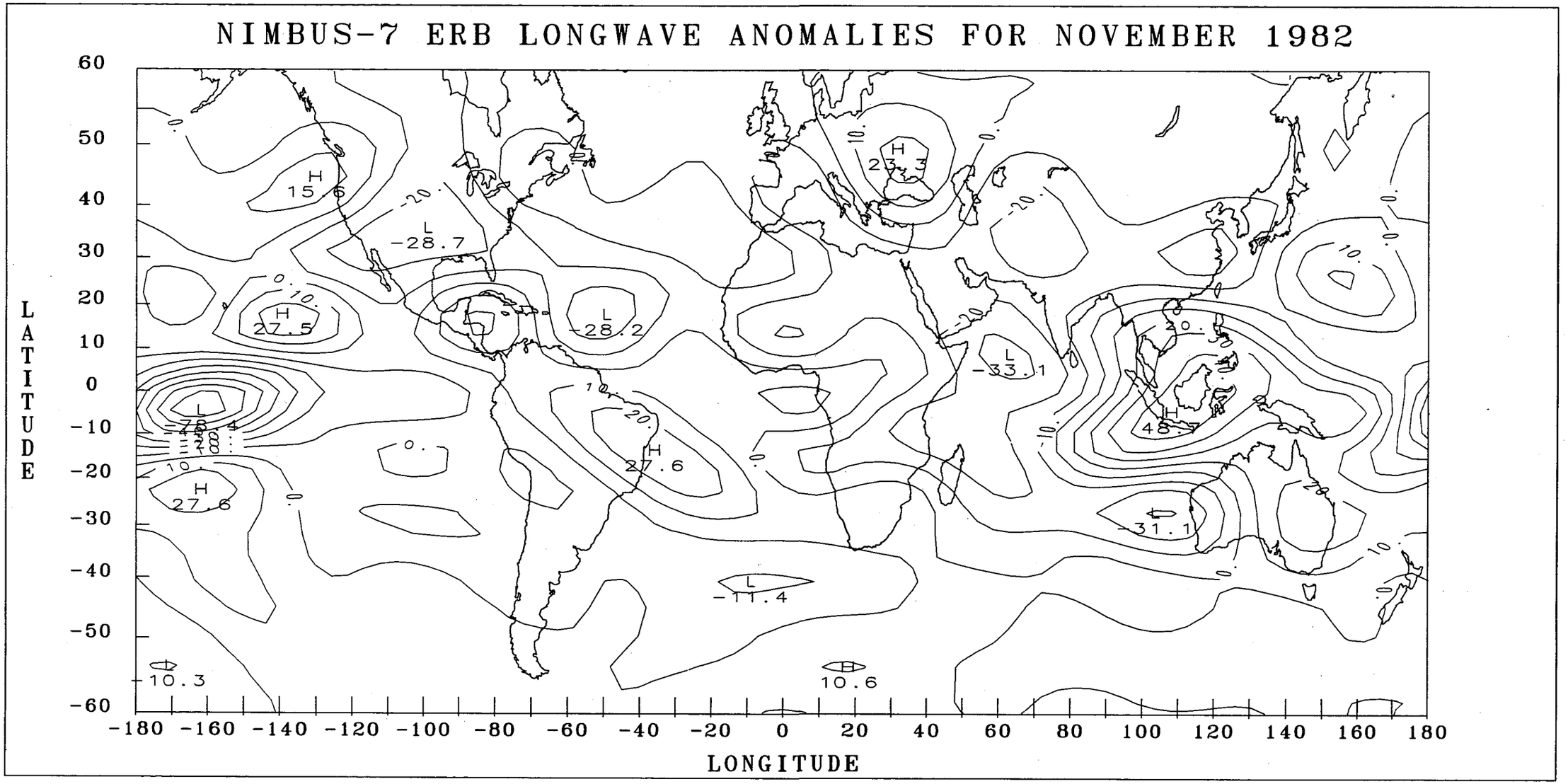
NIMBUS-7 ERB LONGWAVE ANOMALIES FOR NOVEMBER 1982
LATITUDE
LONGITUDE
60
50
40
30
20
10
0
-10
-20
-30
-40
-50
-60
-180 -160 -140 -120 -100 -80 -60 -40 -20 0 20 40 60 80 100 120 140 160 180
H 15.6
L -28.7
H 27.5
L -28.2
H 23.3
L -33.1
H 48.7
L -75.4
H 27.6
H 27.6
L -11.4
-31.1
10.3
10.6

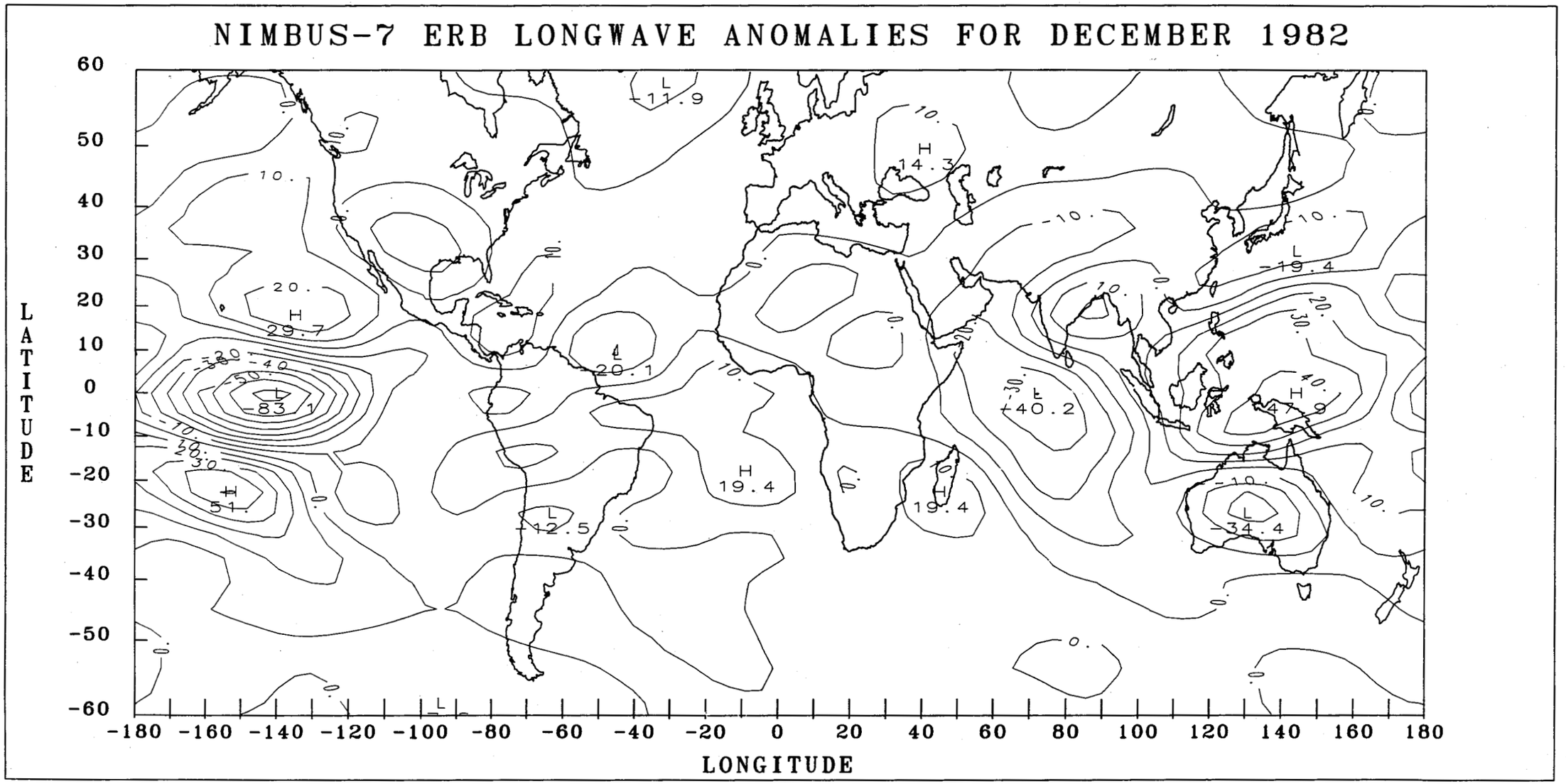
NIMBUS-7 ERB LONGWAVE ANOMALIES FOR DECEMBER 1982
LATITUDE
LONGITUDE
60
50
40
30
20
10
0
-10
-20
-30
-40
-50
-60
-180 -160 -140 -120 -100 -80 -60 -40 -20 0 20 40 60 80 100 120 140 160 180
L -11.9
H 14.3
L -19.4
H 29.7
L -83.1
L 20.1
H 19.4
L -12.5
L -40.2
H 47.9
H 51.
L -34.4
H 19.4

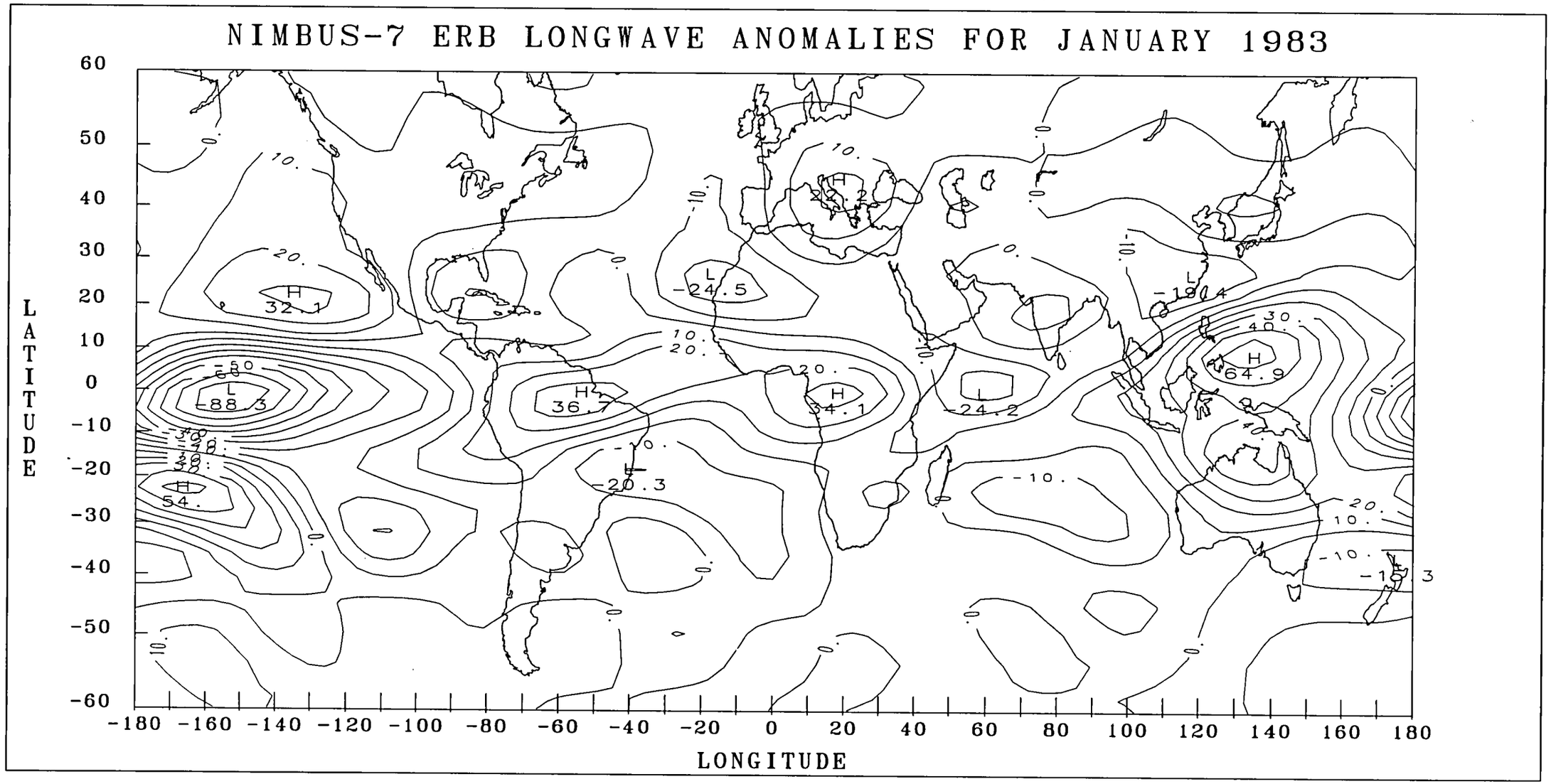
NIMBUS-7 ERB LONGWAVE ANOMALIES FOR JANUARY 1983
LATITUDE
60
50
40
30
20
10
0
-10
-20
-30
-40
-50
-60
-180 -160 -140 -120 -100 -80 -60 -40 -20 0 20 40 60 80 100 120 140 160 180
LONGITUDE
H 32.1
L -88.3
H 54.
H 36.7
L -24.5
H 34.1
H 22.2
L -24.2
L -19.4
H 64.9
L -20.3
10.
20.
30.
40.
-10.
-20.
-30.
-40.
0.

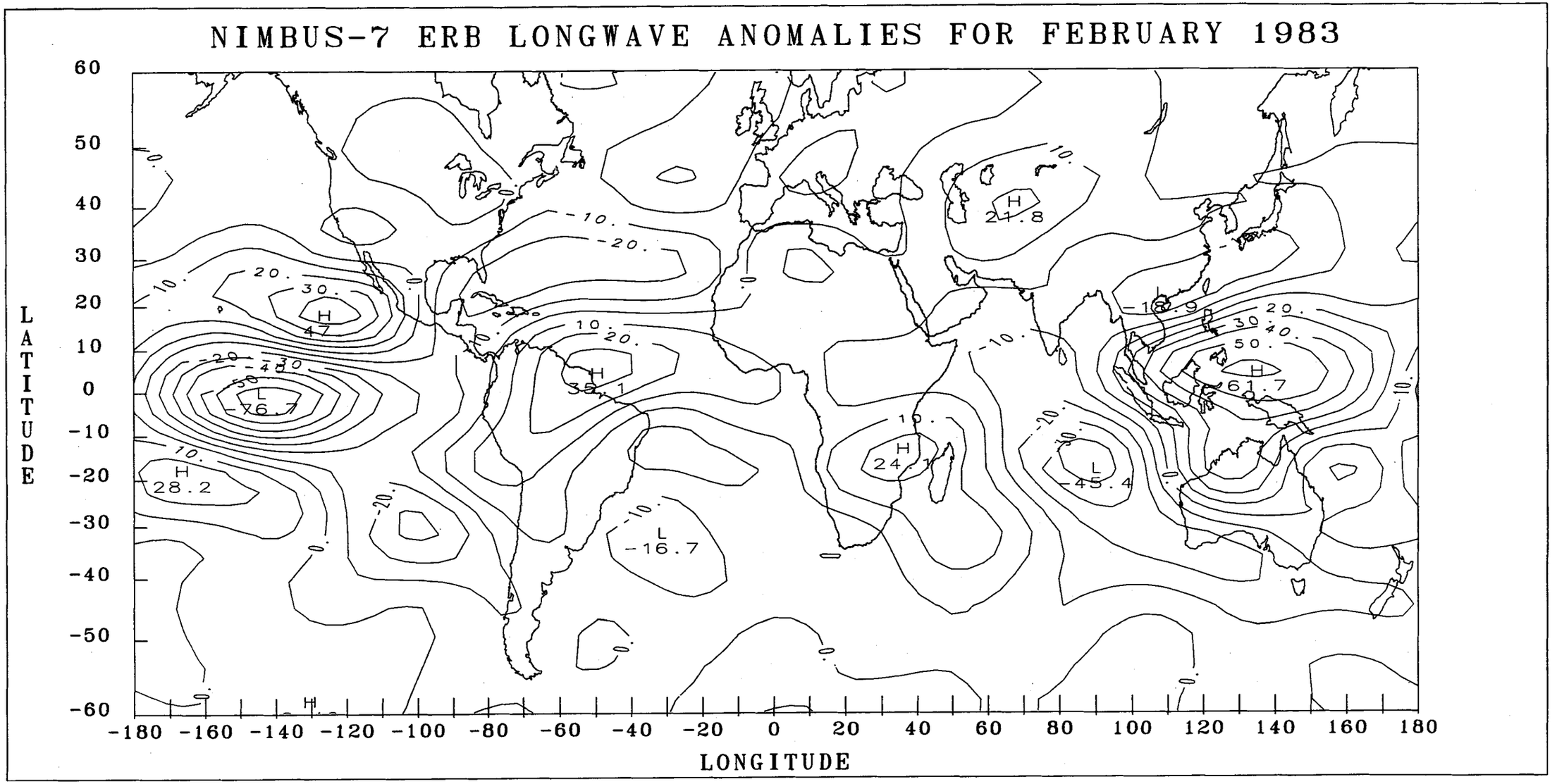
NIMBUS-7 ERB LONGWAVE ANOMALIES FOR FEBRUARY 1983
LATITUDE
LONGITUDE
60
50
40
30
20
10
0
-10
-20
-30
-40
-50
-60
-180 -160 -140 -120 -100 -80 -60 -40 -20 0 20 40 60 80 100 120 140 160 180
H 47
L -76.7
H 28.2
H 39.1
L -16.7
H 24.1
H 24.8
L -45.4
-18.9
H 61.7

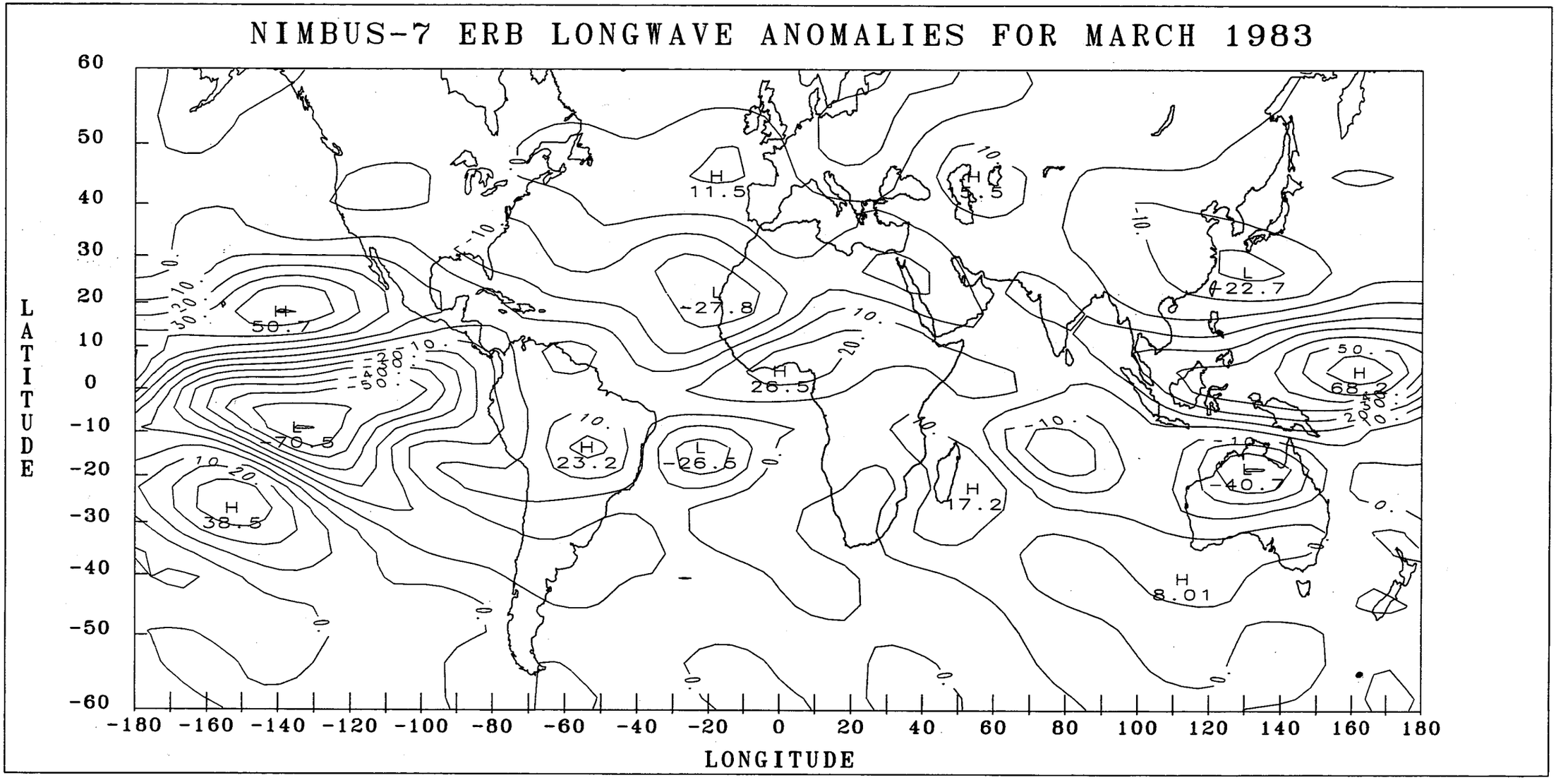
NIMBUS-7 ERB LONGWAVE ANOMALIES FOR MARCH 1983
LATITUDE
LONGITUDE
60
50
40
30
20
10
0
-10
-20
-30
-40
-50
-60
-180 -160 -140 -120 -100 -80 -60 -40 -20 0 20 40 60 80 100 120 140 160 180
H 11.5
H 5.5
L -27.8
L 22.7
H 50.7
L -70.5
H 26.5
H 23.2
L -26.6
H 38.5
H 17.2
L -40.7
H 68.2
H 8.01

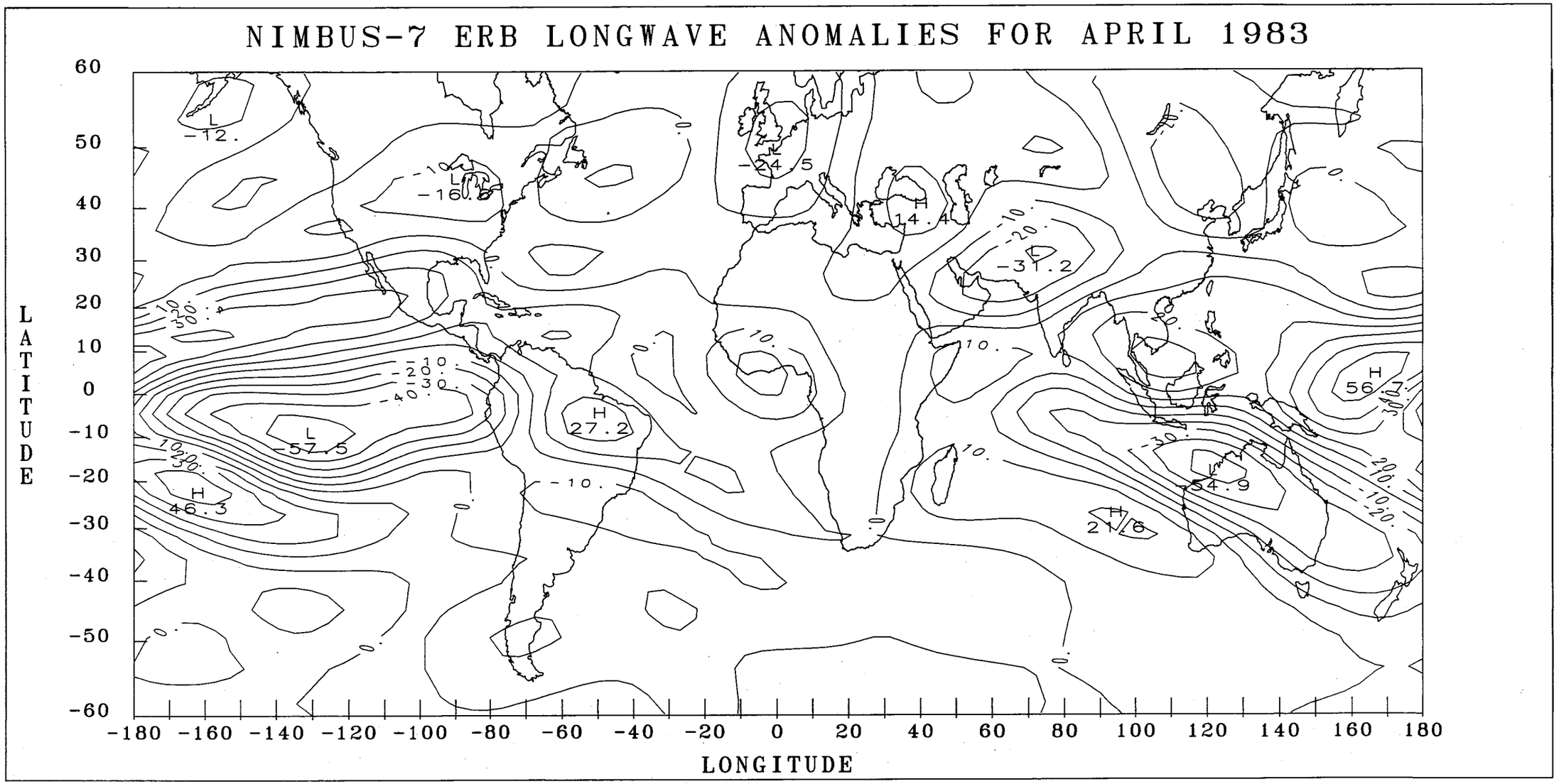
NIMBUS-7 ERB LONGWAVE ANOMALIES FOR APRIL 1983
LATITUDE
LONGITUDE
60
50
40
30
20
10
0
-10
-20
-30
-40
-50
-60
-180 -160 -140 -120 -100 -80 -60 -40 -20 0 20 40 60 80 100 120 140 160 180
L -12.
L -16.8
-24.5
H 14.4
-31.2
H 27.2
L -57.5
H 46.3
H 56.7
L -54.9
H 21.6

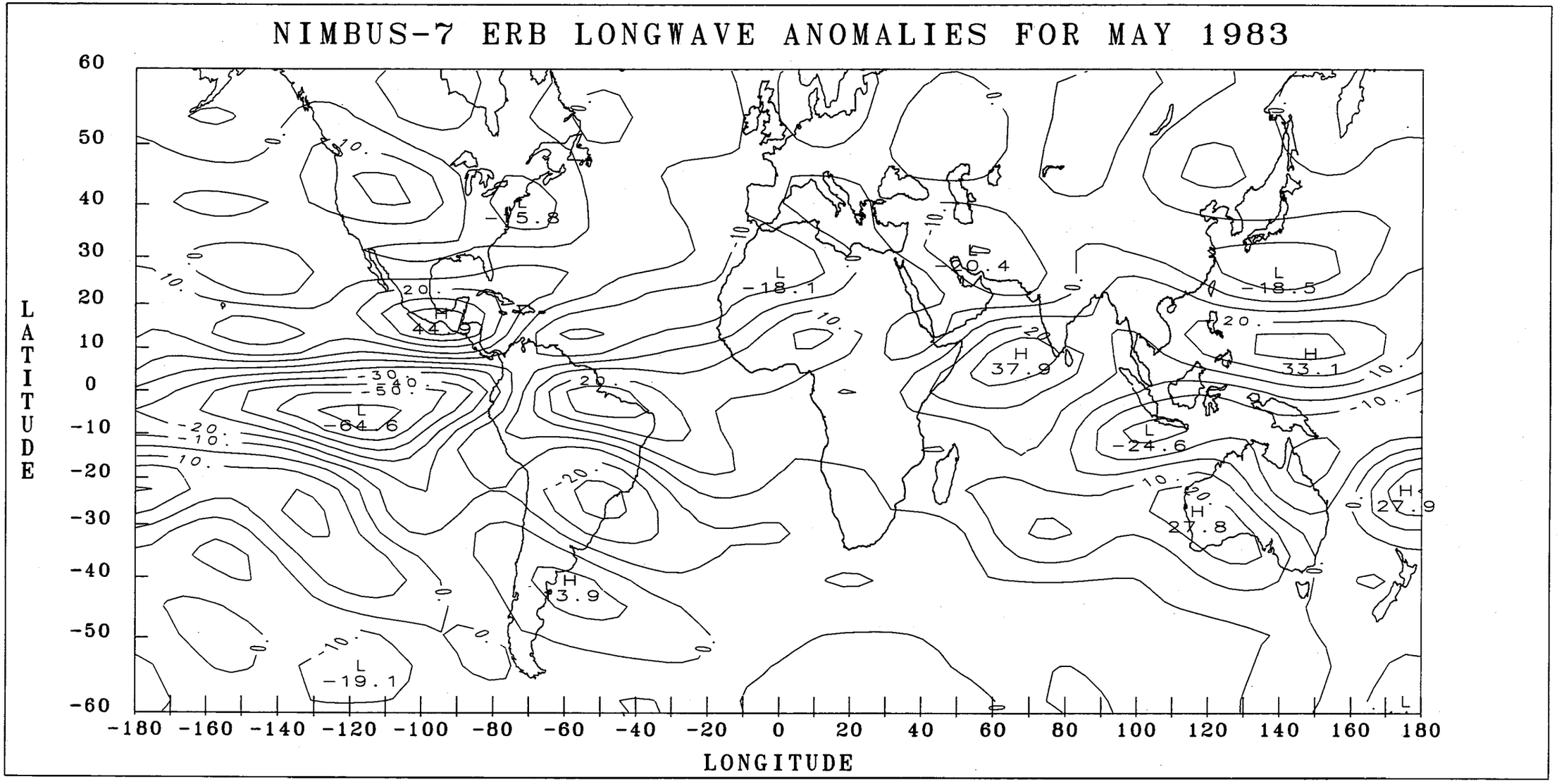
NIMBUS-7 ERB LONGWAVE ANOMALIES FOR MAY 1983
LATITUDE
LONGITUDE
60
50
40
30
20
10
0
-10
-20
-30
-40
-50
-60
-180 -160 -140 -120 -100 -80 -60 -40 -20 0 20 40 60 80 100 120 140 160 180
L -15.8
L -18.1
L -20.4
L -18.5
H 44.9
H 37.9
H 33.1
L -64.6
L -24.6
H 3.9
H 27.8
H 27.9
L -19.1

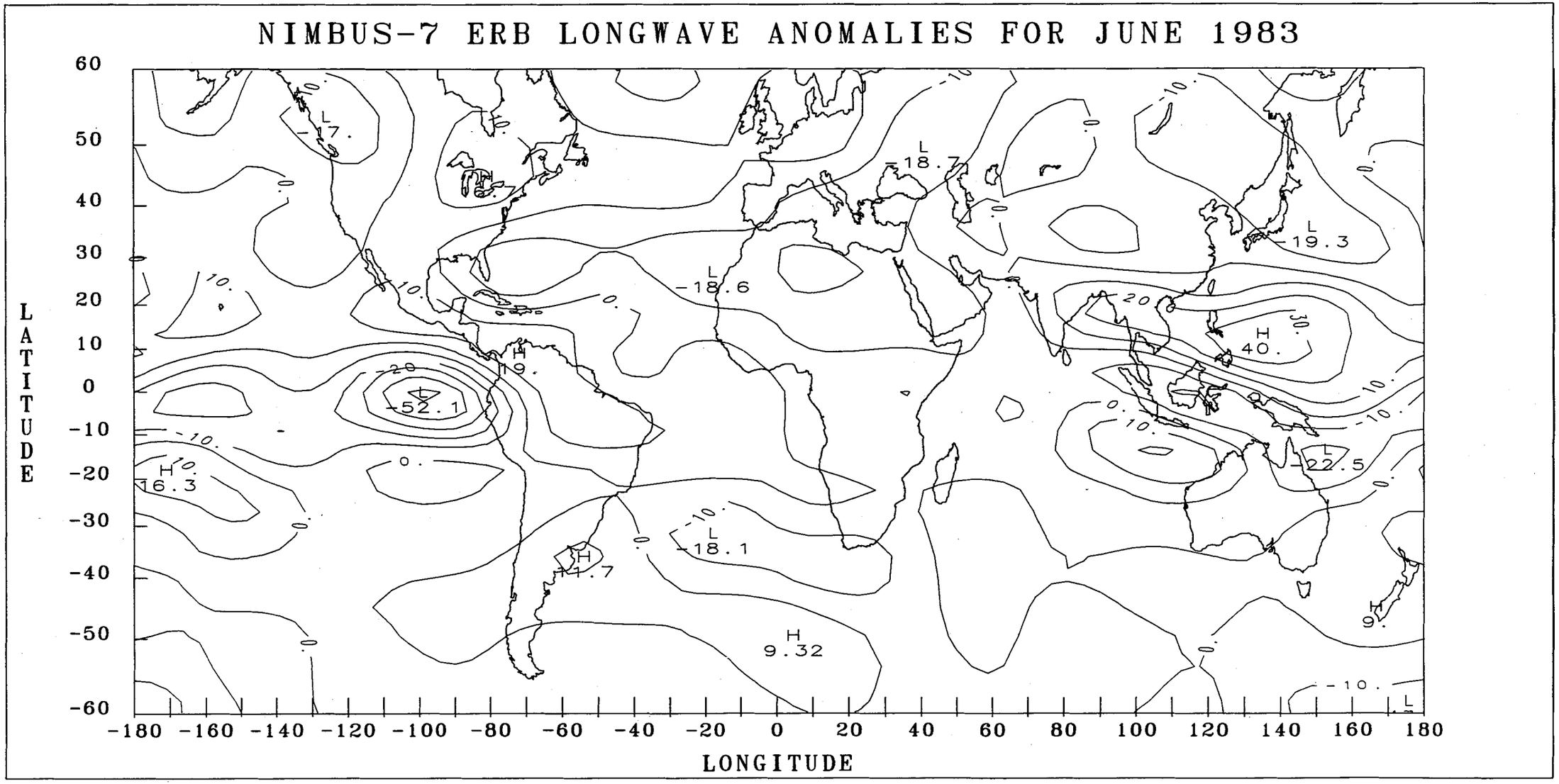
NIMBUS-7 ERB LONGWAVE ANOMALIES FOR JUNE 1983
LATITUDE
LONGITUDE
60
50
40
30
20
10
0
-10
-20
-30
-40
-50
-60
-180 -160 -140 -120 -100 -80 -60 -40 -20 0 20 40 60 80 100 120 140 160 180
L -7.
H 16.
L -18.7
L -19.3
L -18.6
H 19.
H 40.
L -52.1
L -22.5
H 16.3
L -18.1
H 14.7
H 9.32
H 9.
L

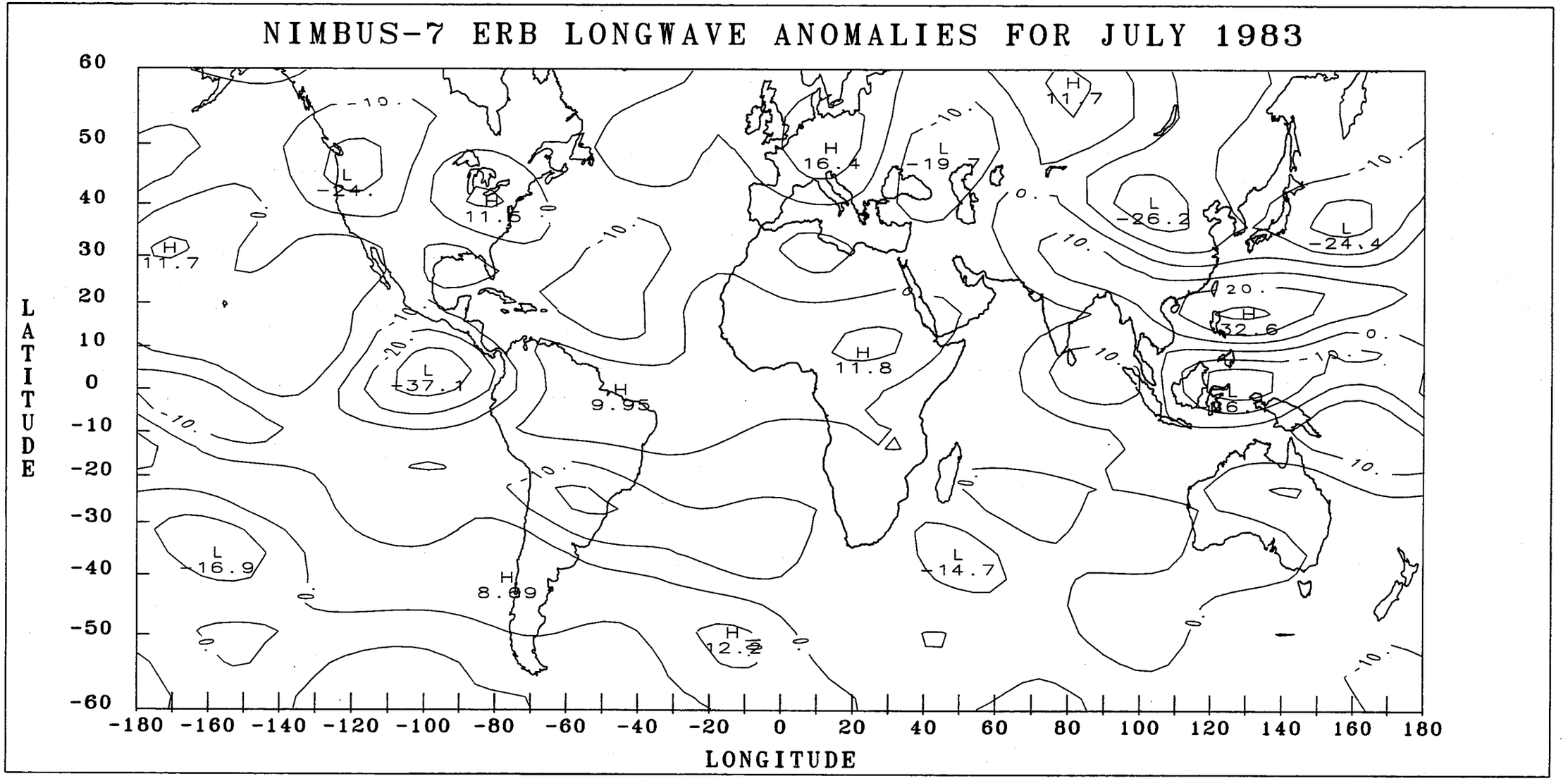
NIMBUS-7 ERB LONGWAVE ANOMALIES FOR JULY 1983
LATITUDE
LONGITUDE
60
50
40
30
20
10
0
-10
-20
-30
-40
-50
-60
-180 -160 -140 -120 -100 -80 -60 -40 -20 0 20 40 60 80 100 120 140 160 180
H 11.7
L -24.
H 11.5
H 16.4
L -19.7
H 11.7
L -26.2
L -24.4
H 11.7
H 32.6
H 11.8
L -37.1
H 9.95
L -16.9
H 8.89
L -14.7
H 12.2
-10.
0.
10.
20.

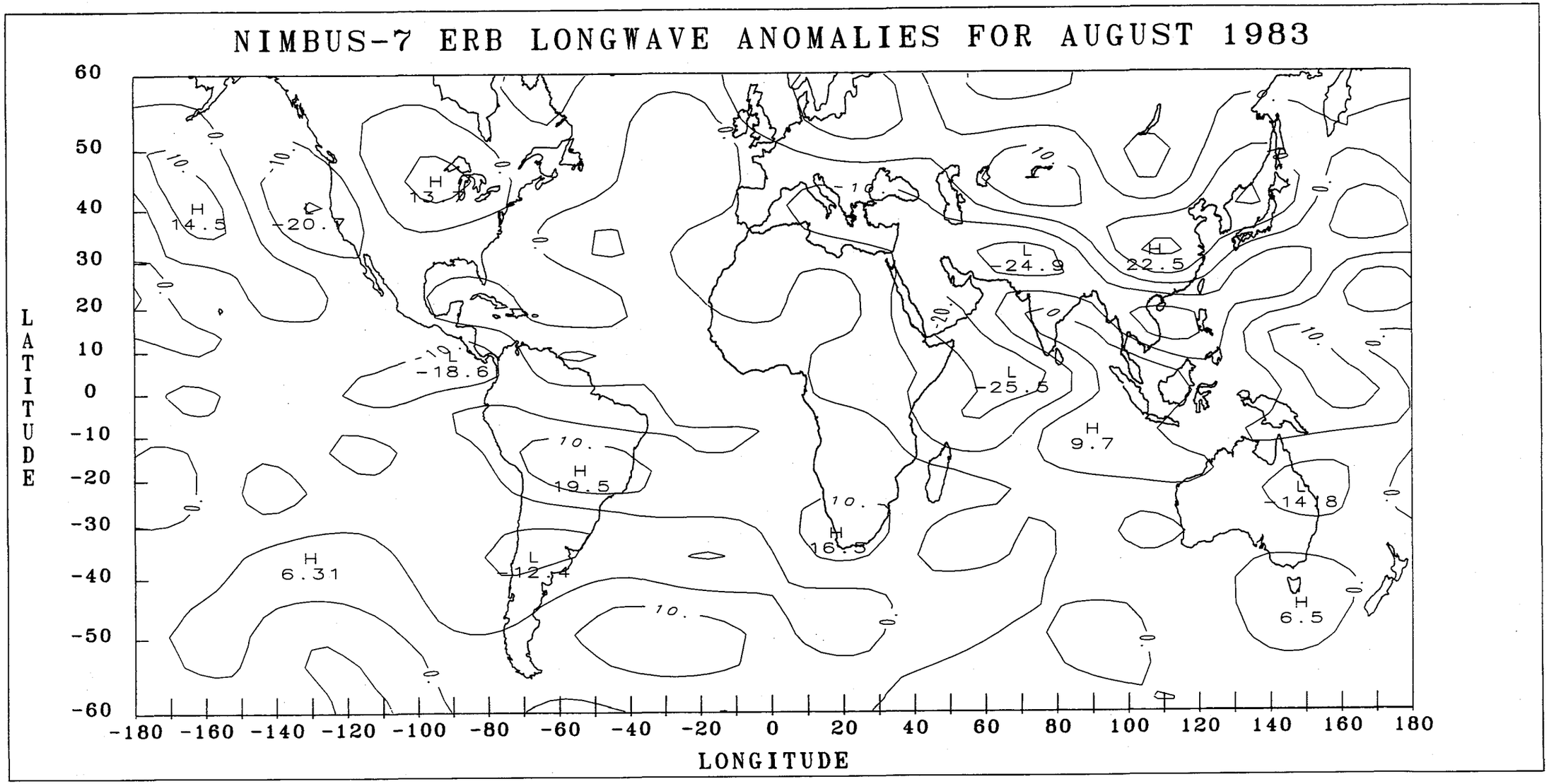
NIMBUS-7 ERB LONGWAVE ANOMALIES FOR AUGUST 1983
LATITUDE
LONGITUDE
60
50
40
30
20
10
0
-10
-20
-30
-40
-50
-60
-180 -160 -140 -120 -100 -80 -60 -40 -20 0 20 40 60 80 100 120 140 160 180
H 14.5
-20.7
H 13
-18.6
H 19.5
H 6.31
L -12.4
H 16.5
L -24.9
H 22.5
L -25.5
H 9.7
L -14.8
H 6.5

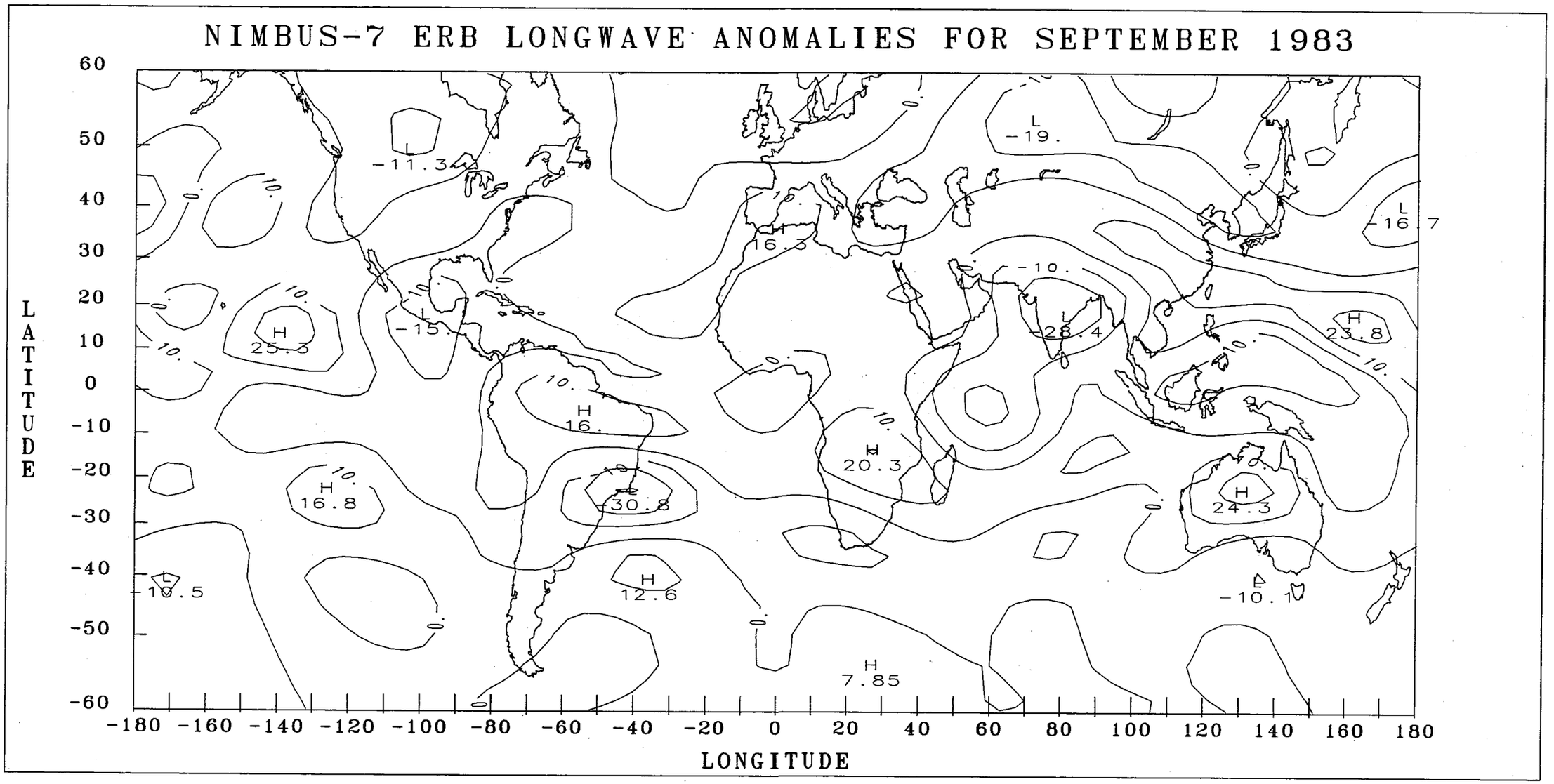
NIMBUS-7 ERB LONGWAVE ANOMALIES FOR SEPTEMBER 1983
LATITUDE
LONGITUDE
60
50
40
30
20
10
0
-10
-20
-30
-40
-50
-60
-180 -160 -140 -120 -100 -80 -60 -40 -20 0 20 40 60 80 100 120 140 160 180
L -11.3
L -19.
L -16.7
16.3
-10.
H 25.3
L -15.
L -28.4
H 23.8
10.
H 16.
H 20.3
H 16.8
30.8
H 24.3
H 12.6
L -10.5
L -10.1
H 7.85

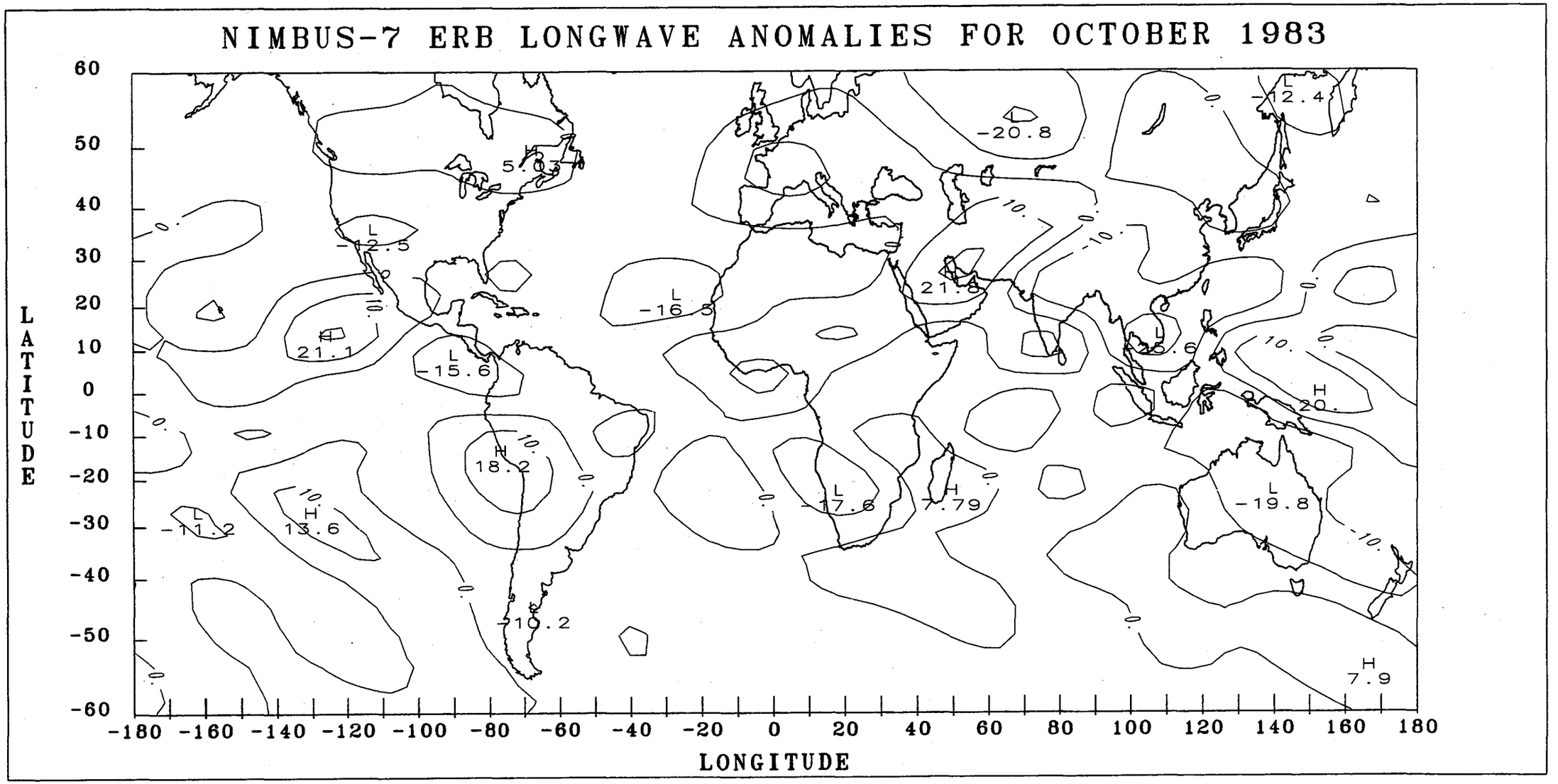
NIMBUS-7 ERB LONGWAVE ANOMALIES FOR OCTOBER 1983
LATITUDE
LONGITUDE
60
50
40
30
20
10
0
-10
-20
-30
-40
-50
-60
-180 -160 -140 -120 -100 -80 -60 -40 -20 0 20 40 60 80 100 120 140 160 180
L -12.4
-20.8
5.03
L -12.5
L -16.5
21.8
21.1
L -15.6
H 18.2
L -17.6
H 7.79
L -19.8
H 20.
L -11.2
H 13.6
-10.2
H 7.9

SEASONALLY AVERAGED FIELDS

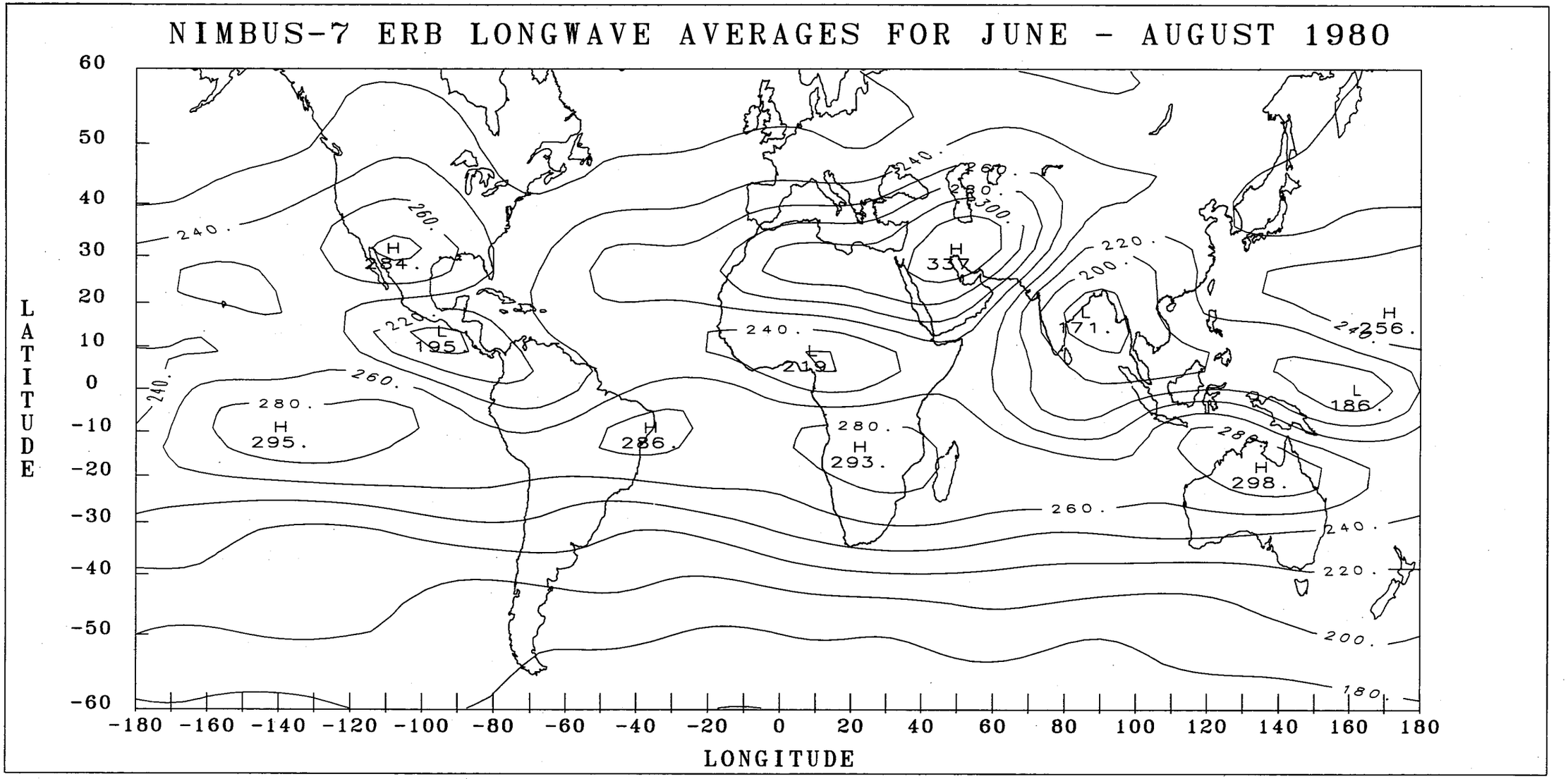
NIMBUS-7 ERB LONGWAVE AVERAGES FOR JUNE - AUGUST 1980
LATITUDE
60
50
40
30
20
10
0
-10
-20
-30
-40
-50
-60
-180 -160 -140 -120 -100 -80 -60 -40 -20 0 20 40 60 80 100 120 140 160 180
LONGITUDE
240.
260.
280.
300.
220.
200.
180.
H
284.
H
295.
H
286.
H
293.
H
298.
H
256.
L
195
L
171.
L
186.
219

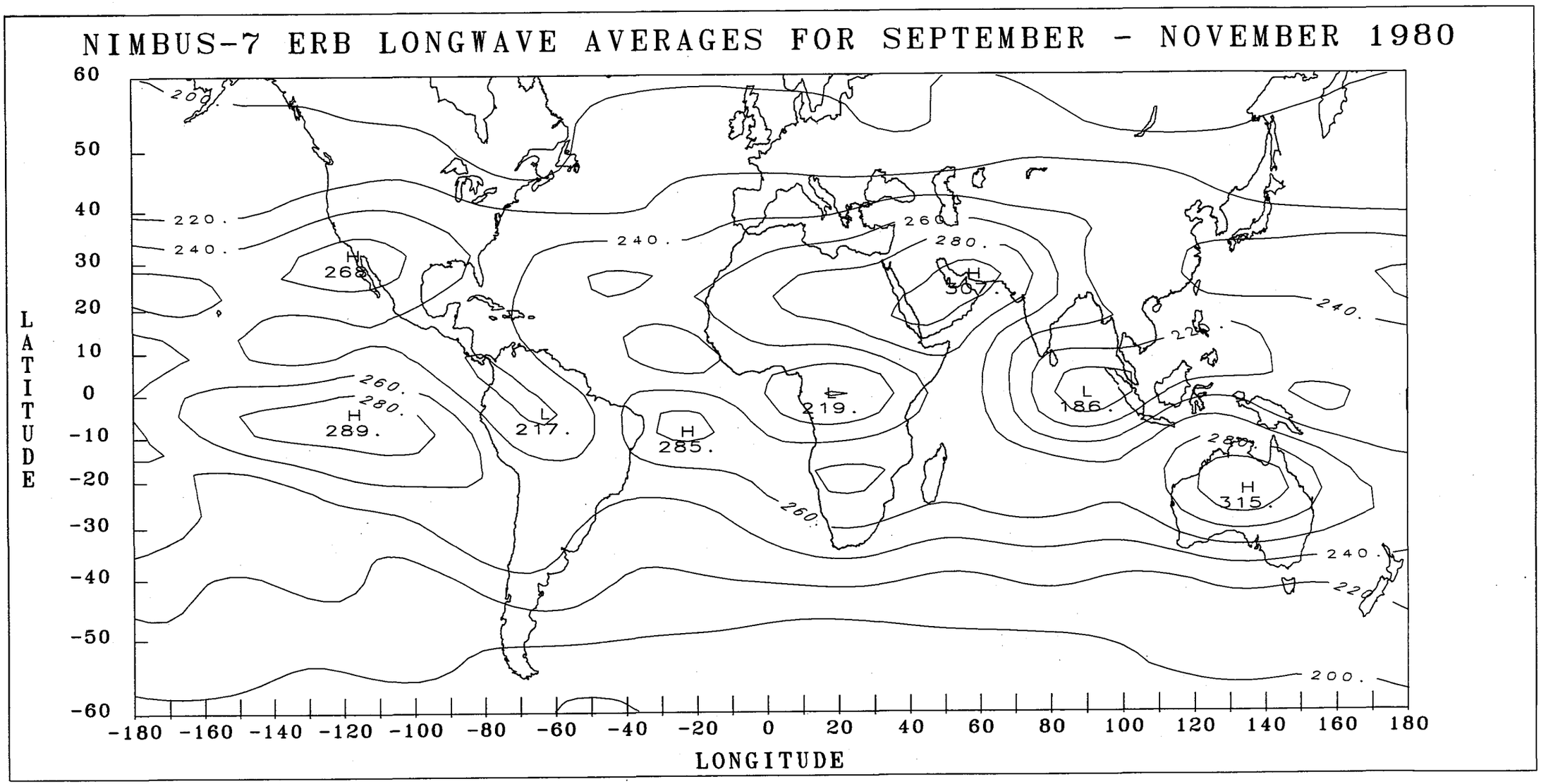
NIMBUS-7 ERB LONGWAVE AVERAGES FOR SEPTEMBER - NOVEMBER 1980
LATITUDE
LONGITUDE
60
50
40
30
20
10
0
-10
-20
-30
-40
-50
-60
-180 -160 -140 -120 -100 -80 -60 -40 -20 0 20 40 60 80 100 120 140 160 180
200.
220.
240.
260.
280.
H
268.
H
307.
L
186.
H
289.
L
217.
H
285.
219.
H
315.

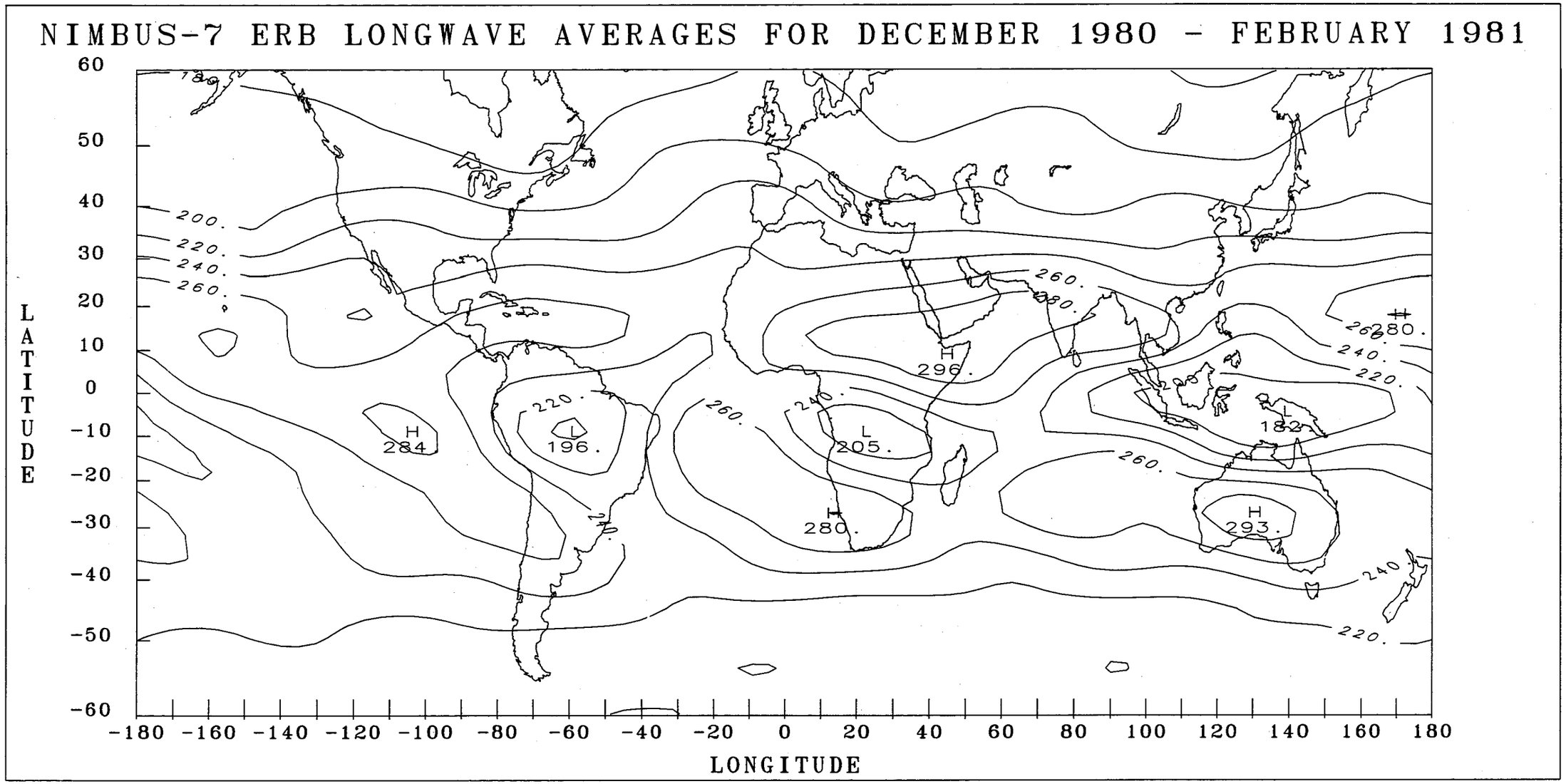
NIMBUS-7 ERB LONGWAVE AVERAGES FOR DECEMBER 1980 - FEBRUARY 1981
LATITUDE
60
50
40
30
20
10
0
-10
-20
-30
-40
-50
-60
LONGITUDE
-180 -160 -140 -120 -100 -80 -60 -40 -20 0 20 40 60 80 100 120 140 160 180
200.
220.
240.
260.
280.
H
284
L
196.
H
296.
L
205.
H
280.
H
293.
L
182

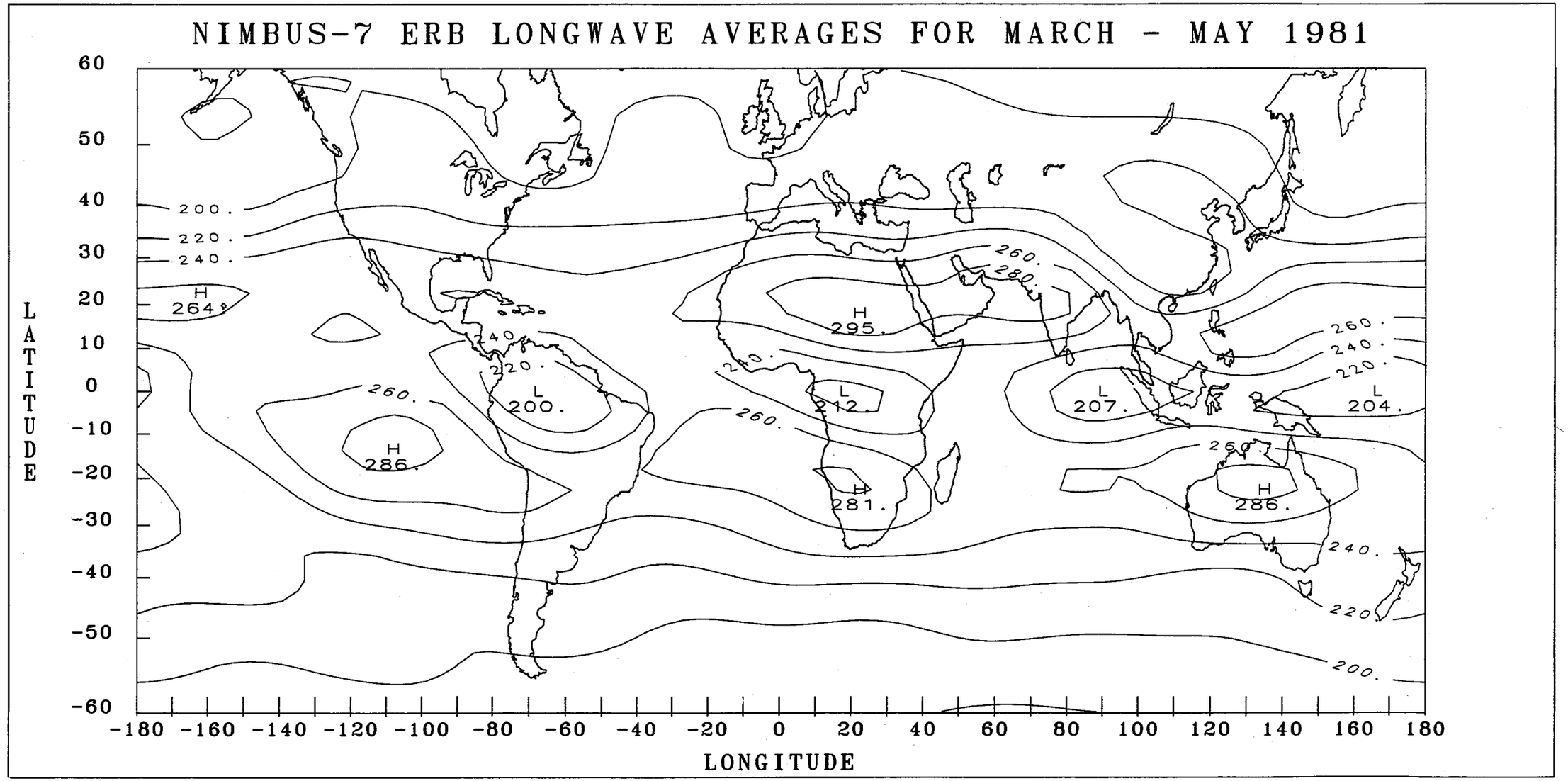
NIMBUS-7 ERB LONGWAVE AVERAGES FOR MARCH - MAY 1981
LATITUDE
LONGITUDE
60
50
40
30
20
10
0
-10
-20
-30
-40
-50
-60
-180 -160 -140 -120 -100 -80 -60 -40 -20 0 20 40 60 80 100 120 140 160 180
200.
220.
240.
260.
280.
H
264.
H
295.
L
200.
L
212.
L
207.
L
204.
H
286.
H
281.
H
286.

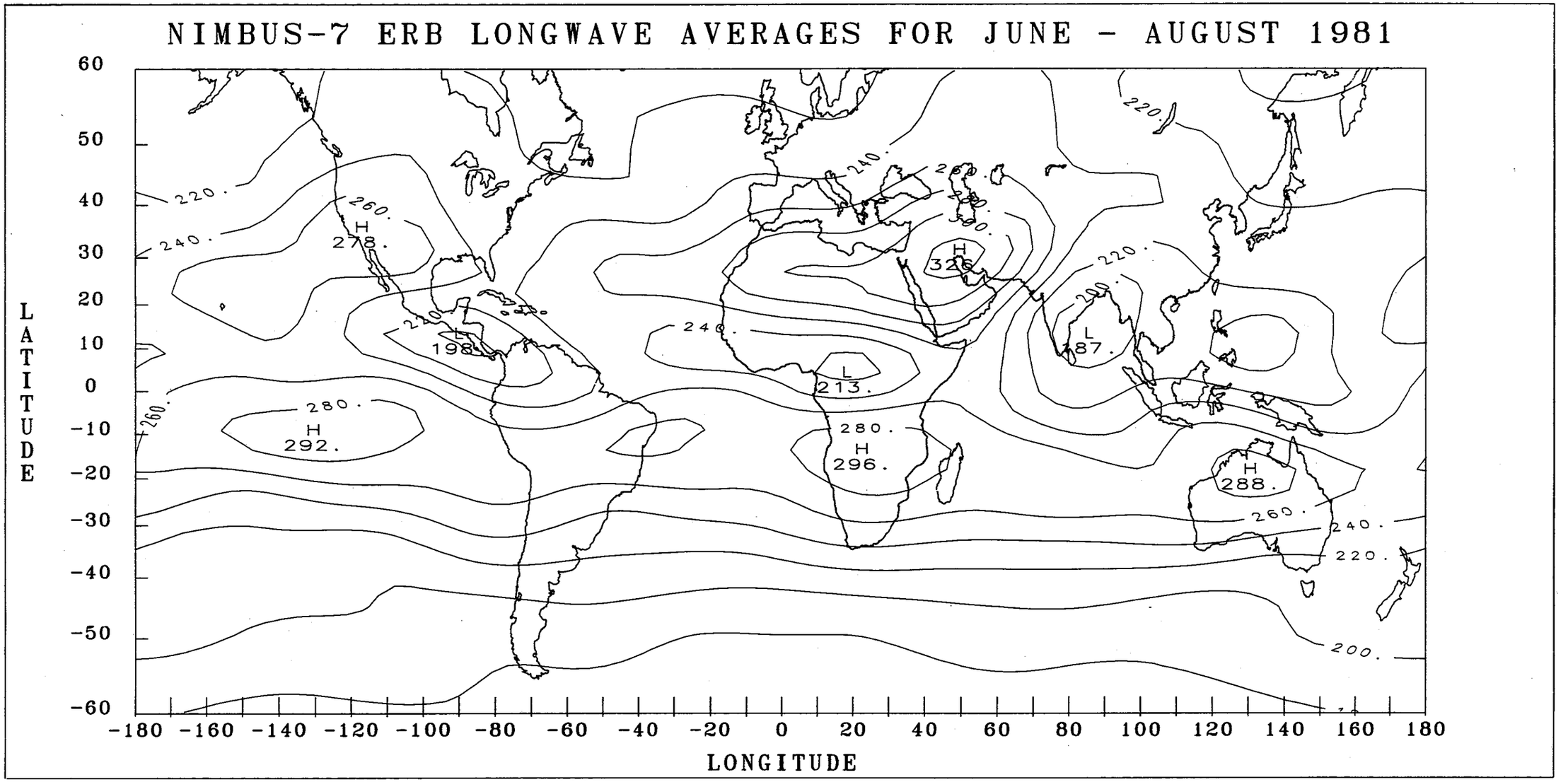
NIMBUS-7 ERB LONGWAVE AVERAGES FOR JUNE - AUGUST 1981
LATITUDE
LONGITUDE
60
50
40
30
20
10
0
-10
-20
-30
-40
-50
-60
-180 -160 -140 -120 -100 -80 -60 -40 -20 0 20 40 60 80 100 120 140 160 180
220.
240.
260.
H
278.
L
198.
280.
H
292.
240.
260.
280.
H
296.
L
213.
H
326.
220.
200.
L
187.
H
288.
260.
240.
220.
200.

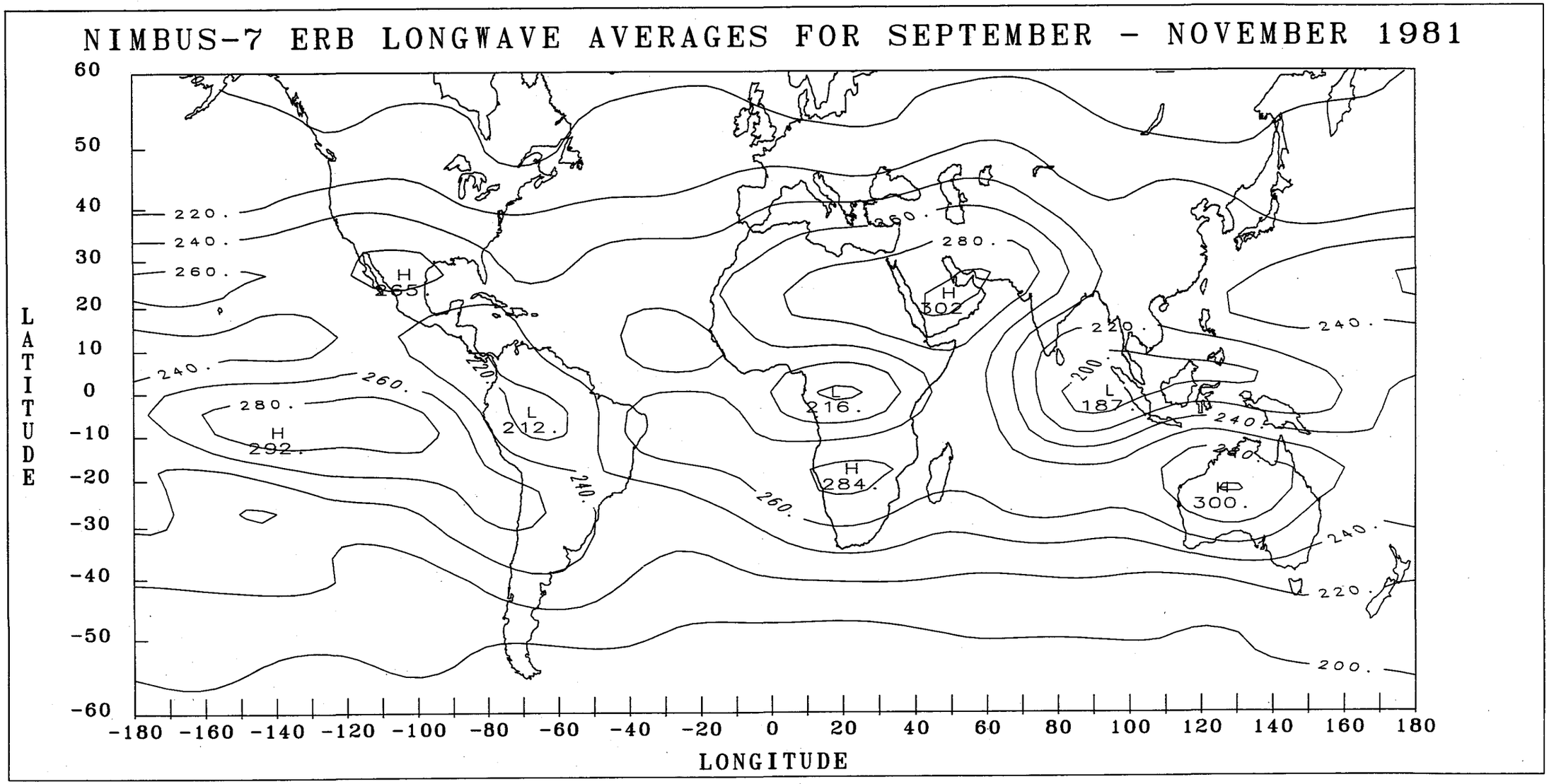
NIMBUS-7 ERB LONGWAVE AVERAGES FOR SEPTEMBER - NOVEMBER 1981
LATITUDE
60
50
40
30
20
10
0
-10
-20
-30
-40
-50
-60
220.
240.
260.
280.
H
265.
H
292.
L
212.
240.
260.
280.
H
302
240.
220.
200.
L
187.
240.
L
216.
H
284.
260.
240.
300.
240.
220.
200.
-180 -160 -140 -120 -100 -80 -60 -40 -20 0 20 40 60 80 100 120 140 160 180
LONGITUDE

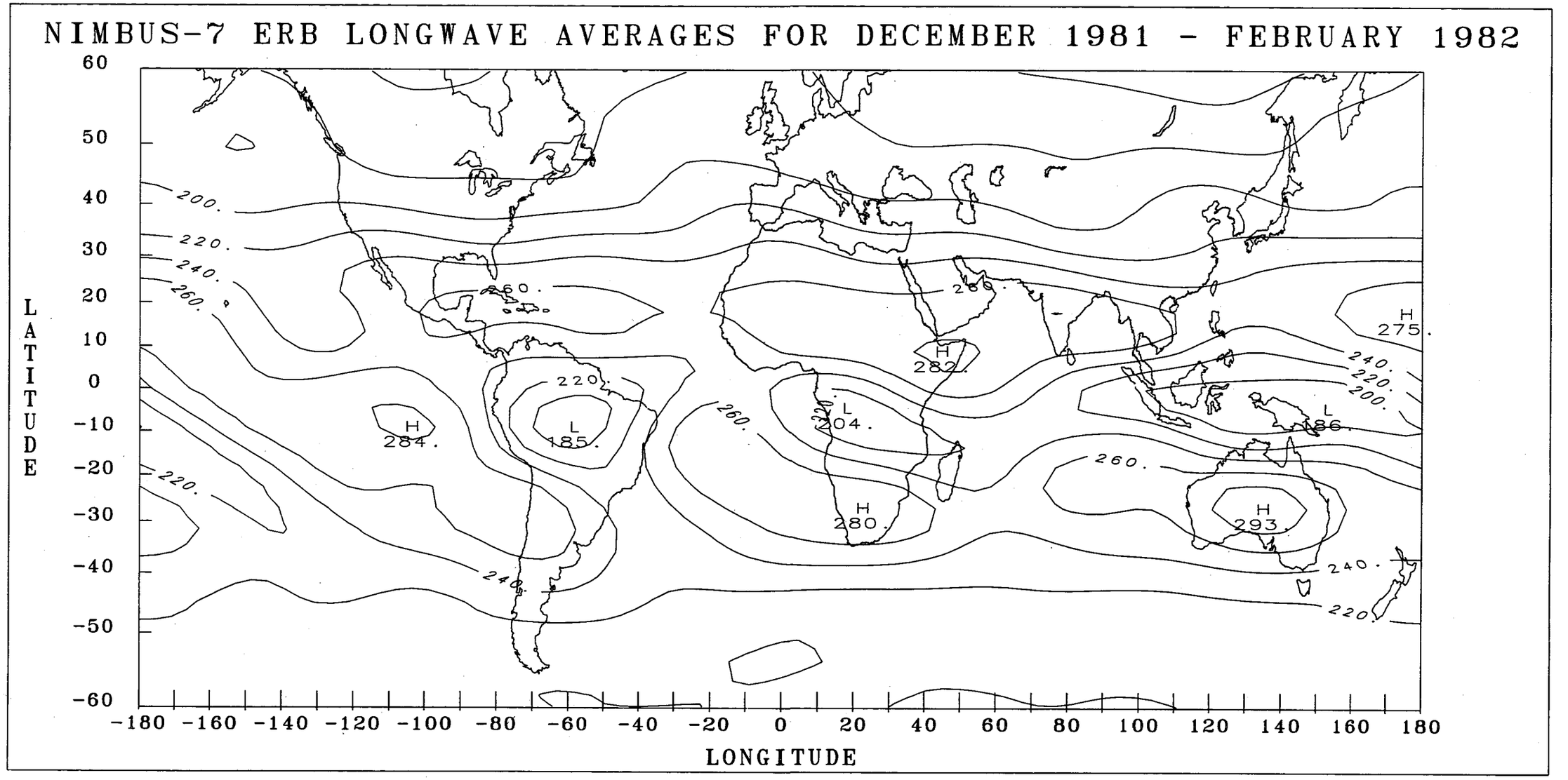
NIMBUS-7 ERB LONGWAVE AVERAGES FOR DECEMBER 1981 - FEBRUARY 1982
LATITUDE
60
50
40
30
20
10
0
-10
-20
-30
-40
-50
-60
LONGITUDE
-180 -160 -140 -120 -100 -80 -60 -40 -20 0 20 40 60 80 100 120 140 160 180
200.
220.
240.
260.
H
284.
L
185.
H
282.
L
204.
H
280.
H
293.
L
186.
H
275.

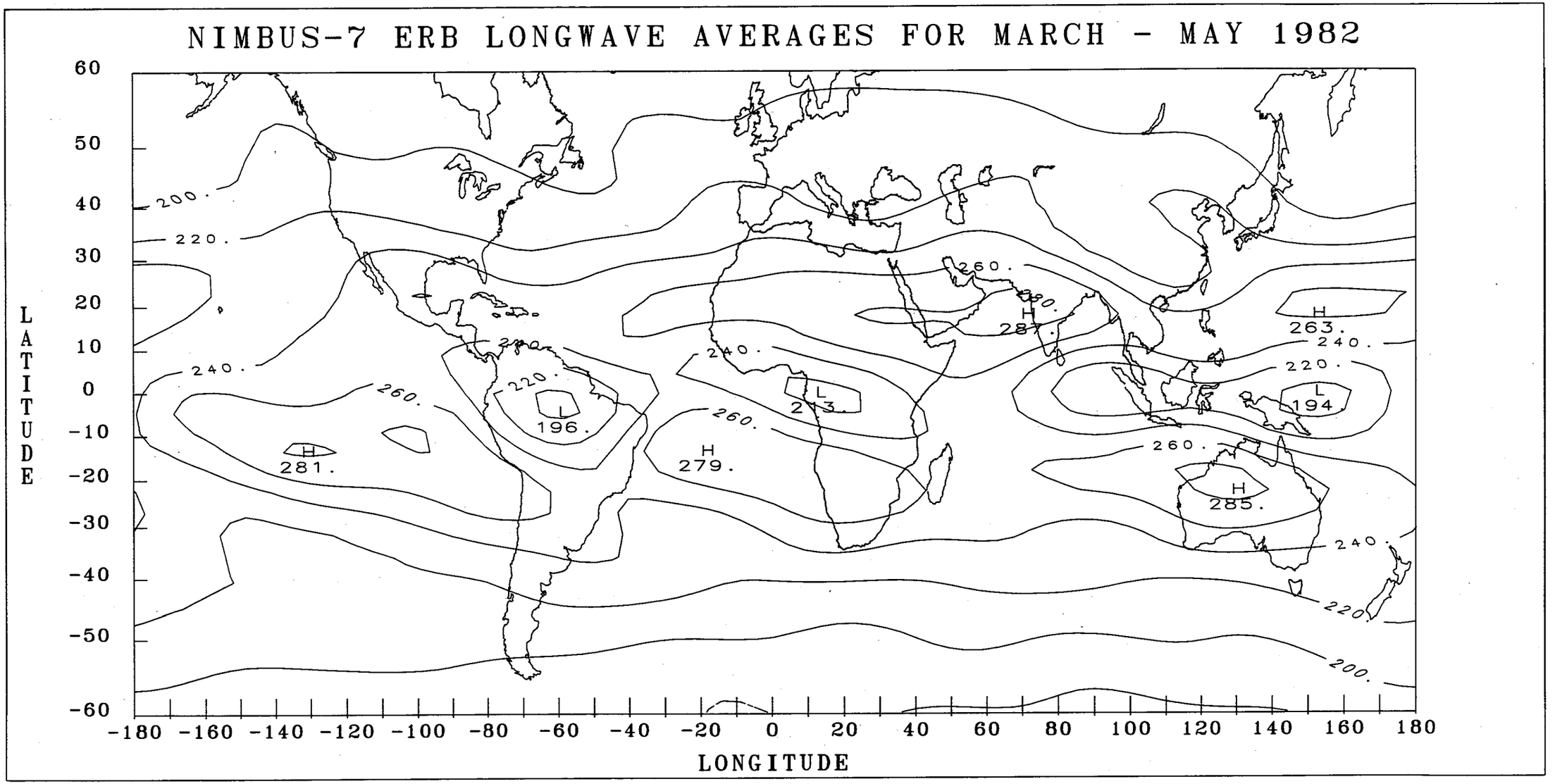
NIMBUS-7 ERB LONGWAVE AVERAGES FOR MARCH - MAY 1982
LATITUDE
60
50
40
30
20
10
0
-10
-20
-30
-40
-50
-60
-180 -160 -140 -120 -100 -80 -60 -40 -20 0 20 40 60 80 100 120 140 160 180
LONGITUDE
200.
220.
240.
260.
280.
H
281.
L
196.
H
279.
L
213
H
287.
H
263.
L
194
H
285.

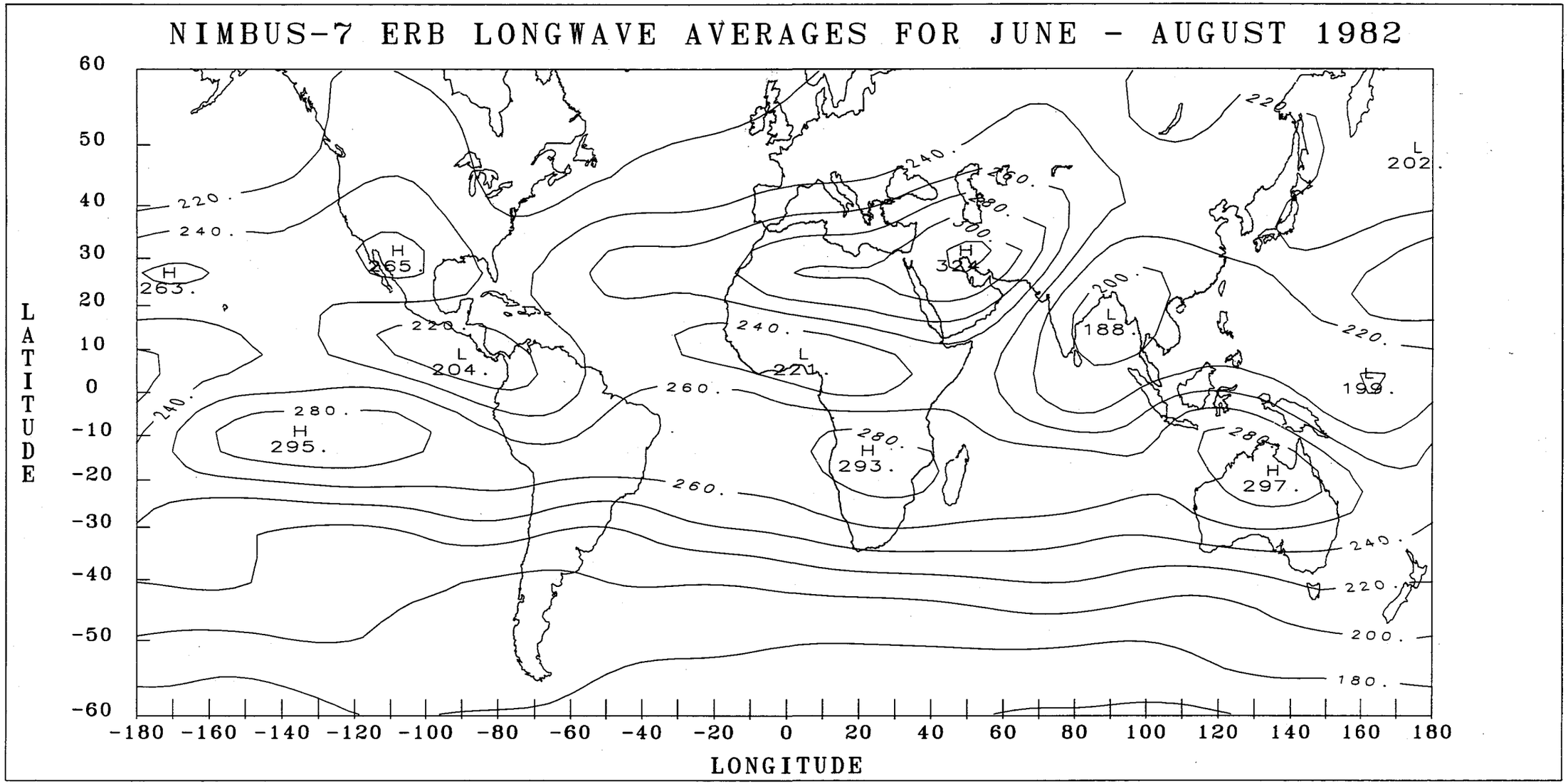
NIMBUS-7 ERB LONGWAVE AVERAGES FOR JUNE - AUGUST 1982
LATITUDE
LONGITUDE
60
50
40
30
20
10
0
-10
-20
-30
-40
-50
-60
-180 -160 -140 -120 -100 -80 -60 -40 -20 0 20 40 60 80 100 120 140 160 180
H 263.
H 265.
L 204.
H 295.
L 221.
H 293.
L 188.
H 297.
L 202.
220.
240.
260.
280.
200.
180.

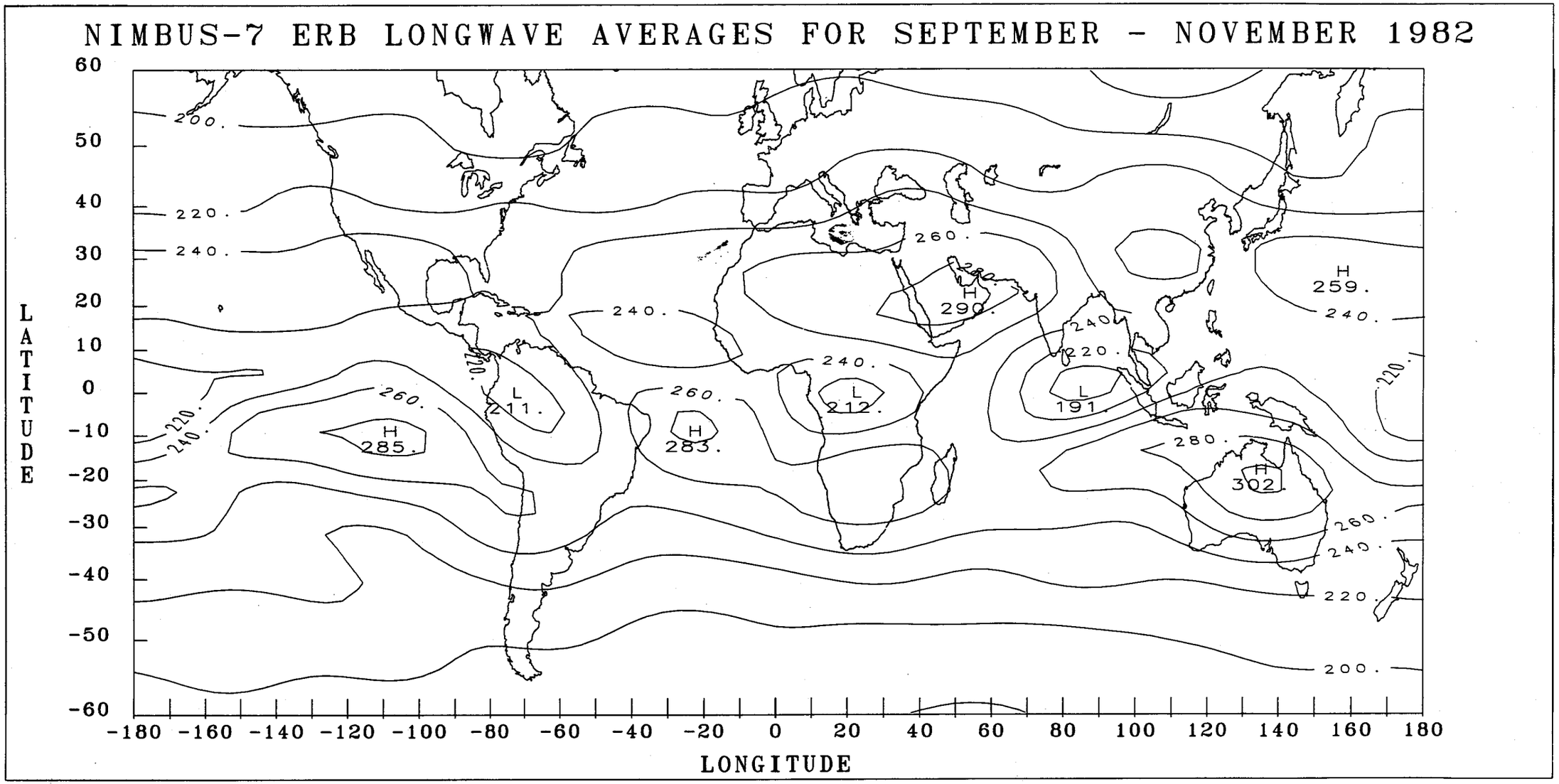
NIMBUS-7 ERB LONGWAVE AVERAGES FOR SEPTEMBER - NOVEMBER 1982
LATITUDE
60
50
40
30
20
10
0
-10
-20
-30
-40
-50
-60
LONGITUDE
-180 -160 -140 -120 -100 -80 -60 -40 -20 0 20 40 60 80 100 120 140 160 180
200.
220.
240.
260.
280.
H 285.
H 283.
H 290.
H 259.
H 302.
L 211.
L 212.
L 191.

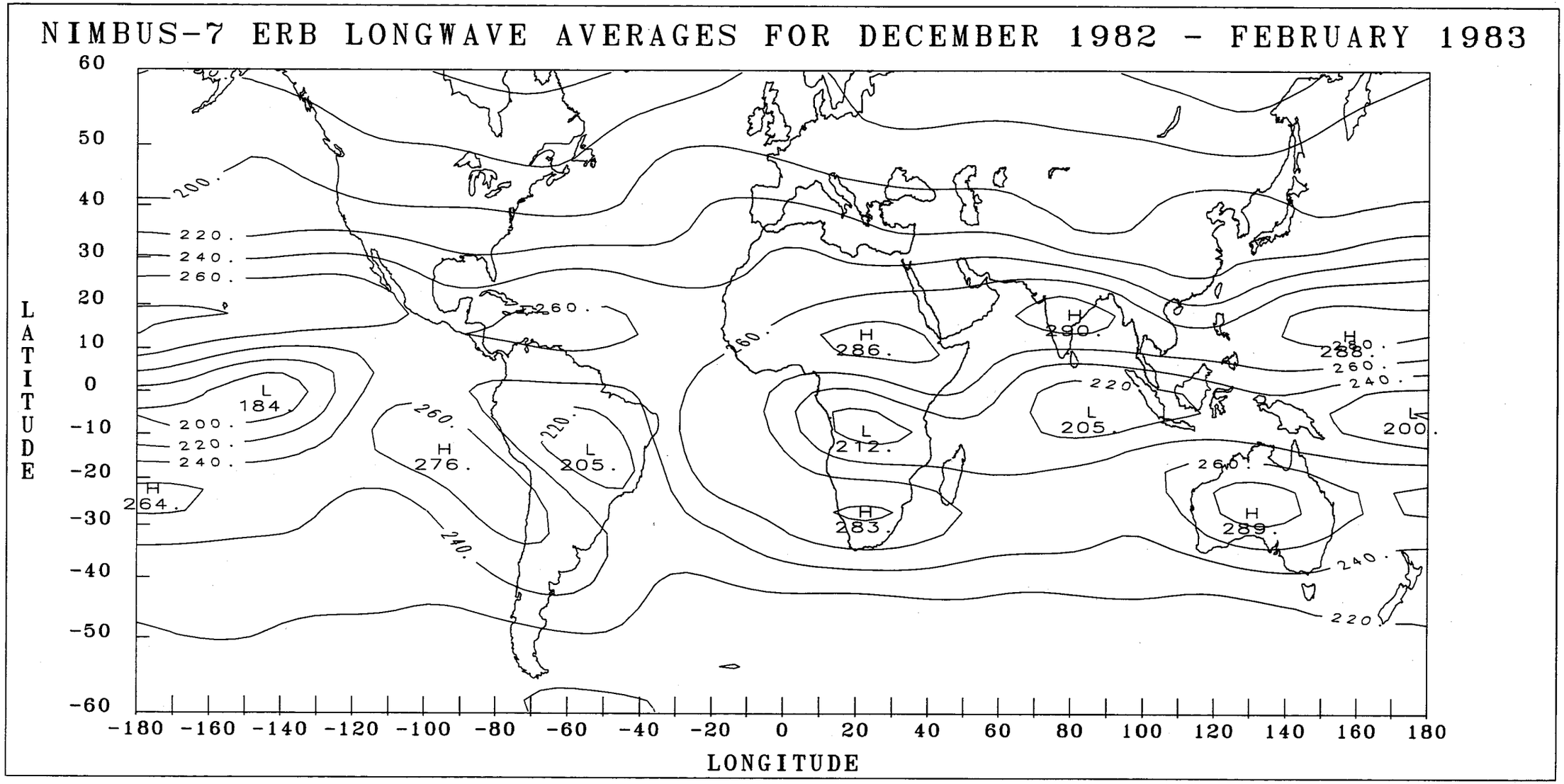
NIMBUS-7 ERB LONGWAVE AVERAGES FOR DECEMBER 1982 - FEBRUARY 1983
LATITUDE
LONGITUDE
60
50
40
30
20
10
0
-10
-20
-30
-40
-50
-60
-180 -160 -140 -120 -100 -80 -60 -40 -20 0 20 40 60 80 100 120 140 160 180
200.
220.
240.
260.
160.
L
184.
H
264.
H
276.
L
205.
H
286.
H
290.
L
212.
L
205.
H
283.
H
289.
H
288.
L
200.

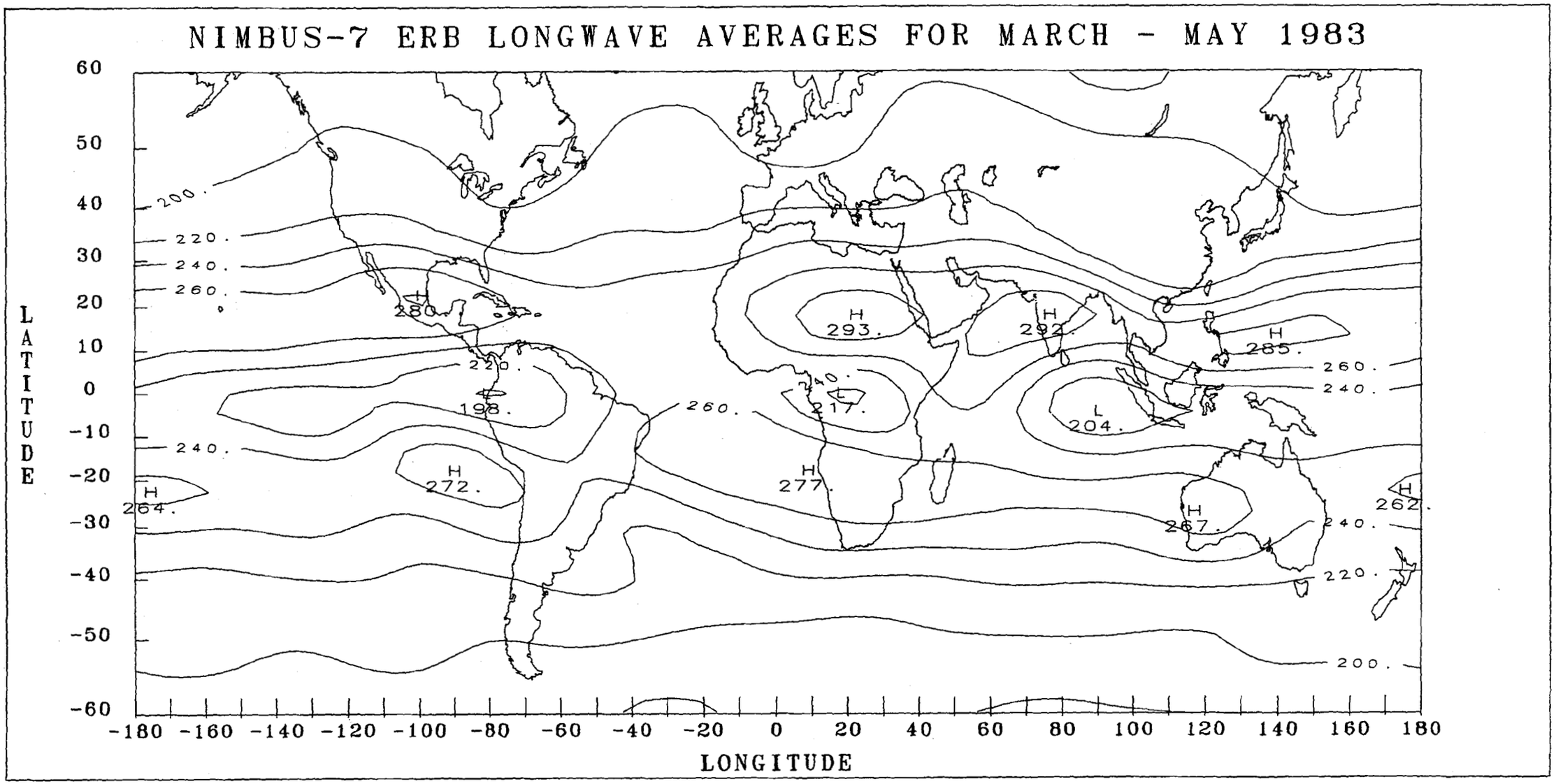
NIMBUS-7 ERB LONGWAVE AVERAGES FOR MARCH - MAY 1983
LATITUDE
LONGITUDE
60
50
40
30
20
10
0
-10
-20
-30
-40
-50
-60
-180 -160 -140 -120 -100 -80 -60 -40 -20 0 20 40 60 80 100 120 140 160 180
200.
220.
240.
260.
H 280.
220.
198.
260.
240.
H 264.
H 272.
H 293.
H 292.
L 217.
H 277.
H 285.
260.
240.
L 204.
H 267.
H 262.
240.
220.
200.

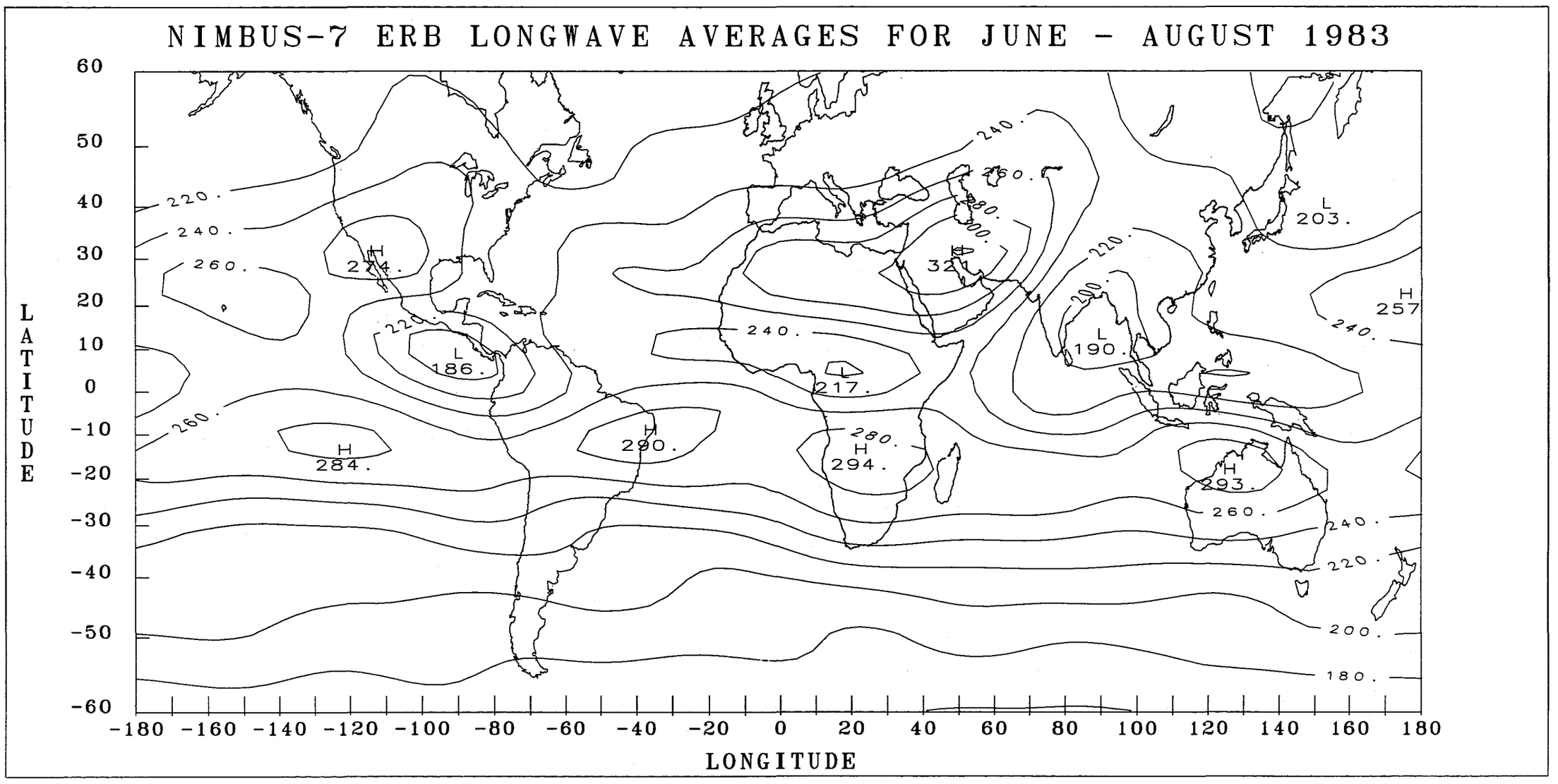
NIMBUS-7 ERB LONGWAVE AVERAGES FOR JUNE - AUGUST 1983
LATITUDE
LONGITUDE
60
50
40
30
20
10
0
-10
-20
-30
-40
-50
-60
-180 -160 -140 -120 -100 -80 -60 -40 -20 0 20 40 60 80 100 120 140 160 180
220.
240.
260.
H 274.
L 186.
H 284.
H 290.
240.
L 217.
280.
H 294.
H 32
240.
220.
200.
L 190.
L 203.
H 257
240.
H 293.
260.
240.
220.
200.
180.

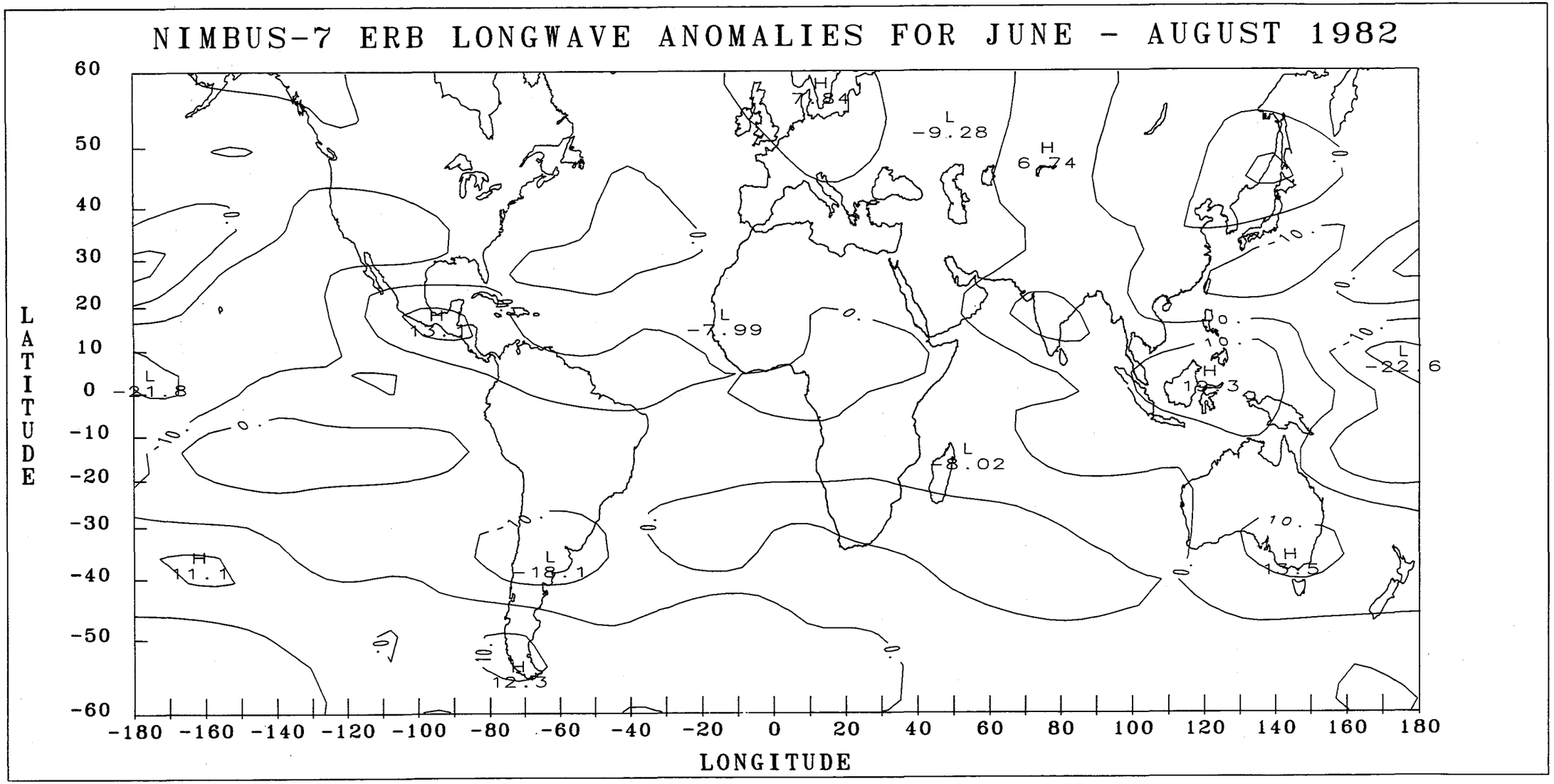
NIMBUS-7 ERB LONGWAVE ANOMALIES FOR JUNE - AUGUST 1982
LATITUDE
LONGITUDE
60
50
40
30
20
10
0
-10
-20
-30
-40
-50
-60
-180 -160 -140 -120 -100 -80 -60 -40 -20 0 20 40 60 80 100 120 140 160 180
H 7.84
L -9.28
H 6.74
H 15.1
L -7.99
L -21.8
L -8.02
L -22.6
H 19.3
H 11.1
L -18.1
H 12.3
H 13.5
0.
-10.
10.

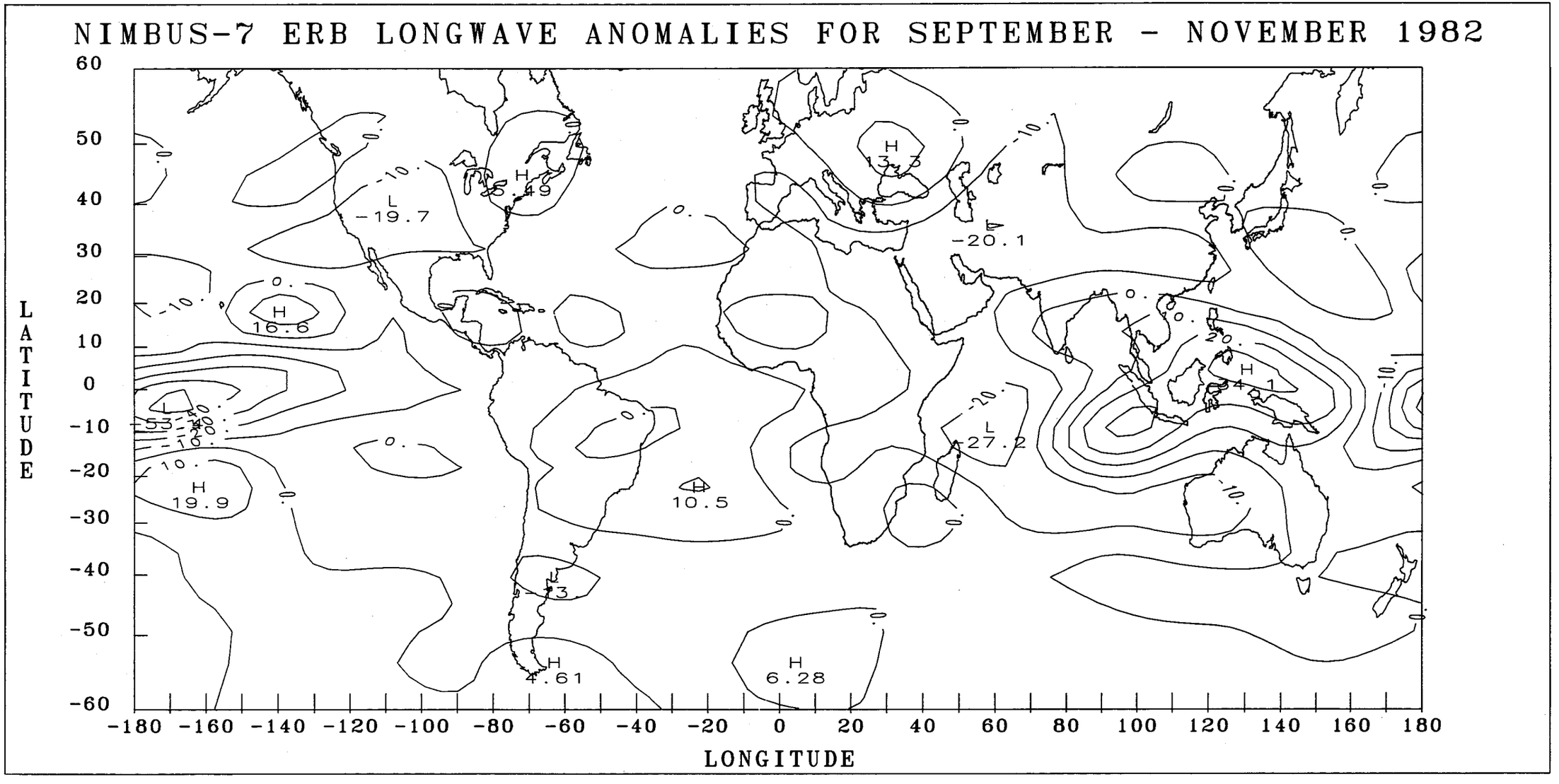
NIMBUS-7 ERB LONGWAVE ANOMALIES FOR SEPTEMBER - NOVEMBER 1982
LATITUDE
LONGITUDE
60
50
40
30
20
10
0
-10
-20
-30
-40
-50
-60
-180 -160 -140 -120 -100 -80 -60 -40 -20 0 20 40 60 80 100 120 140 160 180
H
16.6
L
-19.7
H
5.49
H
3.3
-20.1
H
19.9
10.5
L
27.2
H
4.1
H
4.61
H
6.28

NIMBUS-7 ERB LONGWAVE ANOMALIES FOR DECEMBER 1982 - FEBRUARY 1983

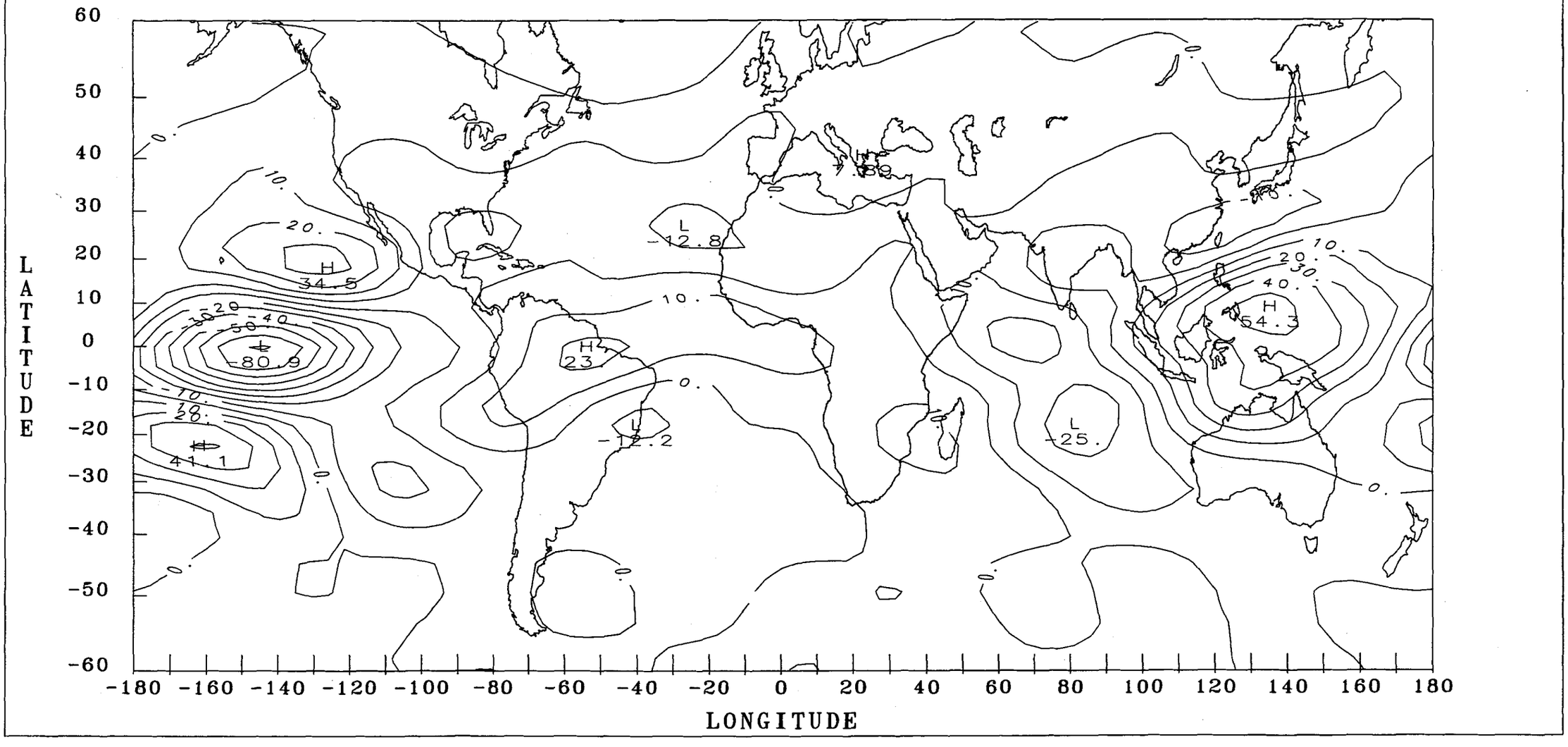

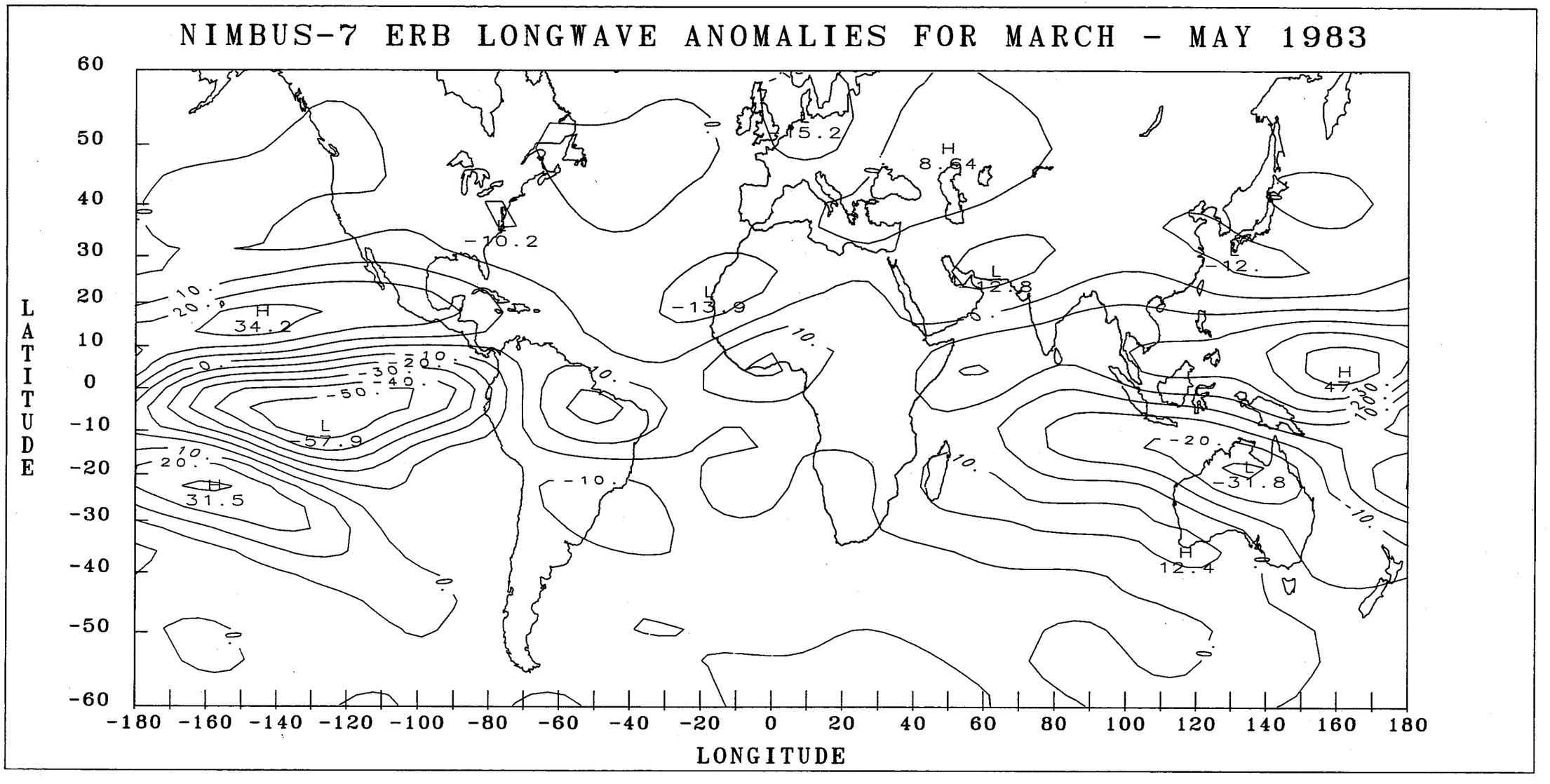
NIMBUS-7 ERB LONGWAVE ANOMALIES FOR MARCH - MAY 1983
LATITUDE
LONGITUDE
60
50
40
30
20
10
0
-10
-20
-30
-40
-50
-60
-180 -160 -140 -120 -100 -80 -60 -40 -20 0 20 40 60 80 100 120 140 160 180
H
34.2
L
-57.9
H
31.5
L
-13.9
-10.2
5.2
H
8.64
L
-2.8
-12.
H
47
L
-31.8
H
12.4

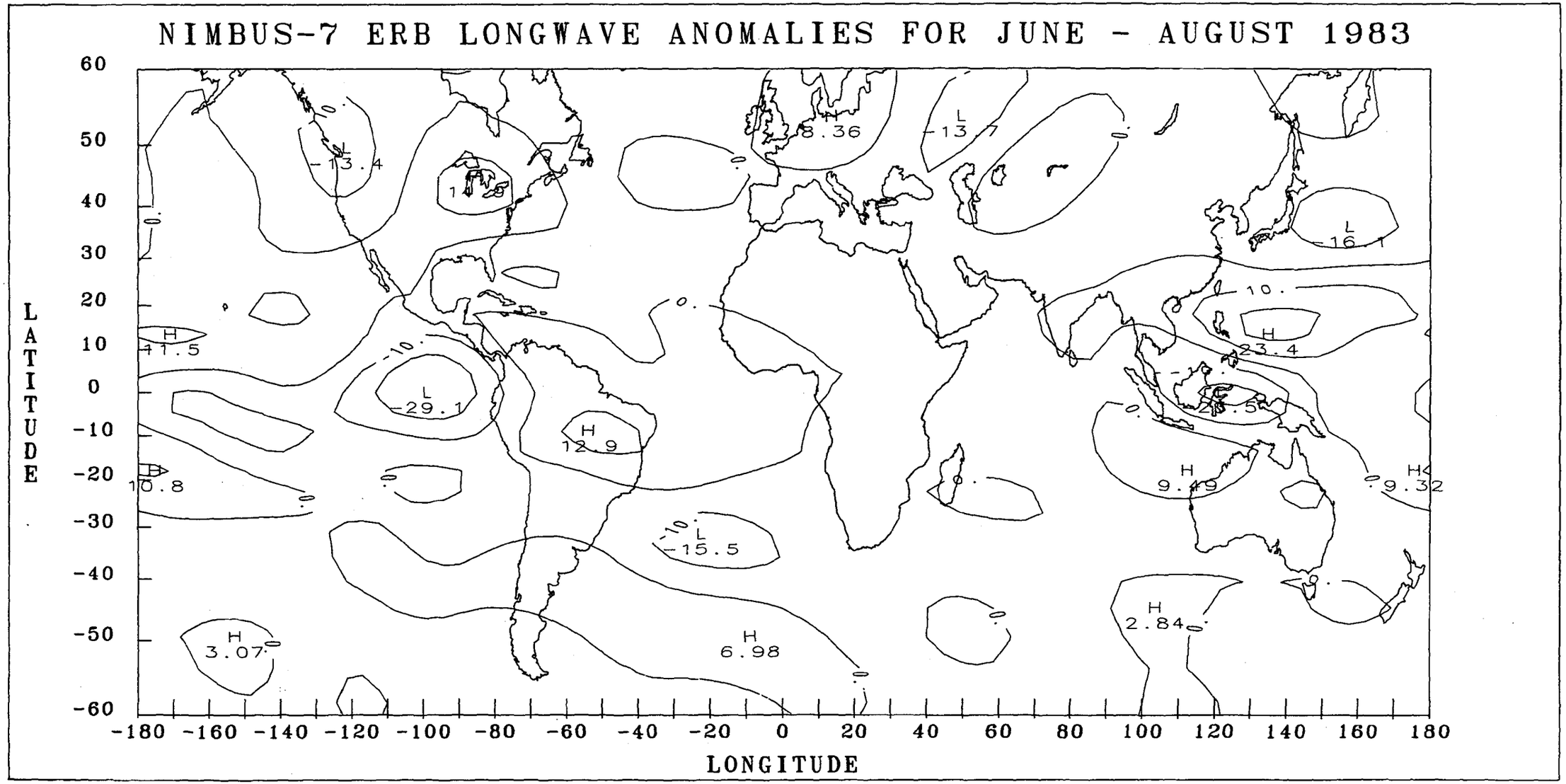
NIMBUS-7 ERB LONGWAVE ANOMALIES FOR JUNE - AUGUST 1983
LATITUDE
LONGITUDE
60
50
40
30
20
10
0
-10
-20
-30
-40
-50
-60
-180 -160 -140 -120 -100 -80 -60 -40 -20 0 20 40 60 80 100 120 140 160 180
H 41.5
L -29.1
H 12.9
10.8
L -15.5
H 6.98
H 3.07
L -13.4
H 8.36
L -13.7
L -16.1
H 23.4
H 9.49
H 9.32
H 2.84

ANNUALLY AVERAGED FIELDS

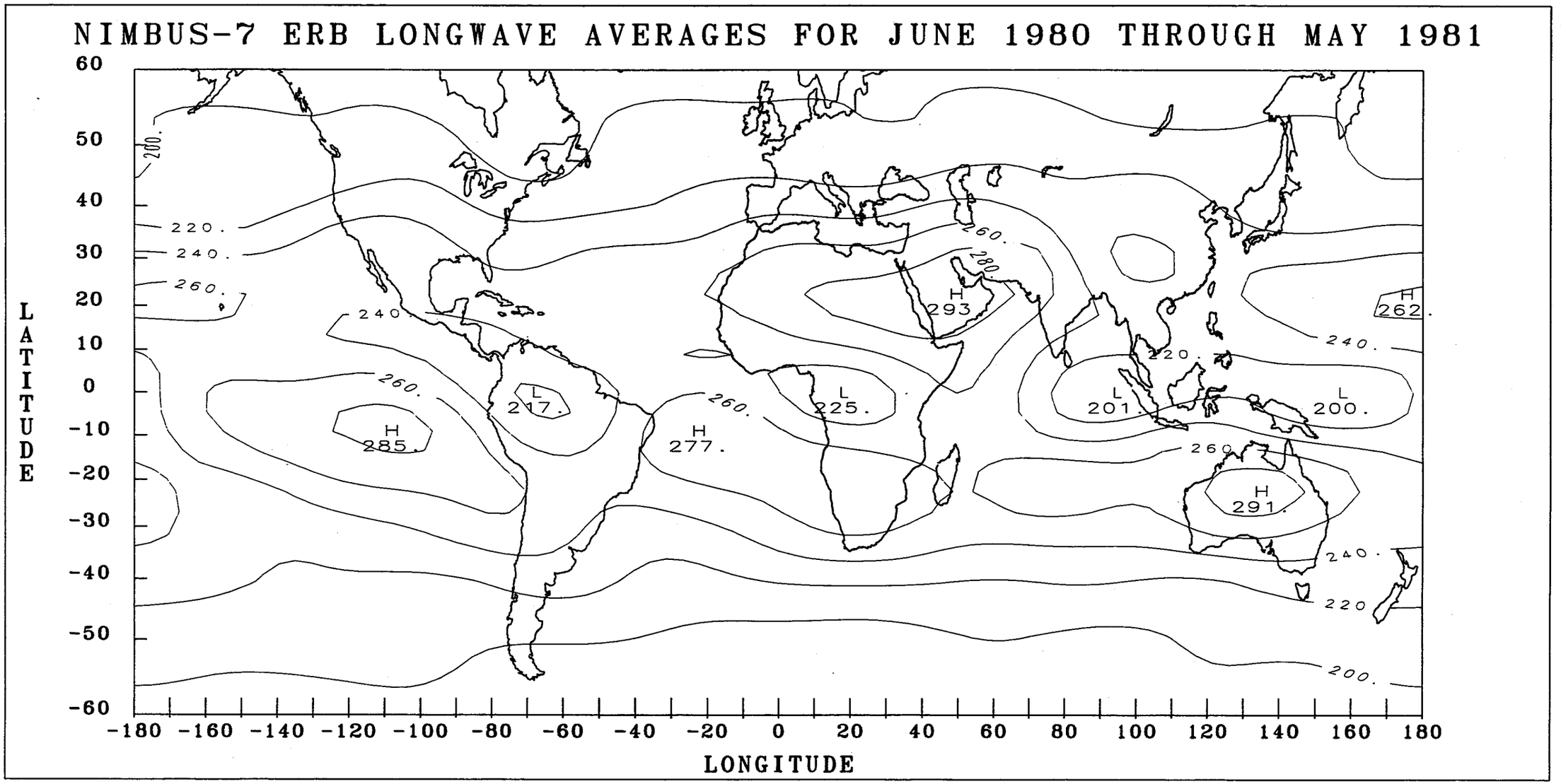
NIMBUS-7 ERB LONGWAVE AVERAGES FOR JUNE 1980 THROUGH MAY 1981
LATITUDE
60
50
40
30
20
10
0
-10
-20
-30
-40
-50
-60
-180 -160 -140 -120 -100 -80 -60 -40 -20 0 20 40 60 80 100 120 140 160 180
LONGITUDE
200.
220.
240.
260.
280.
H 293
H 262.
L 217.
L 225.
L 201.
L 200.
H 285.
H 277.
H 291.

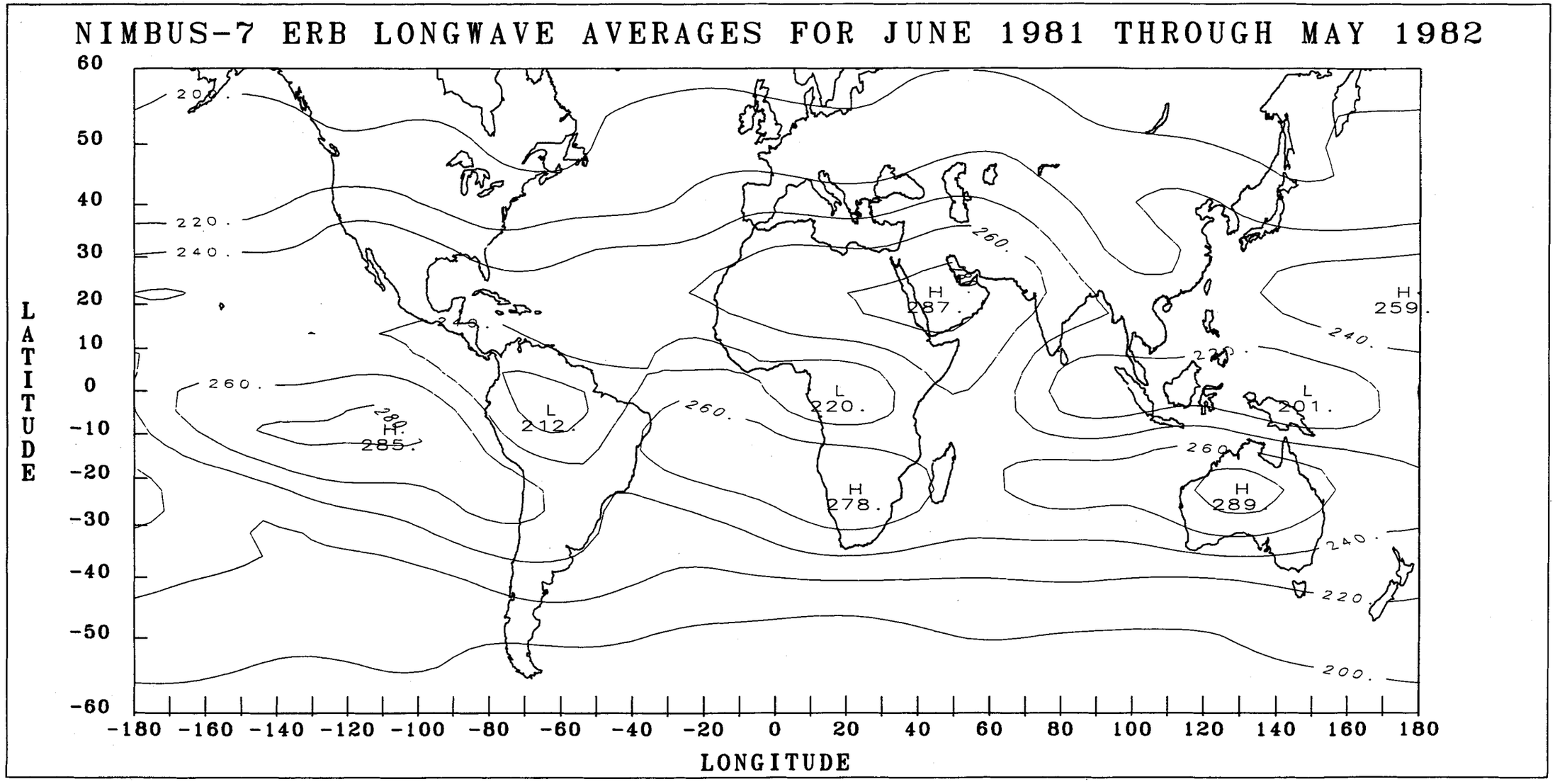
NIMBUS-7 ERB LONGWAVE AVERAGES FOR JUNE 1981 THROUGH MAY 1982
LATITUDE
LONGITUDE
60
50
40
30
20
10
0
-10
-20
-30
-40
-50
-60
-180 -160 -140 -120 -100 -80 -60 -40 -20 0 20 40 60 80 100 120 140 160 180
220.
240.
260.
H
287.
H
259.
L
212.
L
220.
L
201.
H
285.
H
278.
H
289
200.

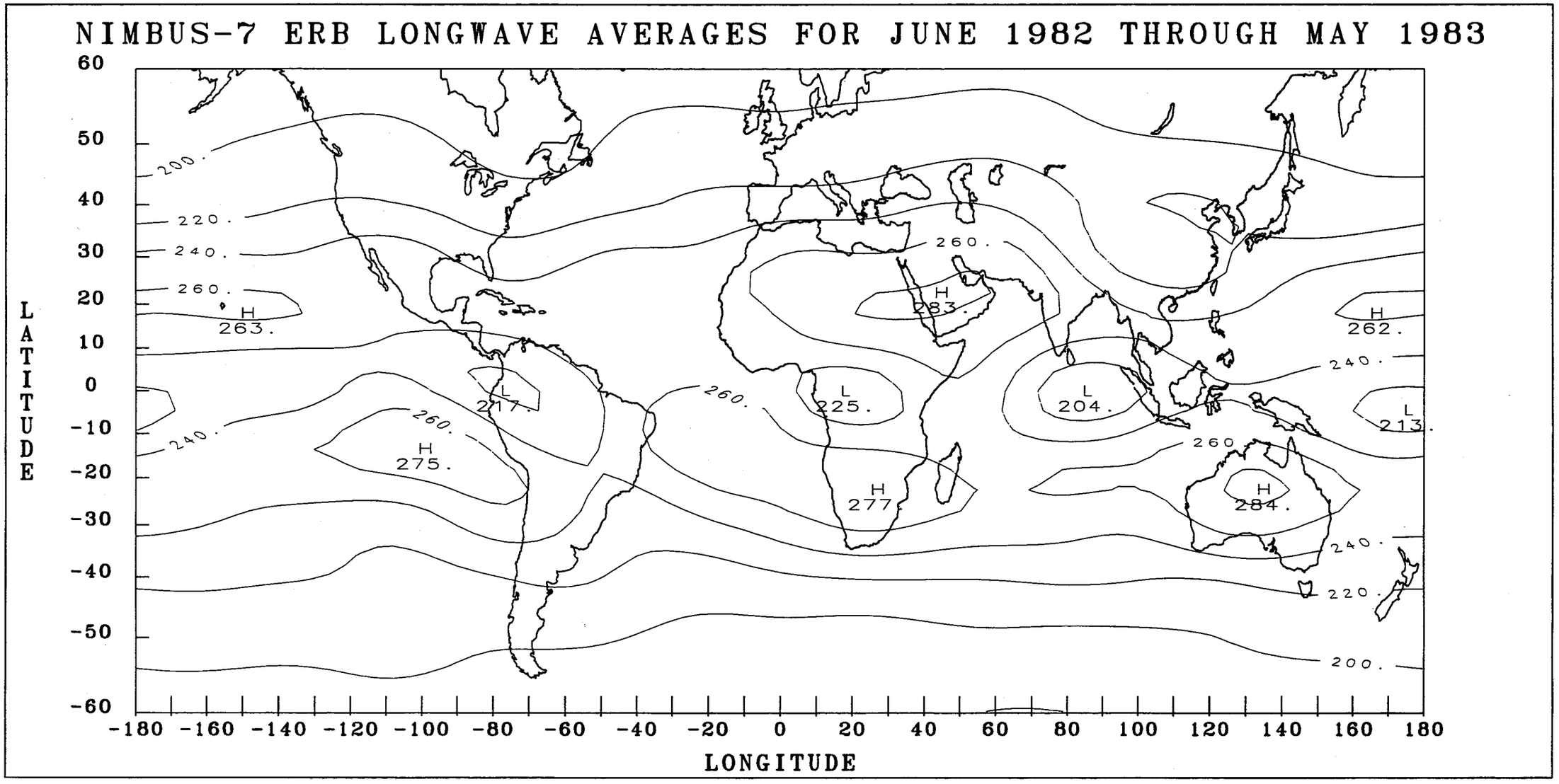
NIMBUS-7 ERB LONGWAVE AVERAGES FOR JUNE 1982 THROUGH MAY 1983
LATITUDE
LONGITUDE
60
50
40
30
20
10
0
-10
-20
-30
-40
-50
-60
-180 -160 -140 -120 -100 -80 -60 -40 -20 0 20 40 60 80 100 120 140 160 180
200.
220.
240.
260.
H
263.
H
283.
H
262.
L
217.
L
225.
L
204.
L
213.
H
275.
H
277
H
284.

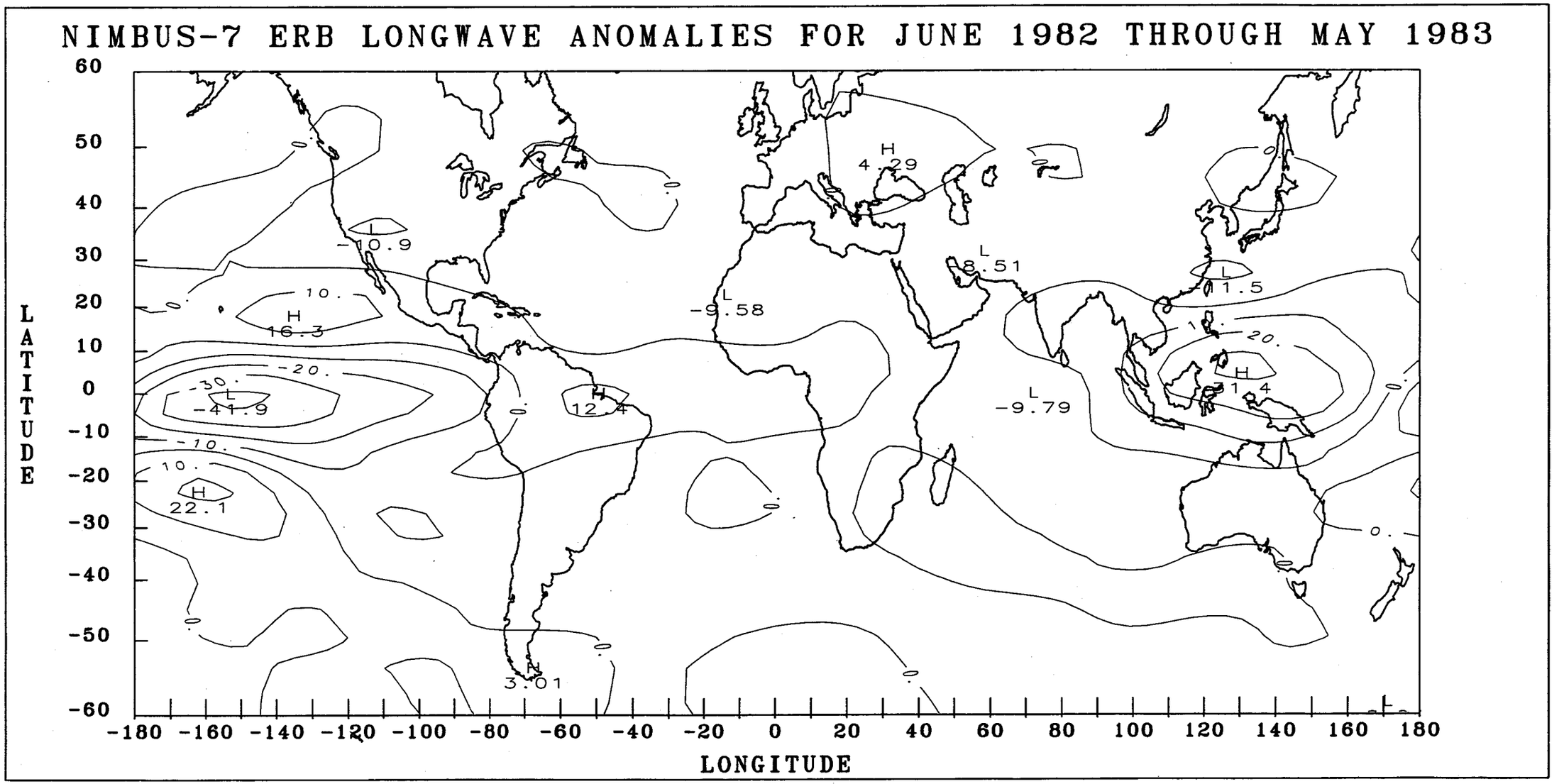
NIMBUS-7 ERB LONGWAVE ANOMALIES FOR JUNE 1982 THROUGH MAY 1983
LATITUDE
60
50
40
30
20
10
0
-10
-20
-30
-40
-50
-60
-180 -160 -140 -120 -100 -80 -60 -40 -20 0 20 40 60 80 100 120 140 160 180
LONGITUDE
L -10.9
H 16.3
L -41.9
H 22.1
H 12.4
H 3.01
L -9.58
H 4.29
L 8.51
L -9.79
L 1.5
H 1.4
10.
-10.
-20.
-30.
0.

1. Report No.	2. Government Accession No.	3. Recipient's Catalog No.
NASA RP-1163		

4. Title and Subtitle	5. Report Date
El Nino and Outgoing Longwave Radiation: An Atlas of Nimbus-7 Earth Radiation Budget Observations	April 1986
	6. Performing Organization Code: 636

7. Author(s)	8. Performing Organization Report No.
H. Lee Kyle, Philip E. Ardanuy,* Richard R. Hucek,* and the Nimbus-7 ERB Experiment Team	85B0565
	10. Work Unit No.: 665-10-70

9. Performing Organization Name and Address	11. Contract or Grant No.
Space Data and Computing Division Goddard Space Flight Center Greenbelt, MD 20771	NAS5-27728
	13. Type of Report and Period Covered: Reference Publication

12. Sponsoring Agency Name and Address	14. Sponsoring Agency Code
National Aeronautics and Space Administration Washington, DC 20546	

15. Supplementary Notes

*Research and Data Systems Corporation, Lanham, MD 20706

16. Abstract

Five years of broad-band Earth Radiation Budget (ERB) measurements taken by the Nimbus-7 ERB experiment have been archived. This five-year period included the 1982-1983 El Nino/Southern Oscillation event, which reached its peak in January 1983 (near the beginning of the fifth data year). An outgoing longwave radiation subset of the data, for the period June 1980-October 1983, has been processed to enhance spatial resolution. This atlas contains the analyses of the resultant fields. In addition, a set of anomaly maps, based on a definition of pre-El Nino climatology, is included. Together, these two sets of maps provide the first broad-band glimpse of the terrestrial outgoing longwave radiative response to the El Nino event.

17. Key Words (Suggested by Author(s))	18. Distribution Statement
Earth's radiation budget outgoing longwave radiation El Nino/Southern Oscillation Nimbus-7 ERB experiment	Unclassified - Unlimited Subject Category 47

19. Security Classif. (of this report)	20. Security Classif. (of this page)	21. No. of Pages	22. Price
Unclassified	Unclassified	98	A05

N-305

For sale by the National Technical Information Service, Springfield, Virginia 22161